Methalox Propellant for Future Launch Vehicles

A comparative study of methalox, hydrolox and kerolox propellant for future launch vehicles

AE5810: Master Thesis (Space)

Swati Shridhar Iyer

Delft University of Technology

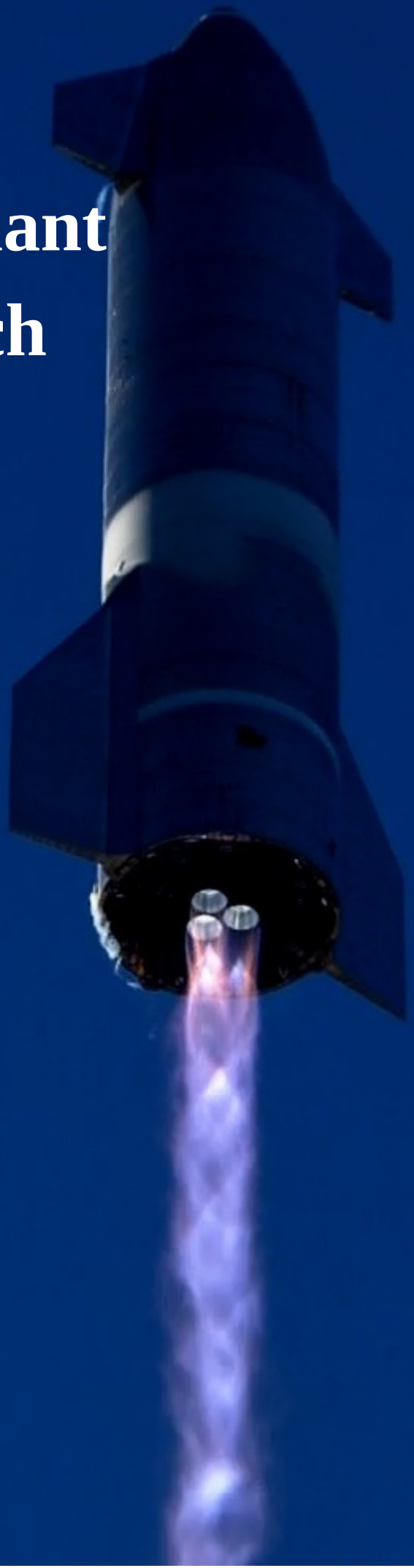

TU Delft

Methalox Propellant for Future Launch Vehicles

A comparative study of methalox, hydrolox and kerolox propellants for future launch vehicles

by

Swati Shridhar Iyer

to obtain the degree of Master of Science

at the Delft University of Technology

Student Number:	5003725
Instructor:	Ir. B.T.C. Zandbergen
Institution:	Delft University of Technology
Place:	Faculty of Aerospace Engineering, Delft
Project Duration:	August 2021 – June 2022

Cover Image: SpaceX Starship SN9 Simulation [61]

TU Delft

Acknowledgement

This document concludes the work of a Master Thesis about a cost based comparison of methalox propellant with existing liquid propellants - hydrolox and kerolox. The study is conducted as a part of my Master of Science at the Delft University of Technology.

I would like to take this moment to thank my supervisor supervisor Ir. B.T.C. Zandbergen for his guidance, constructive criticism, and encouragement throughout this thesis. I feel extremely grateful to have had the opportunity to work under his guidance. I would also like to thank M. Rozemeijer and Stephane Contant whose work served as the basis of this research. In particular, I would like to express my gratitude to M. Rozemeijer for helping and answering any questions I had in regard to the First Stage Recovery Tool.

Furthermore, I would like to thank my parents, and my sister, Shruti, for their constant support and words of encouragement. I would also like to thank Thatha and Nikhil. Thank you also to my close friends Mehreen, Anamika, Pearl and Sreevidhya for supporting me throughout despite the long distance.

Lastly, I would like to thank everyone who has helped me in my endeavour of obtaining this Master's degree.

Swati Shridhar Iyer
Delft, July 2022

Abstract

Contrasting experience with Reusable Launch vehicles—Space Shuttle and Falcon 9— has established that potential of reusable launch vehicles to achieve low launch costs is driven by the design choices made. Methalox propellant is one such design choice that has been touted to power future missions and potentially replace traditional propellants — Hydrolox and Kerolox. The high density of methalox compared to hydrolox and improved specific impulse compared to kerolox, potentially make methalox an ideal propellant choice. To justify any new design choice, cost-based analysis is essential, especially given the persisting issue of high launch cost. Additionally, it is essential to benchmark the performance of any new design choice with existing practices, especially when they are expected to replace current practices. For this, a cost based comparative analysis of methalox based launchers with hydrolox and kerolox launchers is performed using a tool capable of launch vehicle design and cost analysis. Rather than designing a tool from scratch, existing First Stage Recovery Tool (FRT), which was developed by M. Rozemeijer to modify and cost existing expendable launchers to include reusability, was extended to include a launch vehicle design module, which was previously lacking. A Multidisciplinary Design Analysis and Optimization (MDAO) methodology was applied for the design module. The design module was developed by verified and validated models implemented from literature for hydrolox, kerolox and methalox propellants and an optimization scheme to minimize for Gross Lift-Off Mass (GLOM). This design module in conjunction with the FRT enables design and costing of expendable and reusable launcher configurations. For the current study, two missions were considered—15600 kg payload to Low Earth Orbit (LEO) and a 5000 kg payload to Geostationary Transfer Orbit (GTO)—for different propellant combination-based launchers. Additionally, different launcher configurations— expendable, reusable via non-propulsive recovery and reusable via propulsive recovery—were considered, enabling cost comparison of propellants for different scenarios. Results indicate that methalox based launchers are cost-effective solution when compared to hydrolox, regardless of mission type or launcher configuration considered in the current study. Compared to kerolox, only a marginal cost benefit can be achieved, for the case of expendable configuration and in combination with kerolox. For reusable configurations, purely methalox shows potential to achieve costs within 10% of kerolox. Sensitivity analysis showed the potential to reduce this gap by including the lower refurbishment requirement of methalox, given low soot formation possibility. Furthermore, it showed the need for a better engine model for methalox, to refine comparison between methalox and kerolox.The tool, however, is not complete and should be extended to include reliability assessment, especially for methalox systems, which are not flight proven unlike hydrolox and kerolox. There also remains issues with the accuracy and uncertainty in certain models, which make the current version suitable only for comparative studies.

Contents

Nomenclature

Abbreviations

Abbreviation	Definition
RLV	Reusable Launch Vehicle
LOX	Liquid Oxygen
CH_4	Liquid Methane
LH_2	Liquid Hydrogen
RP1	Kerosene
LEO	Low Earth Orbits
GTO	Geostationary Transfer Orbits
ELV	Expendable Launch Vehicle
FRT	First Stage Recovery Tool
MDA	Multidisciplinary Design Analysis
MDO	Multidisciplinary Design Optimization
MDAO	Multidisciplinary Design Analysis and Optimization
DRL	Down Range Landing
RTLS	Return to Launch Site
CEA	NASA Chemical Equilibrium with Applications
TPS	Thermal Protection System
GLOM	Gross Lift-Off Mass
MECO	Main Engine Cut Off
GA	Genetic Algorithm
SQP	Sequential Quadratic Programming
HIAD	Hypersonic Inflatable Aerodynamic Decelerator
MAR	Mid-Air Retrieval
IRT	Ideal Rocket Theory
LpA	Launches per Annum
OAT	One-at-a-time Sensitivity Analysis
MC	Monte Carlo Analysis

Symbols

Symbol	Definition	Unit	Value
P_c	Chamber Pressure	[Pa]	
P_e	Exit Pressure	[Pa]	
t_b	Burn time	[s]	
OF	Mixture ratio	[-]	

Symbol	Definition	Unit	Value
D_e	Engine Exit Diameter	[m]	
D_s	Stage Diameter	[m]	
N_{eng}	Number of Engines	[-]	
I_{sp}	Specific Impulse	[s]	
F_T	Thrust	[N]	
γ	Specific heat ratio	[-]	
T_c	Combustion chamber temperature	[K]	
M	Gas mean molar mass	[mol^{-1}]	
Γ	Vandenkerckhove function	[-]	
ϵ	Geometric Expansion Ratio	[-]	
A_e	Exit Area	[m^2]	
A_t	Throat Area	[m^2]	
P_a	Ambient Pressure	[Pa]	
$\dot{m}$	Mass flow rate	[kg/s]	
g_0	Gravitational acceleration	[m/s^2]	9.81
R_A	Universal Gas constant	[$JK^{-1}mol^{-1}$]	8314
L_{LR}	Length of the Liquid Rocket Stage	[m]	
L_{engine}	Length of the Liquid Rocket Engine	[m]	
L_{tanks}	Length of the Propellant Tanks	[m]	
M_{LR}	Liquid Rocket Stage mass	[kg]	
M_{prop}	Propellant Mass	[kg]	
M_{tanks}	Propellant Tank mass	[kg]	
M_{TPS}	Tank Thermal protection system mass	[kg]	
$M_{intertank}$	Inter-tank mass	[kg]	
SF_t	Safety Factor	[-]	1.4
σ_t	Ultimate Yield Stress	[MPa]	
μ	Relative Mean Error	[%]	
E	Absolute Relative Error	[%]	
σ	Standard Deviation	[%]	
ξ_s	Specific Impulse correction factor	[-]	
C_d	Discharge coefficient	[-]	
ξ_{len}	Methane engine length factor	[-]	
ξ_{mass}	Methane engine mass factor	[-]	

List of Figures

List of Tables

1 Introduction

High launch costs have been a major hindrance to the expansion of the space industry [34]. It is well established that spaceflight components are expensive to build. The reason being that these components must be built to withstand the harsh environment of space, requiring increased research and testing of these components [75]. Crewed missions lead to additional requirements to account for the safety of the crew, eliminating failure through failure tolerant methods such as redundancy, all adding to costs [50]. With the shift in paradigm from political incentives of government funded space agencies to economically driven private companies, the need to offer low launch costs to stay in the launch market competition is more pronounced than ever.

One of the breakthrough solutions to lower the launch costs has been to recover and reuse these high-cost components instead of discarding them after every mission, i.e., Reusable Launch Vehicles (RLV). Only two operational reusable launch vehicles have existed – the Space Shuttle and Falcon 9. Although, both partially reusable, the experience from the two launchers are contrasting. The Space Shuttle was built with the intention of lowering costs and enabling affordable and frequent access to space. Space Shuttle successfully demonstrated technical feasibility of designing systems capable of re-entry and landing for reuse, however failed to achieve the goal of lower cost through reusability. Falcon 9, on the other hand, has successfully lowered launch costs by reusability. From the comparison of these two launchers performed in literature study, it became evident that the benefits of reusability is very much driven by designing a launcher suited for the market, the type of reusability method implemented and how much of the launcher is to be recovered and reused [30].

Another method to lower the launch costs is advanced propulsion technologies –in the form of new propellants, air-breathing engines, and intelligent vehicle health management systems. Liquid Oxygen /Liquid Methane (Methalox) is one such propellant combination that is currently being extensively researched – especially for missions to Mars [43]. Methalox propellant has advantages such as higher density compared to Liquid Oxygen /Liquid Hydrogen (Hydrolox), low soot formation compared to Rocket Propellant or highly refined Liquid Oxygen /Kerosene (Kerolox). The higher density compared to hydrolox has the potential of a much smaller propellant tanks [15], leading to lighter systems, and the low soot formation compared to kerolox can lead to lower need for maintenance [45], an important advantage for reusable

systems. Furthermore, coking is an issue when hydrocarbons such as methalox and kerolox are used, however, literature exists that suggests different methods to prevent coking [47].

Within TU Delft, launch vehicle design research is mostly focused on the small launcher market and reusable launcher research is mostly focused on Propulsive or winged recovery. Most of this research is focused on mass characteristics and trajectory, with a few focusing on cost [12, 55]. And although research is extensive with regard to methalox, most of this research postulates the potential of lower launch costs of these propellant, no evidence of this, however, exists. Therefore, a comparative study must be performed to analyse the cost characteristics of methalox powered launchers and to establish a preliminary cost comparison between methane based launchers and traditional propellants (hydrolox, kerolox) powered launchers, to determine whether there is an incentive to switch from tradition propellants to this new methalox propellant. Furthermore, from literature, it is unclear whether the type of mission or launcher configuration would influence propellant comparison. This leads to the main research question for this study:

"Can Liquid Oxygen/Liquid Methane propellant combination achieve lower costs compared to Liquid Oxygen/Liquid Hydrogen and Liquid Oxygen/ Kerosene ?"

To answer the main research question, a set of sub-questions is established below, followed by the scope within which the main research question is answered:

1. What is the cost optimum propellant for Expendable Launch Vehicle (ELV)?
2. What is the cost optimum propellant for Reusable Launch Vehicle (RLV)?
3. What is the influence of recovery method on propellant comparison?
4. What is the influence of launcher configuration on propellant comparison?
5. What is the influence of target orbit on propellant comparison?

Interest in methalox as a propellant is growing, as potential benefits of methalox for Mars mission is established in literature [43, 13]. For the current study, however, the focus is on missions to Low Earth Orbits (LEO) and Geostationary Transfer Orbits (GTO). This is because for Earth based missions, the advantage of ability of Methane being produced on the surface of Mars has no value, thus enabling a comparative analysis solely based on design and cost. Additionally, market analysis predicts dominance of Low Earth and Geostationary orbit missions in the payload range of medium/heavy lift launchers [30].

For the current study, both expendable and reusable configurations are considered, to analyse whether launcher configuration influences the propellant comparison. In previous research and literature study, it is evident that partially reusable launch vehicles perform much better than fully reusable launchers [54, 53]. Therefore, for reusable configuration only first stage recovery and reuse is considered. Most research on reusable methalox launchers is based on retropropulsive or winged recovery. However, literature study showed vertical takeoff ballistic reusable launch vehicles are much lighter and require lower refurbishment efforts compared to winged landing systems [30]. Therefore, the current study considers ballistic Non-propulsive and Propulsive recovery methods, to not only fill in the gap of reusable methalox launchers with non-propulsive recovery but also determine whether recovery method has an influence

on propellant comparison which is unclear from literature. The current research is also limited to liquid propellant Two-Stage launch Vehicles, as literature indicates Three-Stage are more expensive compared to Two Stage Launchers [12, 57].

Rather than developing a new tool for this study, the existing First Stage Recovery Tool (FRT) [55], developed to resize existing Expendable launchers to include reusability, is extended to include a design module capable of designing a new launcher from scratch. The FRT was selected over the tool developed by Contant [12], mainly as FRT offers more recovery methods compared to Contant that was developed solely for launcher design based on retro-propulsive recovery. Furthermore, the FRT tool is based on ParSim which has most of the essential features of the TuDat environment used in Contant's tool, is validated [55] and is much more user-friendly [12]. Although, Contant's tool has the capability to design new launcher, within the time frame it was much suited to include a design module within the FRT tool rather than incorporate non-propulsive recovery method mass and cost estimation relations and include these recovery method options in the optimization process of Contant's tool.

The report is organized into seven chapters, with the current chapter being the first. This chapter is followed by Background information, which summarizes key findings from literature with regard to methalox propellant, recovery hardware, tools in literature and design process. Chapter 3 describes in detail the propulsion, mass, and geometry models implemented in the current study, along with a verification and validation to establish their validity. In Chapter 4, a description of the extension to the FRT tool is presented, with a detailed overview of the tool architecture, description of the improvements and the optimization method implemented. Chapter 5 presents the different simulation cases performed and discusses in detail the results, that will help answer the main research question. Chapter 6 presents an overview of sensitivity analysis of key launcher design parameters on uncertainty in modelling and identifies parameters that could potentially influence propellant comparison. Finally, Chapter 7 presents the conclusion and recommendations to improve and extend the current study.

Note:

The data in this report is presented rounded to the closest integer, unless the difference is minor or in the case of percentages, the data is presented rounded off to the nearest tenth [16]. In this report, hydrolox represents LOX/LH_2, kerolox is LOX/RP1 and methalox is LOX/CH_4. Additionally, pure propellant combinations are simply referred to as hydrolox, kerolox or methalox. In case of combinations, both the propellants are specified, with the first propellant representing stage 1 propellant, followed by upper stage propellant.

2

Background

This chapter presents a brief discussion on why methalox propellant is currently being extensively researched in literature, followed by key finding from literature study on the comparison of methalox propellant with existing propellant combinations. A discussion on the types of recovery methods is then presented. A set of requirements for the tool that would be required to answer the research question is established. Finally, a description of tools from literature that are suitable for the current study is presented and their shortcomings that must be addressed to meet the tool requirements for the current study is presented.

2.1. Methalox Propellant

Methalox has been extensively studied in recent years as a propellant choice. Liquid methane (CH_4) has emerged as an excellent fuel choice for future missions to Mars, with the potential of being produced on Mars much more efficiently than other propellants, thus eliminating the need of carrying return fuel onboard for future Mars return missions, enabling lighter systems and potential lower costs [43]. Table 2.1 describes the properties of different propellants. Certain properties of methalox such as the boiling point proximity of Liquid Oxygen (LOX) and CH_4 is an advantage in terms of ground operations and storage commonality. Although, for other factors such as density, CH_4 has a higher density compared to Liquid Hydrogen (LH_2) and lower density compared to Kerosene (RP1). This implies that the tank size of CH_4 would be smaller compared to LH2, but larger compared to RP1. Furthermore, methalox has lower specific impulse than hydrolox, but higher specific impulse potential compared to kerolox, Figure 2.1. Again, indicating that to produce the same specific impulse, propellant mass for methalox based launchers would be somewhere between hydrolox and kerolox [30]. Apart from the impact of these properties on design, methalox has the advantage of lower soot production as a consequence of lower carbon content compared to kerolox Figure 2.2. This is advantageous, especially for reusable engine design, as cost savings can be achieved by lower refurbishment requirements.

Propellants	Mixture Ratio, O/F	I_{vac} sec
LOX/LH_2	6.00	460
LOX/CH_4	3.28	365
LOX/Kerosene	2.62	354
LOX/Ethanol	1.81	342
LOX/Ethylene	2.44	366
LOX/Propane	2.86	360
LOX/Propyne	2.05	370
H_2O_2/Kero	7.96	315
N_2O_4/MMH	2.4	336
N_2O_4/Kero	4.6	324
N_2O_4/Propane	5.0	328
N_2O/Propane	8.7	305

Figure 2.1: Performance wise ranking of different green propellants [8, 66]

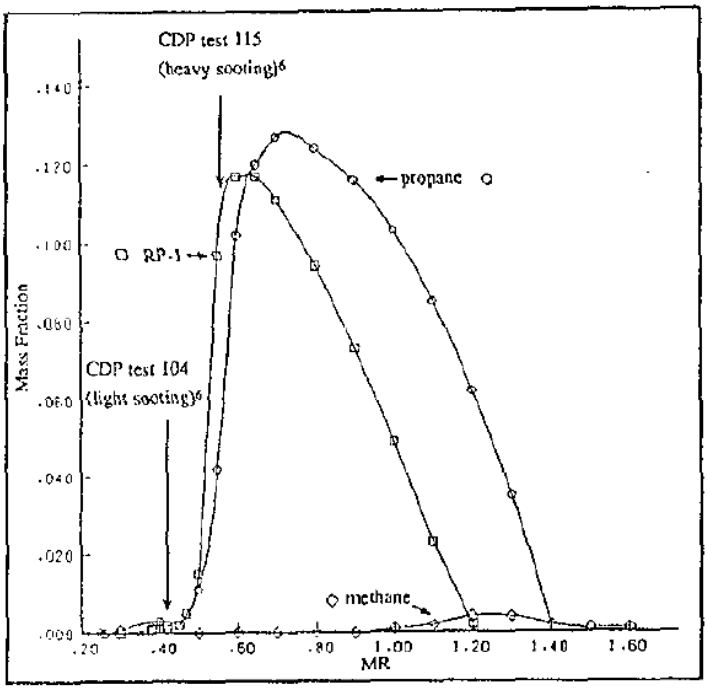

Figure 2.2: Mass fraction of soot formation for different hydrocarbon [45]

How these properties then play out in design process is studied in literature [10, 15]. Dresia et al. compare hydrolox, kerolox and methalox launchers with retro-propulsive recovery using grid fins and landing legs. Their work shows that for the same payload capability, hydrolox launchers have the lowest Gross Lift off Mass (GLOM), followed by methalox and then kerolox. In terms of inert mass, this trend is reversed, with kerolox having the lowest inert mass followed by methalox and then hydrolox, thus agreeing with what is predicted from their properties. How this reflects on cost however is lacking in literature and the extensive research into methalox for earth based missions must then be justified by a cost analysis. A cost analysis would better indicate how the varying mass characteristics of the different propellants reflect on costs and reflect on propellant comparison. Additionally, cost analysis results

can help in identifying the potential cost savings or additional costs that would be incurred by switching from hydrolox or kerolox to methalox.

Property	LH_2	RP1	CH_4	LOX
Normal Boiling Point (K)	20	420	112	90
Freezing Point (K)	14	224	91	54
Density at 16 degree Celsius (kg/m^3)	-	810	-	-
Density at Boiling point (kg/m^3)	71		425	1141
Critical Temperature (K)	33	662	190	154

Table 2.1: Propellant properties [73, 64, 17]

Burkhardt et al. compared methalox and kerolox propellant launcher design with winged recovery. Their analysis reveals a comparable design of the boosters, for similar payload capability, with methane fuelled booster having a slightly larger length and fuselage diameter compared to kerosene fuelled booster. This leads to the higher booster empty mass for methane fuelled booster by 10%. This in turn leads to increased wing mass and landing gear mass required for recovery, and thus leading to a larger overall GLOM for methalox launcher compared to kerolox. Comparing this with the work of Dresia et al. discussed above, shows that in case of retro-propulsion, the methalox booster is just 2% heavier than kerolox. One reason for the difference in inert mass difference can be attributed to the different recovery methods implemented in both the studies. This suggests that the type of recovery method can influence the launcher mass characteristics comparison and can therefore influence the cost comparison. Literature, however, lacks such comparison.

2.2. Recovery Hardware

As mentioned in the previous section, type of recovery can influence the mass characteristics of different launch vehicles. This section discusses the different recovery techniques identified from literature [30]. Only wingless recovery is considered in this study, as literature shows winged recovery hardware is significantly heavier than the grid fins or landing gear hardware required for retro-propulsive recovery [30]. This results in winged recovery system being inherently more expensive than wingless recovery [41].

Recovery of launch vehicle components requires additional hardware that enable reentry, deceleration, and landing. Recovery hardware is typically a combination of deceleration systems and landing systems. Deceleration systems can be classified as Non-Propulsive and Propulsive. Typical Non-propulsive deceleration methods are—subsonic/supersonic parachutes, Hypersonic Inflatable Aerodynamic Decelerator (HIAD), Grid Fins. Landing systems identified from literature are Landing legs, Airbags and Mid-Air Retrieval (MAR). In case of MAR, the recovered system is retrieved by a carrier aeroplane or helicopter. In case landing legs or Airbags are used as the landing system, the recovered launcher component must be retrieved by boat.

A detailed description of these recovery methods is presented below. The mass models and cost models of these recovery methods can be found in the work of Rozemeijer [55] and is not repeated here. These models are not improved upon, as sensitivity analysis performed by [55]

shows variation of recovery hardware mass, within its accuracy levels, shows minimum impact on the cost characteristic (under 0.2%), Appendix E. Furthermore, since the same models are implemented for the different launch vehicles designs, this variation would therefore be noticed across the different designs.

- Parachutes: Parachutes have been extensively used to decelerate the system by creating drag. Parachutes were used to recover the two Solid Rocket Boosters of the Space Shuttle Figure 2.3a and have been routinely used to recover crew capsules and provide safe soft landing or splashdown Figure 2.3b.

(a) Space Shuttle Solid Rocket Booster recovery [21]

(b) Dragon Capsule recovery [62]

Figure 2.3: Parachute based recovery

- Hypersonic Inflatable Aerodynamic Decelerator (HIAD): HIAD is an inflatable deceleration system that is currently being researched for entry into planets or moons with atmosphere. HIAD is a lightweight aeroshell that is capable of generating lift and easier to pack within the launch vehicle Figure 2.4.

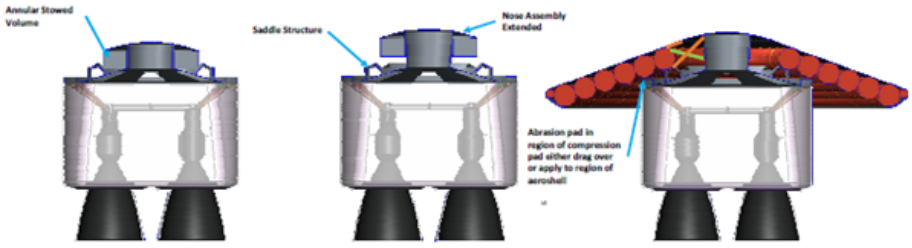

Figure 2.4: HIAD stowed and deployed configuration for Vulcain rocket engine [53]

- Grid fins: Grid fins are deployable structures that are similar to inflatable deceleration system with the main difference being that these structures are rigid unlike inflatables that can change its shape. Grid fins are employed on the SpaceX Falcon 9 first to decelerate and provide precision controlled landing Figure 2.5.

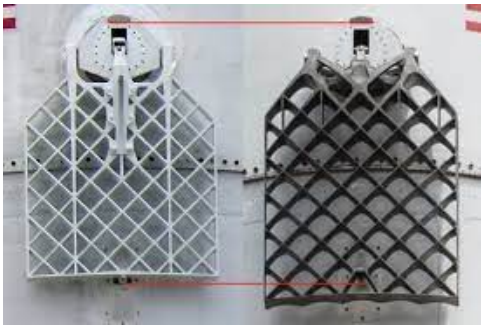

Figure 2.5: Grid fins on Falcon 9 [59]

- Retro-propulsion: Retro-propulsion is the method of decelerating the system using the main engine. The advantage of retro-propulsion is that it does not require any additional hardware. However, the launch vehicle must carry on-board extra propellant for deceleration. Retro-propulsion has been used by SpaceX to decelerate the first stage of the Falcon 9, Figure 2.6.

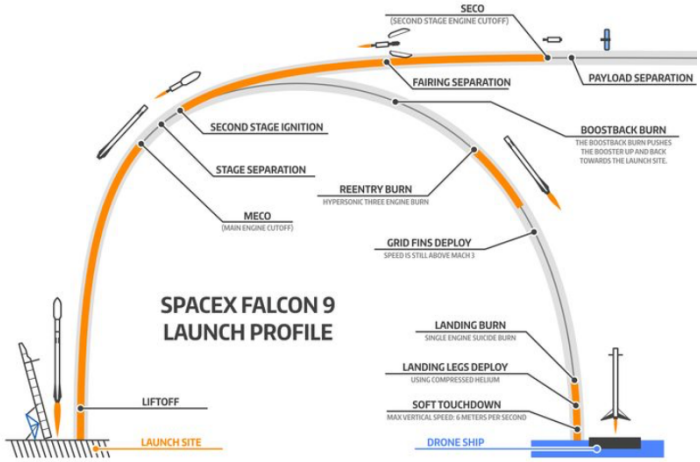

Figure 2.6: Retro-propulsion employed by SpaceX

A typical Mid-Air Retrieval sequence is shown in Figure 2.7. MAR uses an aeroplane or helicopter to catch the reusable launcher component, which is typically initially decelerated using a parachute system, and return it to land. This recovery method is currently under testing by RocketLab. The other method of landing is by using landing legs, which are stowed to the launcher sidewall during ascent and deployed during the landing phase. The landing legs are suited when the reusable component lands either on a drone ship or the launch site. This option is currently used to land the first stage of the Falcon 9 rocket. The final landing option is Airbags, which when deployed create a cushion to absorb the forces.

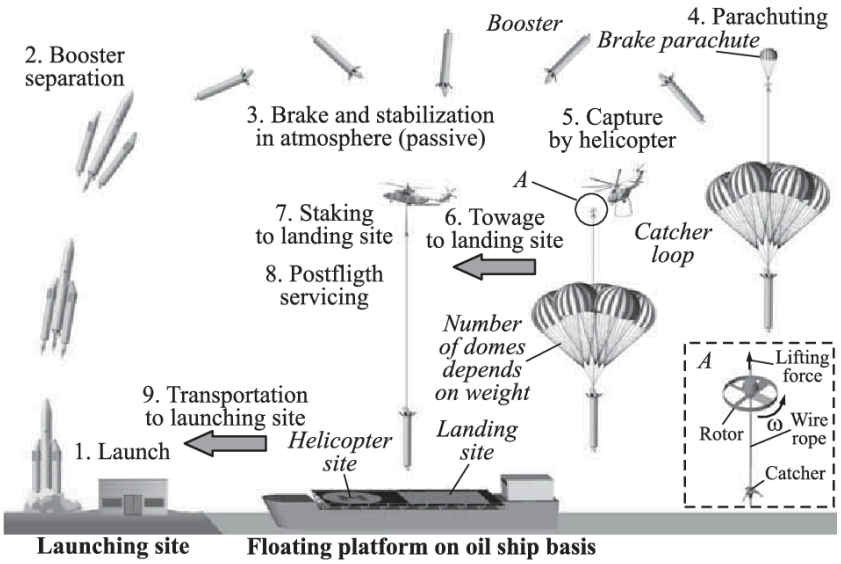

Figure 2.7: Typical MAR Sequence [2]

Different combinations of the above recovery hardware make up the non-propulsive and propulsive recovery method. To analyse the design and cost of a launcher powered by different propellants and recovery hardware, a dedicated tool is required. The tools identified in literature and their comparison in terms of suitability for current study is presented in the following section.

2.3. Tool Comparison and Requirement

To answer the research questions described in Chapter 1, a tool is required. A set of requirements that this tool must meet were established during the literature study [30] and presented listed below:

- REQ-FUNC-001: The tool shall be able to design launch vehicles.
- REQ-FUNC-002: The tool shall be able to incorporate reusability.
- REQ-FUNC-003: The tool shall be able to model Methalox launcher system.
- REQ-FUNC-004: The tool shall include recovery method models for Propulsive and Non-Propulsive ballistic methods.
- REQ-FUNC-005: The tool shall be able to simulate missions to Low Earth Orbit and Geostationary Transfer Orbit.
- REQ-FUNC-006: The tool shall include costing models for both expendable and reusable configuration.
- REQ-FUNC-007: The tool shall be able to output the Expendable launcher Geometry, mass, and cost parameters for comparative analysis.
- REQ-FUNC-008: The tool shall be able to output the Reusable launcher Geometry, mass, and cost parameters for comparative analysis.
- REQ-FUNC-009: The tool shall be able to output optimal ascent and descent trajectory parameters.

During literature study, two potential tools that could be implemented for this study were identified—First Stage Recovery tool (FRT) developed by Rozemeijer [55] and the tool developed by Contant [12]. A brief description of these tools are presented below. It is important to highlight that other tools were identified in the literature study. However, because of lack of data in regard to the tool models and methodology, and the tools not being readily available or open-source, these were not considered further.

2.3.1. Tool developed by Contant

This tool was developed by Contant [12], to perform a cost analysis of small reusable launch vehicles with retro-propulsion as recovery method. The tool is capable of designing a launch vehicle using Multidisciplinary Design Analysis approach followed by implementing a Multidisciplinary Design Optimization (MDO) method to optimize for price per flight. The launch vehicle design consists of the propulsion, geometry and mass models. The recovery method considered for the study is retro-propulsion, with both Return to Launch Site (RTLS) and Downrange Landing (DRL) options considered. The cost model considered was a combination of the TRANSCOST Model and the cost model developed by Drenthe [14]. This is because the TRANSCOST model alone shows high inaccuracy in estimating costs of launchers with payload less than 700 kg. The cost model is further modified to include reusability costs – recovery and refurbishment costs. These models are then incorporated in the MDAO tool. The environment used in this thesis is TuDat tool.

Figure 2.8 shows the overall architecture of the tool developed by Contant. Four different cases for objective function fitness are considered—vehicle design infeasible, vehicle feasible but violates trajectory constraint, vehicle feasible and does not violate trajectory constraint but fails to reach target orbit and vehicle feasible and reaches target orbit. Each of these cases has a different fitness function for the optimization. Depending on the case, the fitness function is selected. First, the launch vehicle design and optimization block is performed, where the design parameters that construct the launch vehicle are selected at random and then fed to the optimization algorithm. If the launcher does not violate the launcher design constraints, it is passed on to the cost modelling followed by trajectory simulation.

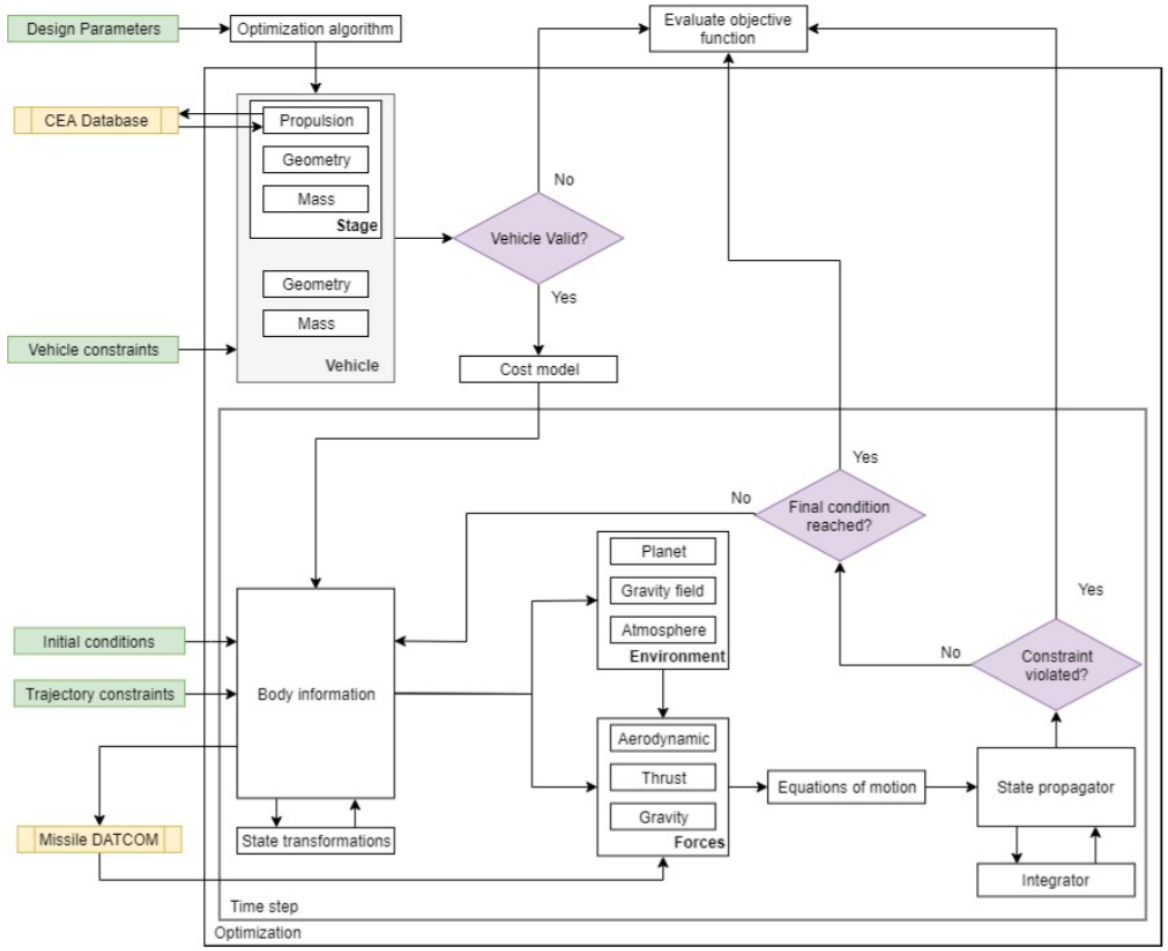

Figure 2.8: Contant Tool Architecture [12]

2.3.2. First Stage Recovery Tool (FRT)

The tool was developed to analyse the best recovery method in terms of cost per kg for a medium/heavy lift reusable launch vehicle. Unlike Contant, Rozermeijer analysed current launch vehicles for this study and modified them in order to incorporate reusability. Therefore, FRT required launcher mass and geometry data as user input. Furthermore, different recovery methods were considered and analysis was not restricted to retro-propulsion only. However, RTLS option was not researched in this study, as previous analysis reveals a payload loss as high as 40-65% [65]. As mentioned, the tool was developed to analyse the medium/heavy lift launch vehicles and thus, the cost model employed – TRANSCOST model – required no changes unlike in the previous tool, as the TRANSCOST model is fairly accurate for cost analysis of launchers with payload greater than 700 kg. The tool was designed in the MATLAB environment.

Figure 2.9 shows the tool architecture. The objective function is similar to that of Contant - minimize cost per flight. However, in this case, the launcher mass and geometry characteristics are input to the tool rather than designed within the tool. Therefore, the FRT inherently assumes that the input launcher is a feasible launcher design, therefore discarding one of the cases considered by Contant - to check for launcher feasibility. Next, the launcher design is

checked for whether it can reach orbit, similar to the third case of Contant. Once this check is performed, the main optimization loop, which the trajectory optimization is performed, where the input launcher is resized to include cost optimum recovery hardware. This is the loop where the second and fourth case of Contant is performed. Apart from launcher design feasibility, FRT can perform the other cases of Contant. Therefore, the two tools serve the same purpose, but are implemented differently.

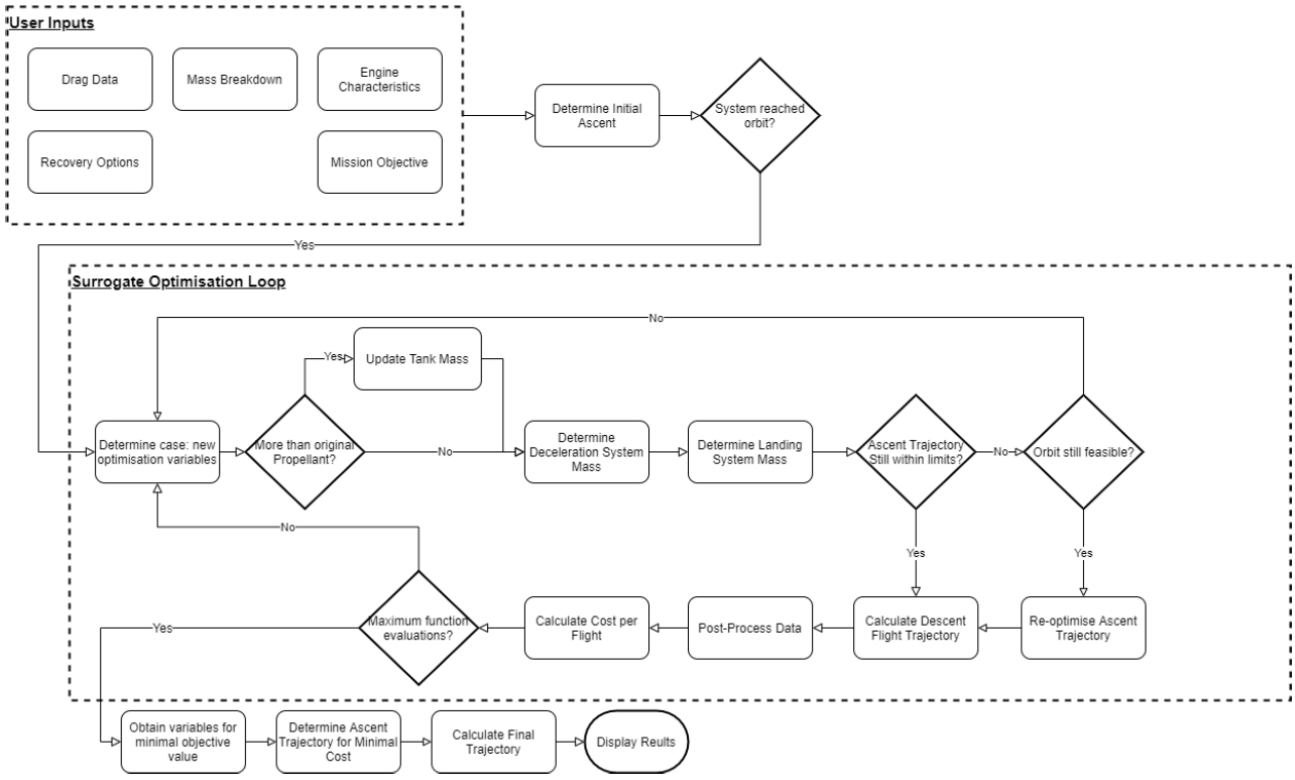

Figure 2.9: First Stage Recovery Tool Architecture [55]

2.3.3. Comparison of tools

Both, the tool developed by Contant and FRT, have been verified and validated. An overview of the accuracy of the models implemented within the tool is presented in Appendix E. The tool architectures can be seen in Figure 2.8 and Figure 2.9. The main difference in the two tools is that for the tool of Contant there exists a module to design the launcher, using a combination of MDA and MDO. This module is not present in the work of Rozemeijer, where it has been replaced by a user input module, implying the launcher data must be entered by the user and this launcher design is feasible. Furthermore, the FRT tool allows the user to select different recovery methods, however no such option is present in the work of Contant, where only retro-propulsive recovery is possible. The tool of Contant was developed in TuDat environment and the FRT developed using existing ParSim tool. The different tools does not vary the trajectory design, as the fundamental trajectory models in both the tools are similar [55]. Furthermore, the trajectory optimization control law is the same in both the works and is based on the work of Van Kesteren [67]. The tool methodology therefore is fairly similar and the differences in the tool is more to do with the tool capabilities. Therefore, the requirements of the tool required for the current study are then compared with the capabilities of these two tools.

ID	Requirement	Contant	FRT
REQ-FUNC-001	The tool shall be able to design launch vehicles.	✓	
REQ-FUNC-002	The tool shall be able to incorporate reusability.	✓	✓
REQ-FUNC-003	The tool shall be able to model Methalox launcher system.		
REQ-FUNC-004	The tool shall include recovery method models for Propulsive and Non-Propulsive ballistic methods.		✓
REQ-FUNC-005	The tool shall be able to simulate missions to Low Earth Orbit and Geostationary Transfer Orbit.	✓	✓
REQ-FUNC-006	The tool shall include costing models for both expendable and reusable configuration.		✓
REQ-FUNC-007	The tool shall be able to output the Expendable launcher Geometry, mass, and cost parameters for comparative analysis.		Partial
REQ-FUNC-008	The tool shall be able to output the Reusable launcher Geometry, mass, and cost parameters for comparative analysis.	✓	✓
REQ-FUNC-009	The tool shall be able to output optimal ascent and descent trajectory parameters.	✓	✓

Table 2.2: Comparison of existing tool capabilities with requirements of tool required for current study

From Table 2.2, it can be seen that both the tools can be implemented for the current study with some addition—extend capability of Contant's tool to include non-propulsive recovery or extend capability of FRT to include design module. It was decided to extend the FRT tool rather than Contant's tool. This extension can be modular and thus not affect the tool architecture. Furthermore, whether Contant's tool can design medium/heavy lift launchers is unclear. Also, incorporating non-propulsive recovery method mass relations can affect Contant's tool architecture significantly and is left as a potential recommendation for further studies.

2.4. Launch Vehicle Design and Optimization

For this current study, it was decided to extend the existing First Stage Recovery Tool to include a design module capable of designing a launcher from scratch. Launch Vehicle design process consists of several subsystems, each interacting with one another. Each of these subsystems are coupled, and the design choices of one subsystem influences the other. The Multidisciplinary Design Analysis and Optimization(MDAO) approach is a widespread approach in literature [3, 11, 12, 67, 68]. The reason for this being the ability of this approach to satisfy the coupling between different subsystems (MDA) and concurrently varying the design variable simultaneously to reach a global optimum (MDO) [12]. Therefore, this methodology is considered for

the current study as well. A typical Launch vehicle design process is shown in Figure 2.10. The dotted lines depict the coupling of the subsystems. The launcher subsystem design models (MDA) and optimization process (MDO) is described in detail in Chapter 3 and Chapter 4.

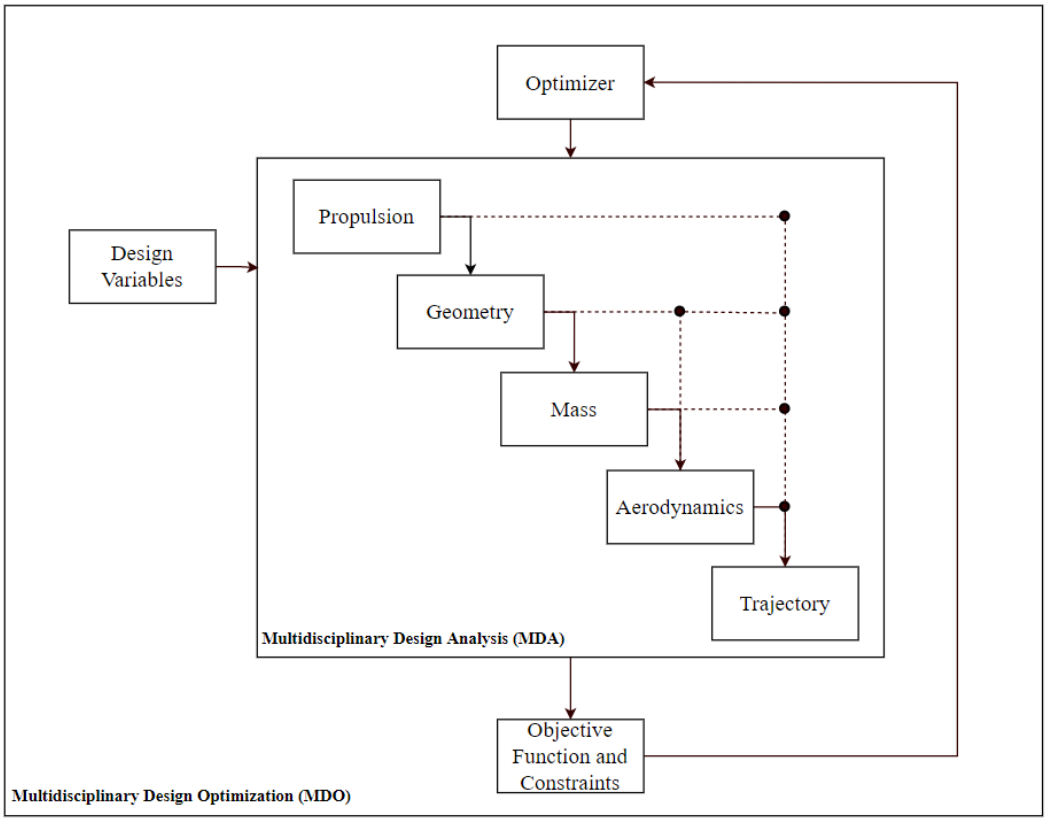

Figure 2.10: Typical Launch Vehicle Design Process

Literature shows 10% accuracy in launcher modelling is necessary to place a level of confidence in the design solutions [11]. This 10% accuracy baseline has been seen in the work of Vandamme, Van Kesteren and Contant [68, 67, 12]. The reason for 10%, although not explicitly stated in these works, can be attributed to the sensitivity analysis performed in these works that show even a 10% variation in certain parameters has minimal impact on the optimal model results. Therefore, for the current study, 10% accuracy level is set as a baseline and is subject to sensitivity analysis in Chapter 6 to determine whether 10% accuracy is good enough. The design models implemented by Contant can achieve this accuracy level and are thus implemented in this study as well [12]. Table 2.3 shows the accuracy levels of different models implemented by Contant. Certain models partially meet the requirements and are therefore looked at in detail in Chapter 3, especially engine mass and length estimation relations. Engine mass and length estimation relations are propellant specific, and exists in literature for hydrolox and kerolox. For methalox engines, typical practice in literature is to use kerolox relations itself. However, whether this approach is correct is unclear and is also looked at in detail in Chapter 3.

ID	Requirement	Source	Status
REQ-PER-001	The design module shall be able to model the liquid stage thrust within 10% accuracy.	[67, 68]	✓
REQ-PER-002	The design module shall be able to model the liquid stage Specific Impulse within 10% accuracy.	[67, 68]	✓
REQ-PER-003	The design module shall be able to model the Engine Length within 10% accuracy.	[67, 68]	Partial
REQ-PER-004	The design module shall be able to model the Engine Mass within 10% accuracy.	[67, 68]	Partial
REQ-PER-005	The design module shall be able to model the Launch Vehicle Inert Mass within 10% accuracy.	[67, 68]	Partial
REQ-PER-006	The design module shall be able to model the Launch Vehicle stage length within 10% accuracy.	[67, 68]	Partial
REQ-PER-006	The design module shall be able to model the Launch Vehicle Gross Lift-Off Mass within 10% accuracy.	[67, 68]	✓

Table 2.3: List of Performance Requirements for the designed tool

2.4.1. Optimization Algorithm

Typical optimization algorithms identified in literature are gradient-based algorithms or heuristic algorithms [4]. The gradient algorithm is based on differentiating the objective function and constraints to determine the optimum solution. Therefore, this algorithm requires smooth, differentiable objective and constraint functions. Typical gradient based algorithms are Newton's Method, Sequential Quadratic Programming (SQP), Steepest Descent. Heuristic algorithms on the other hand are stochastic method, that are suitable for non-differentiable functions as well. Typical heuristic algorithms are Genetic Algorithm (GA), Simulated Annealing (SA), Particle Swarm Optimization (PSO), Differential Evolution (DE). A brief description of these algorithms is presented below:

- **Genetic Algorithm (GA)**: This optimization algorithm is an evolutionary process that is based on the concept of survival of the fittest. The algorithm first generates an initial population of the design variables (chromosomes). Each population is then evaluated through multiple different combinations (generations) and the best design variables (chromosomes) from each generation is retained until convergence [12].
- **Differential Evolution (DE)**: This optimization is similar to GA, however uses actual real numbers rather than the binary formulation used in GA. DE also works by iteratively improving candidate solutions by having populations of potential solutions (agents) that move around the search space [12].
- **Particle Swarm Optimization (PSO)**: The optimization works on the basis of a popula-

tion (swarm) of candidate solutions (particles). These particles move around the search space, replicating a flock of birds [68]. The particle movement is determined by both their own best known position and the swarm's best known position in the search space.

- **Simulated Annealing (SA)**: It is a stochastic method to determine global optimum, especially for search space that are discrete. The optimization process changes one variable at a time to determine impact on solution [12].

Launcher design is complex, with non-linear formulation. Therefore, heuristic optimization algorithms are preferred. Typically, Genetic Algorithm is implemented in launcher design optimization [5, 12, 42, 31] and Particle Swarm algorithm is implemented in trajectory optimization [55, 1]. The no free lunch theorem states, "any two optimization problem are equivalent when their performance is averaged across all possible problems", implying that there is no clear optimum optimization algorithms for a given problem. This is confirmed in the work of Rozemeijer, where results of optimization with GA were compared to that with PSO. The results showed negligible difference in values, but relatively significant difference in computation time—with GA trajectory optimization taking significantly longer compared to PSO. Therefore, for the trajectory optimization, no changes in algorithm are made. For launch vehicle design process, which is a constrained non-linear design process, work by Rafique et al. [52] shows that although PSO is computationally efficient, the quality and robustness of results obtained by GA outperforms that of PSO and SA. Therefore, for the MDO process in the design module extension to FRT, Genetic Algorithm is selected.

3

Launch Vehicle Design Models

As described in Chapter 2, launch vehicle design is multidisciplinary and coupled. Typical launch vehicle design process is a Multidisciplinary Design Analysis and Optimization (MDAO) process. This chapter describes in detail the modelling assumptions and equations implemented for the current study, which make up the MDA part of the launcher design process. Most models are implemented from the work of Contant and Castellini [12, 11] as these have been verified and validated. In addition to these models, relations for methalox propellant are detailed in this section. Furthermore, a Verification and Validation is performed to determine the accuracy and validity of the results that can be achieved with these models.

3.1. Propulsion Model

Modelling a launch vehicle starts with modelling the launcher propulsion system. This is because most geometry and mass models depend on propulsion parameters such as Specific Impulse (I_{sp}) and thrust (F_T). This is also noticed in literature, as most design analysis and optimization considers propulsion system parameters as the optimization design variables [12, 15, 3, 68].

Propulsion system modelling begins with the estimation of the launch vehicle performance parameters using the Ideal Rocket Theory (IRT) [73]. For any design analysis and optimization problem, the design variables must be selected such that they represent the overall system and significantly impact both the objective and constraints [32]. The design variables considered for the current study are listed in Table 3.1.

Description [units]	**Symbol**
Chamber Pressure [bar]	P_c
Exit Pressure [bar]	P_e
Mass Mixture Ratio [-]	OF
Engine Exit Diameter [m]	D_e
Stage Diameter [m]	D_s
Burn Time [s]	t_b
Number of Engines [-]	N_{eng}

Table 3.1: Design Parameters for launch vehicle modelling

This section presents a description of the CEA relations to determine the complex combustion parameters, implemented in the current study. This is followed by a description of the Ideal Rocket Theory relations and a discussion on the correction factors implemented is presented.

3.1.1. CEA Relations

For a given propellant choice, chamber pressure and mixture ratio, important properties such as the specific heat ratio, γ and the combustion chamber temperature, T_c and combustion gas mean molar mass, M, are typically calculated using existing tools such as NASA Chemical Equilibrium with Applications (CEA) tool. This approach is considered in the work of Contant, as the TuDat environment has the ability to access CEA program. However, implementation of the existing CEA in conjunction with launcher modelling in MATLAB resulted in a time-consuming launcher design process. For this reason, in the current study, approximate interpolation relations are derived based on chemical equilibrium assumption CEA results for different propellant combinations, for a range of chamber pressures and mixture ratio [18]. These interpolation equations are described below. Linear interpolation relations are considered as the mixture ratio considered is in the optimum range [6] and are therefore propellant specific. These relations are subject to verification and validation performed in Section 3.4.

Specific heat ratio equations

The interpolation equation for specific heat ratio is given by Equation 3.1, where a and b are calculated as presented in Table 3.2 for different propellant combinations.

$$\gamma = a + (b - a) \times \left(\frac{200 - P_c}{200 - 30} \right) \tag{3.1}$$

Propellant	a	b
LOX/LH_2	$a = 1.1506 - 0.016 \times \frac{OF-5}{6-5}$	$b = 1.1667 - 0.0194 \times \frac{OF-5}{6-5}$
LOX/RP1	$a = 1.1666 - 0.0389 \times \frac{OF-2}{3-2}$	$b = 1.1869 - 0.0506 \times \frac{OF-2}{3-2}$
LOX/CH_4	$a = 1.2527 - 0.1254 \times \frac{OF-1.35}{3.35-1.35}$	$b = 1.2290 - 0.0922 \times \frac{OF-1.35}{3.35-1.35}$

Table 3.2: Interpolation equation for specific heat ratio calculation

Combustion chamber temperature equations

The interpolation equation for combustion chamber temperature is given by Equation 3.2, where a and b are calculated as presented in Table 3.3 for different propellant combinations.

$$T_{cc} = a + (b - a) \times \left(\frac{200 - P_c}{200 - 30} \right) \tag{3.2}$$

Propellant	a	b
LOX/LH_2	$a = 3218.3 + 170.76 \times \frac{OF-5}{6-5}$	$b = 3352.33 + 243.1 \times \frac{OF-5}{6-5}$
LOX/RP1	$a = 3274.74 + 297.62 \times \frac{OF-2}{3-2}$	$b = 3402.37 + 464.87 \times \frac{OF-2}{3-2}$
LOX/CH_4	$a = 1401.87 + 2033.23 \times \frac{OF-1.35}{3.35-1.35}$	$b = 1546.98 + 2134.66 \times \frac{OF-1.35}{3.35-1.35}$

Table 3.3: Interpolation equation for combustion chamber temperature calculation

Gas mean molar mass equations

The interpolation equation for Gas Mean Molar Mass is given by Equation 3.3, where a and b are calculated as presented in Table 3.4 for different propellant combinations.

$$M = a + (b - a) \times \left(\frac{200 - P_c}{200 - 30} \right) \tag{3.3}$$

Propellant	a	b
LOX/LH_2	$a = 11.744 + 1.589 \times \frac{OF-5}{6-5}$	$b = 11.899 + 1.711 \times \frac{OF-5}{6-5}$
LOX/RP1	$a = 20.716 + 3.706 \times \frac{OF-2}{3-2}$	$b = 20.955 + 4.158 \times \frac{OF-2}{3-2}$
LOX/CH_4	$a = 12.756 + 8.546 \times \frac{OF-1.35}{3.35-1.35}$	$b = 13.371 + 8.45 \times \frac{OF-1.35}{3.35-1.35}$

Table 3.4: Interpolation equation for gas mean molar mass calculation

The supported range of pressure and mixture ratio for the estimated relations is shown in Table 3.5.

Propellant	$P_{c,min}$ [bar]	$P_{c,max}$ [bar]	OF_{min}	OF_{max}
Hydrolox	30	200	5	6
Kerolox	30	200	2	3
Methalox	30	200	1.35	3.35

Table 3.5: CEA relations supported range of pressure and mixture ratio

3.1.2. Ideal Rocket Relations

Once the important combustion properties are determined, the Vandenkerckhove function, Γ, is calculated from Equation 3.4.

$$\Gamma = \sqrt{\gamma}. \left(\frac{2}{\gamma + 1} \right)^{\frac{\gamma+1}{2(\gamma-1)}} \tag{3.4}$$

Next, the expansion ratio, ϵ, is calculated from Equation 3.5. For a given exit diameter, the throat area can be calculated using Equation 3.5.

$$\epsilon = \frac{A_e}{A_t} = \frac{\Gamma}{\sqrt{\frac{2\gamma}{\gamma-1}. \left(\frac{P_e}{P_c} \right)^{\frac{2}{\gamma}} . \left(1 - \left(\frac{P_e}{P_c} \right)^{\frac{\gamma-1}{\gamma}} \right)}} \tag{3.5}$$

The mass flow rate is calculated as shown in Equation 3.6, where R is the specific gas constant, calculated from the gas mean molar mass and the Universal Gas constant, R_A (8314 $J.K^{-}1.mol^{-}1$) Equation 3.7.

$$\dot{m} = \frac{P_c.A_t.\Gamma}{\sqrt{R.T_c}} \tag{3.6}$$

$$R = \frac{R_A}{M} \tag{3.7}$$

The characteristic velocity c* and the thrust coefficient C_F are calculated from Equation 3.8 and Equation 3.9.

$$c^* = \frac{1}{\Gamma}\sqrt{R.T_c} \tag{3.8}$$

$$C_F = \Gamma\sqrt{\frac{2\gamma}{\gamma-1}\left(1-\left(\frac{P_e}{P_c}\right)^{\frac{\gamma-1}{\gamma}}\right)} + \left(\frac{P_e}{P_c}-\frac{P_a}{P_c}\right).\frac{A_e}{A_t} \tag{3.9}$$

The exhaust velocity is then calculated using Equation 3.10.

$$V_e = c^*.C_F \tag{3.10}$$

The specific impulse and thrust can now be calculated using Equation 3.11 and Equation 3.12. It is important to note that the influence of pressure difference on thrust is already considered while calculating the Thrust coefficient Equation 3.9.

$$I_{sp} = \frac{V_e}{g_0} \tag{3.11}$$

$$F_T = \dot{m}.I_{sp}.g_0 \tag{3.12}$$

The specific impulse and thrust equations described above estimate the ideal performances that can be achieved. However, in reality, there are losses that must be accounted for. These losses are typically accounted for by taking into account appropriate correction factors. Therefore, the corrected thrust is calculated using Equation 3.13, ξ_s is the specific impulse correction factor and C_d is the discharge coefficient.

$$F_T = \xi_s.C_d\left(\dot{m}.I_{sp}.g_0\right) \tag{3.13}$$

3.1.3. Correction Factors

Literature suggests a range of valid correction factors for specific impulse, ξ_s [29]. Contant considers this factor to be 0.92, whereas Rozemeijer considers it 0.97 and the work of Ernst considers 0.9 [12, 55, 18]. For discharge coefficient, Contant considers this factor to be 1, whereas Rozemeijer considers it to be 0.94. No reasoning for selection of respective correction factors was provided, as implementation any of these corrections factor would comply with the tool performance requirements Table 2.3. Therefore, it was decided to derive correction factors from engine data available in literature. It is important to note that the derived correction factor depends on the quality of data collected. For this reason, in addition to the reason that no single value could be identified from literature, these correction factors are subject to a sensitivity analysis in Chapter 6.

Engine	**Actual I_{sp}[s]**	**IRT I_{sp} [s]**	**Correction Factor**
RS-68 A	411	443	0.93
Rocketdyne H-1	289	315	0.92
Merlin 1A	300	330	0.91
Merlin 1C	304	330	0.92
Merlin 1D	311	332	0.94
RD-108	315	336	0.94
RD-171	337	346	0.97
Vulcain 2	434	465	0.93
Vulcain 1	431	467	0.92
RD-180	339	346	0.98
Rocketdyne F1	304	332	0.92
NK-33	331	343	0.97
RS-27	295	315	0.94
Rocketdyne J-2	421	454	0.93
RD-120	350	366	0.96
HM7B	445	482	0.92
RL10A-4-2	451	479	0.94
Merlin 1D Vacuum	347	371	0.94
RL-10B-2	462	498	0.93
RD-0109	323	359	0.90
		Average	**0.93**

Table 3.6: Specific Impulse Correction Factor Derivation [17, 56, 19]

Table 3.6 shows that the IRT overestimates the specific impulse. This trend is visible across the different engines. For specific impulse, a correction factor of 0.93 is considered.

Engine	Actual $\dot{m}$ [kg/s]	IRT $\dot{m}$ [kg/s]	Correction Factor
RS-68 A	776	958	1.2
Rocketdyne H-1	244	147	0.3
Merlin 1D	236	226	0.9
RD-108	76	53	0.6
Vulcain 2	327	285	0.9
Vulcain 1	236	230	0.9
Rocketdyne F1	2578	2632	1.0
NK-33	518	542	1.0
RS-27	361	308	0.8
Rocketdyne J-2	241	282	1.1
RD-120	243	258	1.1
HM7B	15	14	0.9
RL10A-4-2	16	22	1.3
Merlin 1D Vacuum	237	218	0.9
RL-10B-2	24	27	1.1
RD-0109	17	15	0.8
		Average	**0.95**

Table 3.7: Mass Flow Rate Correction Factor Derivation [17, 56, 19]

Unlike in the case of specific impulse, for mass flow rate, compared to value from literature, no particular trend is noticed in the value of IRT. In particular, for the case of Rocketdyne H-1 and RD-108, the mass flow rate estimated by IRT is fairly poor. However, no particular reason could be singled out for the poor estimation of mass flow rate by IRT for the cases of Rocketdyne H-1 and RD-108 engine. One reason could be attributed to the ambiguity around the engine conditions for the mass flow rate values from literature. Not considering the Rocketdyne H-1 and RD-108 engines, results in a discharge coefficient of 0.97. Therefore, for the current set of engine data, on average the IRT overestimates the mass flow rate, which explains the discharge coefficient less than 1. A comparison between the discharge coefficient considered in the current study and in that of Contant is presented in Appendix B.

Table 3.8 shows the correction factor therefore implemented in this study. Although, the models implemented have already been validated by Contant, validation of the propulsion model is performed again in Section 3.4 to check whether these new correction factors influence the performance requirement defined in Table 2.3. Furthermore, as mentioned previously, deriving correction factor depend on the quality of data as seen in the ambiguity around discharge coefficient, this correction factors are therefore subject to a sensitivity analysis in Chapter 6.

Parameter	Correction Factor
Mass Flow Rate	0.95
Vacuum Specific Impulse	0.93

Table 3.8: Propulsion Correction Factors

3.2. Geometry and Mass Model

This section presents the geometry and mass relations. Since there is lack of literature with respect to Methane based engine relations, a particular attention to the accuracy levels of these relations for Methane engine is presented. The geometry and mass models for liquid rocket stages are given as Equation 3.14 and Equation 3.15.

$$L_{stage} = L_{interstage} + L_{tanks} \tag{3.14}$$

$$M_{stage} = M_{propsys} + M_{interstage} + M_{avionics} + M_{EPS} \tag{3.15}$$

$$M_{propsys} = M_{prop} + M_{engine} + M_{tanks} + M_{TPS} + M_{intertank} \tag{3.16}$$

3.2.1. Geometry Models

The engine length estimation relations are implemented from literature [74] and are shown in Equation 3.17. ξ_{len} is the minor factor introduced to differentiate kerolox and methalox based engines. Methalox based engine relations are lacking in literature, and typical practice is to use the same relations as that of kerolox. Table 3.9 shows that kerolox relations underestimate methalox engine length. Incorporating a correction factor lowers the absolute error of methalox engine estimate from 23% to 19%. These errors can be further reduced by analysing more methalox based engines, however data in regard to methalox engine is lacking in literature. Since this approach is different from that in literature, ξ_{len} is subject to a sensitivity analysis in Chapter 6. The engine length for different propellants is calculated by Equation 3.17. It is important to note these relations are applicable for non-extendable nozzles. The thrust levels these equations are valid within are shown in Table 3.10. For methalox engine the upper limit of validity range is 2 MN, as that is the range for the engines considered in Table 3.9.

Engine	**Actual L_{engine} [m]**	**Estimated L_{engine} [m]**	**Correction Factor**	**Corrected L_{engine}[m]**
RD-161-1	1.7	1.3	1.3	1.5
RD-182	2.8	3.1	0.9	3.6
RD-185	3.3	2.1	1.54	2.5
TQ-12	3.9	3.0	1.1	3.5
		Average	**1.2**	

Table 3.9: Methane Engine Length Correction Factor [17, 70]

$$L_{engine} = \begin{cases} 0.1667\mathrm{F}_T^{0.2238}, & \text{if LOX/LH}_2 \\ 0.1362\mathrm{F}_T^{0.2279}, & \text{if LOX/RP1} \\ \xi_{len}.\ (0.1362F_T^{0.2279}), & \text{if LOX/CH}_4 \end{cases} \tag{3.17}$$

Propellant	Validity Range
LOX/LH_2	50 kN to 3.5 MN
LOX/RP1	20 kN to 8.0 MN
LOX/CH_4	20 kN to 2.0 MN

Table 3.10: Validity Range for Engine length estimation relations [74]

The propellant tanks are considered as a cylindrical tank with spherical cap ends as shown in Figure 3.1. The grey area accounts for the empty volume, as shown in the work of Vandamme [68]. The tank diameters are assumed to be the same as the stage diameter. The total tank length is calculated using Equation 3.18, where V_{ullage} is set to 10% of the total tank volume [11]. Sensitivity analysis of this parameter was performed by Contant and a variation of 10% showed minimal impact on cost parameter [12]. The oxidizer and fuel mass is calculated from the total propellant mass and the propellant mixture ratios.

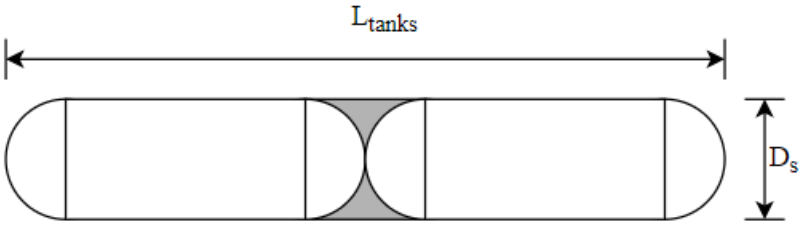

Figure 3.1: Propellant Storage Tank Configuration

$$L_{tanks} = \left(\frac{M_{ox}}{\rho_{ox}} + \frac{M_f}{\rho_f} + \frac{\pi D_s^3}{6} \right) .(1 + V_{ullage}).\frac{4}{\pi D_s^2} \tag{3.18}$$

Other components of the launch vehicle such as the interstage and fairing lengths are calculated using Equation 3.19 and Equation 3.20. For the liquid first stage, the interstage length is given by the engine length plus a factor of $0.2D_s$, validated by Castellini [11]. The upper stage interstage is the Vehicle Equipment Bay (VEB), given by the length of engine plus $0.287D_s$ [11]. The payload fairing length is derived by Contant from existing launch vehicles as a function of Payload diameter [12].

$$L_{interstage} = \begin{cases} L_{engine}+0.2D_s & \text{if liquid stage} \\ L_{engine}+0.287D_s & \text{if liquid upper stage} \end{cases} \tag{3.19}$$

$$L_{fairing} = 1.1035 D_s^{1.6385} + 2.3707 \tag{3.20}$$

3.2.2. Mass Models

The propellant mass is calculated from the propulsion system performance parameters Equation 3.21. K_u is a percentage of unused propellant, typically found in the valves, pipes or wetting the tank walls. For the current study, this value is set to 0.32% [12, 55]. Sensitivity analysis of this parameter was performed by Contant and a variation of 50% showed minimal impact on cost parameter [12].

$$M_{prop} = (\dot{m}.t_b) \,.\, (1 + K_u) \tag{3.21}$$

The mass of the engine is calculated using Equation 3.22. The relation includes the thrust chamber assembly, propellant feed systems, turbo-pumps and other miscellaneous parts such as the gas generators or pre-burners, manifolds and the electrical, control and instrumentation systems [74]. Similar to the case of engine length estimation, a parameter, ξ_{mass}, is introduced to account for minor differences between kerolox and methalox engines. Like in the case of engine length estimation, Table 3.11 shows that kerolox relations for most cases underestimates methalox engine mass. Incorporating a correction factor lowers the absolute error of methalox engine mass estimation from 30% to 26%. This parameter is also subject to a sensitivity analysis in Chapter 6.

Engine	**Actual M_{engine}[kg]**	**Model M_{engine} [kg]**	**Correction Factor**	**Corrected M_{engine} [kg]**
RD-0120-CH	2370	1768	1.3	2303
RD-0120M-CH	2600	1927	1.4	2510
RD-0234-CH	390	516	0.8	-
RD-0256-Methane	770	951	0.8	672
RD-182	1500	1024	1.5	1334
RD-185	415	225	1.8	294
TQ-12	1222	911	1.41	1187
		Average	**1.3**	

Table 3.11: Methane Engine Mass Correction Factor [17, 70]

$$M_{engine} = \begin{cases} 1.866 \times 10^{-10}.F_T^2 + 0.00130F_T + 77.4, & \text{if LOX/LH}_2 \\ 1.104 \times 10^{-3}F_T + 27.702, & \text{if LOX/RP1} \\ \xi_{mass}(1.104{\times}10^{-3}F_T + 27.702), & \text{if LOX/CH}_4 \end{cases} \tag{3.22}$$

Propellant	**Validity Range**
LOX/LH_2	50 kN to 3.5 MN
LOX/RP1	20 kN to 8.0 MN
LOX/CH_4	20 kN to 2.0 MN

Table 3.12: Validity Range for Engine Mass estimation relations [74]

The mass of the propellant tank can be calculated from the propellant tank volume and tank material. The propellant tank thickness is calculated using Equation 3.23, where P_{tank} is the tank pressure, SF_t is the safety factor and σ_t is the tank material stress. For the current study, the tank pressure is set to 4 bar, which is in the typical range for pump-fed systems [24, 73].

$$t_{tank} = \frac{P_{tank} SF_t . D_s}{2\sigma_t} \tag{3.23}$$

Furthermore, cryogenic propellants require sufficient thermal protection (TPS) on these propellant tanks to ensure they are maintained at the cryogenic temperatures. The mass of thermal

protection required for LOX is given by Equation 3.24. Unlike RP1, which is a storable propellant, LH_2 and CH_4, which are cryogenic, propellant tanks require TPS, which add to the overall mass of the propellant storage system. Thermal protection system mass relations exist for LH_2, however for CH_4 no such equations are available. From literature, it can be deduced that one of the advantages of methalox systems is the proximity of the storage temperatures of the fuel and oxidizer, leading to potentially similar thermal management systems [44]. Therefore, for the current study the mass of the TPS system for methane based systems is assumed to be the same as that of the LOX system, Equation 3.25.

$$M_{ox,TPS} = 0.9765(\pi D_s L_{tank} + \pi D_s^2) \tag{3.24}$$

$$M_{f,TPS} = \begin{cases} 1.2695(\pi D_s L_{tank} + \pi D_s^2), & \text{if LOX/LH}_2 \\ 0, & \text{if LOX/RP1} \\ 0.9765(\pi D_s L_{tank} + \pi D_s^2), & \text{if LOX/CH}_4 \end{cases} \tag{3.25}$$

The mass of the inter-tank, which is the structure between the fuel and oxidizer tanks, is given by Equation 3.26. The total inert propellant storage mass is therefore the sum of the tank mass, thermal protection system mass and the inter-tank mass.

$$M_{intertank} = \begin{cases} 5.4015\pi D_s^2 (3.2808 D_s)^{0.5169}, & \text{if Stage 1} \\ 3.8664\pi D_s^2 (3.2808 D_s)^{0.6025}, & \text{otherwise} \end{cases} \tag{3.26}$$

Apart from the propulsion system, other launcher components that has a significant mass contribution are modelled. The payload fairing mass is estimated using Equation 3.27.

$$M_{fairing} = 49.3218(L_{fairing} D_s)^{0.9054} \tag{3.27}$$

The interstage mass differs for the first stage and the upper stages. The interstage mass is calculated using Equation 3.28, where k_{sm} is a factor that accounts for the type of fairing material, 1.0 for classical Al-alloy material, 0.7 for advanced composite structures [11] and S_{int} is the surface area of the interstage.

$$M_{interstage} = \begin{cases} k_{sm}.7.7165.S_{int}(3.3208 D_s)^{0.4856}, & \text{if Stage 1} \\ k_{sm}.5.5234.S_{int}(3.3208 D_s)^{0.5210}, & \text{if upper stage} \end{cases} \tag{3.28}$$

The mass of the payload adapter, for a given payload mass M_{pay}, is calculated using Equation 3.29.

$$M_{PLA} = 0.00477536 M_{pay}^{1.01317} \tag{3.29}$$

The avionics and power subsystem mass is calculated using Equation 3.30 and Equation 3.31.

$$M_{avionics} = 0.25.(246.76 + 1.3183.D_s.L_{vehicle}) \tag{3.30}$$

$$M_{EPS} = 0.3321.M_{avionics} \tag{3.31}$$

The mass of the pad interface that connects the first stage to the launch pad is estimated using Equation 3.32.

$$M_{pad} = \begin{cases} 25.736\pi\frac{D_s^2}{4}(3.2808D_s)^{0.5498}, & \text{if Stage 1} \\ 0, & \text{otherwise} \end{cases} \tag{3.32}$$

For a given propellant choice, material choice and design variables, a conceptual launcher can be modelled using the above equations. These models are verified and validated in the Section 3.4.

3.3. Aerodynamics Model

To model the launcher aerodynamics, external tool RASAero II is implemented. The RASAero II is a well known open source tool that calculates drag coefficient for a given launcher configuration. The drag model is based on the equation presented in Equation 3.33, where C_D is the drag coefficient, q is the dynamic pressure and S represents the wetted area.

$$F_D = C_D.q.S \tag{3.33}$$

The general drag model, treats the entire launcher as a lumped mass and the C_D varies only with the Mach Number for a given launcher design. However, from the design point of view and from Equation 3.33, it can be seen that C_D also depends on geometry, i.e, S. A slender launcher design is preferable from the point of view of lower drag, however from a structural point of view, a slender launcher may run into risks of failure to sustain launch loads. The current design module does not consider the aerodynamics modelling, as it is already included in the existing FRT tool. However, to ensure a realistic design is obtained, a design constraint is included in the design process, discussed in detail in Chapter 4. This method eliminates the need to incorporate high fidelity aerodynamics tools such as Missile DATCOM in the design process, leading to increased complexity and simulation time [71], while considering variation of drag coefficient with Mach, unlike literature that considers drag coefficient as constant [15]. The disadvantage of this method is that the designed launch vehicle, does not necessarily have optimum aerodynamic shape.

The RASAero II tool is already verified and validated in literature and therefore is not repeated in Section 3.4. A comparison of the Altitude prediction of RASAero II, showed an average error of 3.38% and 78% of the simulation cases have all parameters within 10% of the flight data. Other widely used drag prediction model is the Missile DATCOM. However, this model is not open source and is a high fidelity tool, which as mentioned may increase complexity and run time [71].

3.4. Verification and Validation

Verification and Validation is an essential process to determine the credibility of the models to represent real-world systems. Larson et al. define verification as “proof of compliance with design solution specifications and descriptive documents”, whereas Validation is defined as “proof that the product accomplishes the intended purpose based on stakeholder expectations” [38]. In this section, verification is simply performed by evaluating these models for a test case from literature [12], Section 3.4.1. The models implemented in the current study are already validated [11, 12]. However, the correction factors implemented in the current study vary to

those implemented in [11, 12]. To ensure the modelling can still be achieved the performance level set in Table 2.3, validation is performed.

3.4.1. Verification

For the current study, models are implemented from the work of Contant [12]. Therefore, a verification of this implementation is performed by replicating a case from Contant's work shown below, and the design variables are listed in Table 3.13. An overview of this verification is shown in Table 3.14.

Contant Case Overview

- Payload Mass: 500 kg
- Apogee Altitude: 650 km
- Perigee Altitude: 650 km
- Propellant: Hydrolox
- Number of Engines (Stage 1): 9
- Number of Engines (Stage 2): 1

Parameter	**Stage 1**	**Stage 2**
Propellant	LOX/LH_2	LOX/LH_2
Chamber Pressure [bar]	199.1	200.0
Exit Pressure [bar]	0.48	0.01
Mixture Ratio[-]	6.3	6.5
Burn Time [s]	122.7	396.9
Stage Diameter [m]	1.51	1.51
Engine Exit Diameter [m]	0.37	1.30
Number of Engines [-]	9	1

Table 3.13: Design Variables for Verification [12]

Parameter	**Contant [12]**		**Verification**		**% Difference**	
	Stage 1	Stage 2	Stage 1	Stage 2	Stage 1	Stage 2
Vacuum Thrust [kN]	603.9	41.6	604.3	41.7	0.1	0.2
Specific Impulse [s]	-	-	426	479	-	-
Engine Mass [kg]	1489	131.8	1490	131.9	0.1	0.1
Stage Length [m]	32.7	8.6	34	8.6	3.9	0
GLOM [ton]	26.9		26.6		-1.1	
Fairing Mass [kg]	270.6		280.5		-3.6	

Table 3.14: Verification Overview

The implementation of the propulsion model is verified, with negligible difference attributed to rounding error and difference CEA equations implementation. Significant difference is noticed in the stage length determination, however this is attributed to ambiguity in what components

are considered for total stage length calculation in the case of Contant. Variation is also noticed in the fairing mass calculation, although the reason for this cannot be deduced. However, this significant difference has minimal impact on the Gross Lift-Off Mass (GLOM) and is thus accepted. Overall, the verification process shows that results within 5% can be achieved, and most error is attributed to model ambiguity, rounding error and difference in CEA equations implementation.

3.4.2. Validation

The process of verification does not confirm if the modelling is credible. In order to establish the credibility of the modelling, validation with existing engines and launchers is necessary, thereby allowing modelling inaccuracy estimation. The statistical parameters used in the current study are the relative mean error μ , the absolute relative error E and the standard deviation σ [12]. The mean relative error indicates how well the model can predict relative to the actual values, whereas the absolute relative error indicates the percentage error of the model. The standard deviation indicates the variation in a set of values. The statistical relations are presented through Equation 3.34, Equation 3.35 and Equation 3.36.

$$\mu = \frac{100\%}{n} \sum_{i=1}^{n} \frac{(y_i - \bar{y_i})}{y_i} \tag{3.34}$$

$$E = \frac{100\%}{n} \sum_{i=1}^{n} \left| \frac{y_i - \bar{y_i}}{y_i} \right| \tag{3.35}$$

$$\sigma = 100\%. \sqrt{\frac{1}{n-1} \sum_{i=1}^{n} \left(\mu - \frac{(y_i - \bar{y_i})}{y_i} \right)^2} \tag{3.36}$$

where,
y_i: Actual value from literature
$\bar{y_i}$: Estimated value from models
n: Number of Samples

CEA Equations Validation

Work by Ernst shows that results from NASA CEA typically overestimate propulsion parameters. This is verified in Table 3.15. It is confirmed that NASA CEA overestimates specific impulse by 8%. Table 3.16 shows the verification of the interpolation equations compared to CEA tool. Results indicate that these equations can estimate, on average, γ within 1%, T_{cc} within 3% and M within 1% accuracy. The overestimation of NASA CEA results, and thus the interpolation equations, is accounted for in the derivation of specific impulse correction factor Table 3.6 and therefore no separate correction factor for this overestimation is considered.

Engine	Propellant	P_c [bar]	OF [-]	Literature I_{sp} [s]	Model I_{sp}[s]	Error [%]
RS-68 A	LOX/LH_2	102.6	6	411	443	7.8
Rocketdyne H-1	LOX/RP1	40	2.2	289	315	9.1
Merlin 1A	LOX/RP1	53.9	2.2	300	330	9.9
Merlin 1C	LOX/RP1	67.7	2.2	304	330	8.4
Merlin 1D	LOX/RP1	97	2.3	311	332	6.6
RD-108	LOX/RP1	51	2.4	315	336	6.6
Vulcain-2	LOX/LH_2	116	6.7	434	465	7.2
Vulcain 1	LOX/LH_2	100	5.3	431	467	8.4
Rocketdyne F1	LOX/RP1	70	2.3	304	332	9.1
NK-33	LOX/RP1	145.7	2.8	331	343	3.5
RS-27	LOX/RP1	49	2.3	295	315	6.9
Rocketdyne J-2	LOX/LH_2	52.6	5.5	421	454	7.8
RD-120	LOX/RP1	162.8	2.6	350	366	4.6
HM7B	LOX/LH_2	37	5	444.6	482	8.5
RL10A-4-2	LOX/LH_2	39	5.5	451	479	6.3
Merlin 1D Vacuum	LOX/RP1	97.2	2.4	347	371	6.9
RL-10B-2	LOX/LH_2	44.1	5.9	462	498	7.7
RD-0109	LOX/RP1	50	2.1	323.5	359	11.1
					Average	8%

Table 3.15: NASA CEA Validation

	CEA Tool			Interpolation		
Engine	γ	T_{cc}	M	γ	T_{cc}	M
RS-68 A	1.14	3521.85	13.47	1.14	3500.93	13.44
Vulcain 2	1.14	3623.35	14.58	1.13	3635.58	14.62
Vulcain 1	1.15	3386.60	12.37	1.15	3361.14	12.33
Rocketdyne J-2	1.15	3372.93	12.63	1.16	3451.25	12.73
HM7B	1.15	3235.22	11.76	1.17	3346.81	11.89
RL10A-4-2	1.14	3343.93	12.60	1.16	3464.87	12.74
RL-10B-2	1.14	3417.25	13.21	1.15	3549.84	13.38
Rocketdyne H-1	1.15	3473.11	21.88	1.17	3499.52	21.89
Merlin 1A	1.15	3487.72	21.81	1.17	3472.68	21.74
Merlin 1C	1.16	3511.46	21.86	1.17	3459.62	21.71
Merlin 1D	1.15	3633.10	22.57	1.16	3487.71	22.21
RD-108	1.14	3574.10	22.62	1.17	3559.85	22.53
Rocketdyne F1	1.15	3534.57	22.00	1.17	3487.23	21.99
NK-33	1.14	3808.08	24.40	1.14	3596.34	23.87
RS-27	1.15	3506.94	22.02	1.17	3499.65	21.96
RD-120	1.14	3793.43	23.76	1.15	3503.20	23.05
Merlin 1D Vacuum	1.15	3642.93	22.66	1.16	3495.47	22.29
RD-0109	1.16	3438.47	21.51	1.18	3449.68	21.50

Table 3.16: Interpolation equation Validation

Propulsion model validation

The design variables of the Engines used for the validation is presented in Table 3.17.

		Design Parameters						
Engine	**Launcher (Stage)**	**P_c [bar]**	**P_e [bar]**	**OF [-]**	**t_b [s]**	**D_e [m]**	**D_s [m]**	**Propellant**
HM7B	Ariane 5 (2)	37	0.04	5	945	0.99	5.4	LOX/LH_2
LE5B	H-IIB (2)	36	0.03	5	499	1.71	4	LOX/LH_2
LE7A	H-IIA (1)	121	0.23	5.9	390	1.82	4	LOX/LH_2
RL10B2	Delta IV 4 (2)	44	0.04	5.88	850	2.15	4	LOX/LH_2
RL10A42	Atlas V (2)	42	0.04	5.5	842	1.17	3.05	LOX/LH_2
Vinci	Ariane 6 (2)	61	0.02	5.8	800	2.15	5.4	LOX/LH_2
Vulcain 2	Ariane 5 (1)	109	0.23	5.3	540	1.76	5.4	LOX/LH_2
RD191	Angara 1.2 (1)	262.6	0.75	2.6	215	1.45	2.9	LOX/RP1
YF100	Long March 7 (Booster)	180	0.55	2.6	180	1.34	2.25	LOX/RP1
Merlin 1D	Falcon 9 v1.1 (1)	97.2	0.53	2.34	180	1.07	3.7	LOX/RP1
RD120	Zenit (2)	178.1	0.13	2.6	315	1.95	3.9	LOX/RP1
RD58M	Zenit (3)	79	0.02	2.82	650	1.4	3.7	LOX/RP1

Table 3.17: Engine Propulsion Data from Literature [17, 19, 56, 39, 12]

Table 3.18 shows the validation of the propulsion modelling. The Ideal Rocket Theory overestimates both the specific impulse and the thrust, which is expected as the IRT assumes an ideal behaviour. In order to correct this overestimation, correction factors are implemented. In the current study, both the Specific Impulse and the Mass flow rate are corrected with correction factors 0.93 and 0.95 respectively, Table 3.8. The corrected specific impulse now has a relative error of 0.9%, percentage error of 1.4% and standard deviation of 1.6%. The thrust estimation has an absolute error of 4.3%, Table 3.19.

	Literature Value		**Ideal Rocket Theory**		**Corrected Value**	
Engine	I_{sp} [s]	F_T [kN]	I_{sp} [s]	F_T [kN]	I_{sp} [s]	F_T [kN]
HM7B	446	64.8	482	71.5	450	63.2
LE5B	447	137	487	159.2	455	140.7
LE7A	438	1098	466	1186.5	436	1048.6
RL10B2	466	110.1	499	125.5	466	110.9
RL10A42	451	99.2	479	112.6	447	99.5
Vinci	467	180	497	198.8	464	175.7
Vulcain 2	439	1113	467	1140.8	437	1008.2
RD191	338	2084.9	347	2232.2	324	1972.7
YF100	335	1340	347	1405.9	324	1242.5
Merlin 1D	320	742.4	337	778.2	315	687.7
RD120	350	912	367	953.7	343	842.9
RD58M	361	85	382	95.1	357	84.0

Table 3.18: Propulsion Parameter Validation

	Ideal Rocket Theory			Corrected Value		
Parameter	μ [%]	E [%]	σ [%]	μ [%]	E [%]	σ [%]
F_T	-9.0	9.0	4.4	3.6	4.3	3.8
I_{sp}	-5.9	5.9	1.7	0.9	1.4	1.6

Table 3.19: Propulsion Model Statistical Errors

Engine Length and Mass estimation model validation

The Engine length and mass relations validation is shown in Table 3.20. For the case of RL10B2 and Vinci the stowed engine lengths are considered, as the engine length estimation relations are suitable only for stowed lengths [74]. The statistical errors of the engine mass and length estimates are presented in Table 3.21. The absolute error for engine mass estimation is above 10%. There are equations in literature that can be implemented to lower this error [74], although such equations require engine cycle type specification, which is not considered in the current study to ensure universal applicability. Therefore, engine mass model error is subject to sensitivity analysis in Chapter 6. The engine length estimation for stowed engines, shows accuracy levels within 10%.

	Literature Value		Model Value	
Engine	M_{engine} [kg]	L_{engine} [m]	M_{engine} [kg]	L_{engine} [m]
HM7B	165	2.01	160	1.98
LE5B	269	2.8	264	2.4
LE7A	1800	3.7	1646	3.65
RL10B2	301	2.19	224	2.2
RL10A42	168	2.3	209	2.2
Vinci	280	2.37	312	2.5
Vulcain 2	1300	3.1	1578	3.7
RD191	2290	4	2206	3.7
YF100	-	-	1399	3.3
Merlin 1D	476	2.92	787	2.91
RD120	1125	3.8	958	3.1
RD58M	340	2.3	120	1.8

Table 3.20: Engine Mass and Length Validation [17, 19, 56, 39, 12]

Parameter	μ [%]	E [%]	σ [%]
M_{engine}	-0.1	22.2	9.8
L_{engine}	4.0	9.0	11.5

Table 3.21: Engine Mass and Length Estimation Model Statistical Errors

Launcher geometry and mass model validation

The launcher geometry and mass models of components such as the intertank, interstage, payload adapter etc have been validated in the work of Castellini [11] and therefore, in this section

the overall launcher geometry and mass validation is performed. The launcher inert mass and length estimate validation is presented in Table 3.22. For the current study, the launcher stage length is considered as the sum of the propellant tank length and the interstage length. The launcher stage inert mass is the sum of the engine mass, propellant tank mass, inter-tank mass, interstage mass, avionics and EPS mass. In addition to this, for first stage the pad interface mass is considered and for upper stage the payload interface mass is also considered. Given the ambiguity in literature with what components are considered for launcher inert mass and stage length, accurate validation is not possible. However, with the existing mass and geometry models a relative error of 9.7% and 5.5% is obtained for mass and geometry relations respectively. These modelling errors are also subject to sensitivity analysis in Chapter 6.

	Literature Value		**Model Value**	
Launcher (Stage)	M_{inert} [kg]	L_{stage} [m]	M_{inert} [kg]	L_{stage} [m]
Ariane 5 (2)	4540	4.7	5401	7.9
H-IIB (2)	4000	11	3226	9.6
H-IIA (1)	11200	37	8742	30
Delta IV 4 (2)	2850	12	3236	10
Atlas V Centaur (2)	2316	12.7	2102	12.8
Ariane 5 (1)	14700	24	13920	26
Angara 1.2 (1)	9800	26	5473	28

Table 3.22: Launcher Inert Mass and Length Validation [12, 39]

Parameter	μ [%]	E [%]	σ [%]
M_{inert}	9.7	18.9	27.1
L_{stage}	-5.5	19.1	21.6

Table 3.23: Launcher Mass and Length Estimation Model Statistical Errors

Multidisciplinary Design Analysis (MDA) validation

Launch vehicle design process, as described in Chapter 2, is highly coupled. Therefore, a validation of the entire design module is performed by running launch vehicle case from literature—Falcon 9 v1.1 and Delta IV M. The design variables for the validation is presented in Table 3.24. Table 3.25 shows that the relative error of the MDA process is within 10%. Significant difference is in the inert mass estimation, which is expected as from the validation of inert mass performed previously.

		Design Parameters									
Launcher	**Stage**	**P_c [bar]**	**P_e [bar]**	**OF [-]**	**t_b [s]**	**D_e [m]**	**D_s [m]**	**N_{eng}[-]**	**Propellant**	**Engine**	**Tank Material**
Falcon 9 v1.1	1	97.2	0.53	2.34	180	1.07	3.7	9	LOX/RP1	Merlin 1D	Al-Li Alloy
	2	97.2	0.04	2.34	375	3.3	3.7	1	LOX/RP1	Merlin 1DV	
Delta IV M	1	102.6	0.58	5.97	245	2.43	5.1	1	LOX/LH_2	RS-68A	Al-Li Alloy
	2	44	0.04	5.88	850	2.15	4	1	LOX/LH_2	RL10B2	

Table 3.24: Launcher Data from Literature [17, 19, 39]

Launcher	**Falcon 9 v1.1**			**Delta IV M**		
Parameter [unit]	**Literature**	**Model**	**% Error**	**Literature**	**Model**	**% Error**
Payload Mass [kg]	3960			4400		
Total Length [m]	68	72	6	63	67	6
Total M_{dry} [ton]	23	21	-9	31	28	-9.6
Stage 1 I_{sp} [s]	311	309	-0.6	411	413	0.5
Stage 2 I_{sp} [s]	340	346	2	466	467	0.2
Stage 1 F_T [kN]	6672	6043	-9	3363	3694	-9.8
Stage 2 F_T [kN]	934	956	2.4	110	106	-4
GLOM [ton]	506	487	-4	260	267	3

Table 3.25: Multidisciplinary Design Analysis Validation [39, 19, 17]

MDA validation is only performed for two launcher cases. More cases may be needed to be calculated to refine the inert mass modelling. Furthermore, MDA run for a Methane based launcher, such as Blue Origin's New Glenn, could not be performed as the design parameters required could not be found in literature available.
A sensitivity analysis is performed and presented in Chapter 6 to determine the sensitivity of model output to the design variables, correction factors and modelling errors and to identify the most sensitive parameters whose modelling must be done carefully and to identify whether any of these modelling errors could impact the results of the propellant comparison.

The above models make up the Multidisciplinary Design Analysis (MDA) part of the launch vehicle design process described in Chapter 2. The aerodynamics, trajectory, and cost models are not included in this process here. The reason for this is that these models are already included in the FRT tool and described briefly in Appendix C. However, it is important to take into account the effect of drag and losses incurred during flight into the launcher process. This is done by linking the FRT flight data back to the design process and running a loop. This is discussed in detail in the following section Chapter 4. An overview of these model accuracy is presented in Appendix E.

4

First Stage Recovery Tool Design Module

In the previous chapter, the models that make up the MDA part of the design module were discussed, verified and validated. In this section, Multidisciplinary Design Optimization process is described (MDO) in detail. This is followed by a discussion on the overall MDAO architecture and how this design module is incorporated into the existing FRT tool.

4.1. Design Module

The design module represents the launch vehicle design process that is to be incorporated into the existing FRT tool. The models for the design module are already discussed in Chapter 3. In this section, the multidisciplinary design optimization scheme adopted is described. This design optimization is different from the work of Contant, as Contant's work was focused on small launch vehicles and that is not the case for the current study, which is focused on medium/heavy lift launchers. The difference is mainly in the range bounds of the design variables. Whether the current study design constraints are different to that of Contant's cannot be determined, as Contant's work does not elaborate on these constraints. Nevertheless, the constraints in the current study are implemented based on what is typically found in literature. It is important to remember this following section solely focuses on the new design module. The design module is modular and therefore can be run without running the FRT.

A typical MDO formulation is presented in Equation 4.1, where $f(x, y, z)$ represents the main objective function, z represents the global and local design variables. Design variables are those variables that are allowed to change during the design optimization. Typical design variables are those that pertain to the propulsion system—chamber pressure, mixture ratio, engine exit diameter etc. To ensure that realistic launcher designs are attained, inequality, $g(x, y, z)$, and equality, $h(x, y, z)$ constraints are considered. Inequality constraints typically deal with ensuring the design values are within the allowable ranges, whereas the equality constraint is typically related to the target orbit requirements. $c(x, y, z)$ are the coupling functions between the different subsystems, which consider typical coupling variables—specific impulse, stage diameter, stage length, inert mass. What these parameters are for the current study is detailed in the following sections.

$$\begin{aligned} \underset{z}{\text{minimize}} \quad & f(x,y,z) \\ \text{subject to} \quad & g(x,y,z) \leq 0 \\ & h(x,y,z) = 0 \\ & \forall i, \forall j \neq i, y_i = \{c_{ij}(x_j, y_j, z_j)\}_j \end{aligned} \tag{4.1}$$

4.1.1. Objective Function

The main objective function for the launcher design module is minimization of the overall Gross Lift-Off Mass (GLOM). From literature, it is seen that for conceptual launcher design, classical objective function is minimizing the GLOM [4]. Although, from the perspective of costs there are literature that consider minimization of dry mass as the objective function [15], as the propellant costs are relatively insignificant compared to structural costs [53] and claim a lower dry mass design would lead to lower costs. However, the work by Braun et al. [7] shows that minimum dry mass design and minimum cost design are not equivalent. The minimum cost design seeks to minimize the total propulsion system mass. The total propulsion system mass makes up most of the launcher lift off mass [53]. Therefore, it was decided to follow suit of typical practices in literature and set minimization of GLOM as the objective function.

4.1.2. Design Variables

Design variables are those that are allowed to vary during the design optimization. The design variables considered in this study are mostly propulsion system design variables. Most literature consider similar design variables, as the overall launch vehicle design is dependent on the propulsion system design and thus the propulsion system parameters [12, 7, 15, 68]. Table 4.1 shows the design variables and their bounds considered for the current study. The bounds for the parameters are based on the propulsion parameters of existing rocket engines found in literature.

The upper bound of the chamber pressure was set to 200 bar, which is typically used in current rocket engines [73]. Furthermore, since the current study does not differentiate between different engine cycles, the range of chamber pressure extended to 200 bar covers the pressure ranges of the different engine cycles [11]. The mixture ratio range for the different propellants is considered to be within their optimum mixture ratio ranges identified from literature, [6]. The engine diameter range is dependent on the stage diameter and number of engines ranges, to ensure realistic engine configuration is possible. No indication of optimum number of engines for launcher design from perspective of mass or cost was found in literature. Therefore, number of engines is considered as a design variable. Other parameters such as Material, tank pressure, structure safety factor are identified from literature and listed in Appendix D.

Description [units]	Symbol	Lower Bound	Upper Bound
Stage 1			
Chamber Pressure [bar]	P_{c1}	30	200
Exit Pressure [bar]	P_{e1}	0.05	1
LOX/LH_2 Mixture Ratio [-]	OF_1	5	6
LOX/RP1 Mixture Ratio [-]	OF_1	2	3
LOX/CH_4 Mixture Ratio [-]	OF_1	1.35	3.35
Engine Exit Diameter [m]	D_{e1}	0.52	5
Stage Diameter [m]	D_{s1}	3	5.5
Burn Time [s]	t_{b1}	100	300
Number of Engines [-]	N_{eng1}	1	9
Stage 2			
Chamber Pressure [bar]	P_{c2}	30	200
Exit Pressure [bar]	P_{e2}	0.001	0.1
LOX/LH_2 Mixture Ratio [-]	OF_2	5	6
LOX/RP1 Mixture Ratio [-]	OF_2	2	3
LOX/CH_4 Mixture Ratio [-]	OF_2	1.35	3.35
Engine Exit Diameter [m]	D_{e2}	0.94	5
Stage Diameter [m]	D_{s2}	3	5.5
Burn Time [s]	t_{b2}	100	500
Number of Engines [-]	N_{eng2}	1	3

Table 4.1: Design Variable Bounds

4.1.3. Constraints

The optimization constraints are considered to ensure the designed launcher is geometrically realistic. Additionally, as stated previously, the current design module does not consider the trajectory simulation and thus, required ΔV is considered as constraint, with assumed trajectory loss values which are corrected for with an iterative loop discussed in Section 4.2. The constraints are listed in Table 4.2.

Constraint	Description	Constraint Formulation
Trajectory Constraints		
Minimum ΔV Constraint	The main objective of any launcher is to deliver required payload to desired orbit. In order to do this the launcher must have sufficient ΔV. The ΔV_{actual} is consistent with the minimum ΔV required in the FRT simulation.	$\Delta V_{actual} \geq \Delta V_{required}$
Minimum Thrust-to-Weight Constraint	The overall Thrust to Weight ratio of the launcher must be greater than 1.00 to ensure the launcher lifts off from the launch pad. From literature, typical launcher Thrust-to-Weight ratios are compared and 1.36 is considered as the minimum requirement for this study [39].	$T_W \geq 1.36$
Geometry Constraints		
Slenderness Ratio Constraint	Launch Vehicles are typically slender to reduce drag. However, for L/D ratios greater than 15, the structure becomes more flexible and the interaction between elastic deformation and rigid motion is no longer negligible [40, 28].	$\frac{L}{D} \leq 15$
Surface Filling Constraint	The engine exit diameter must not exceed the stage diameter. In case of multiple engines, the number of engines with a particular engine diameter must not exceed the launcher diameter. To consider the multiple engine configuration, surface filling efficiency[1] is considered [11]. These efficiencies and the engine configurations are shown in Table 4.3 and Figure 4.1 .	$N_{eng}.D_e^2 \leq \eta_{surface}.D_S^2$
Engine Constraints		
Upper Stage Engine Expansion Ratio Constraint	For upper stage engines, that operate in space, thrust always increases with expansion ratio. However, this increased expansion ratio comes at the cost of increased mass. Therefore, the expansion ratio is typically increased until this added mass costs more than the extra performance generated [46]. For the current launcher engine design, this limit is set from existing upper stage engines [17, 19, 56]. Furthermore, because the current engine length equations are suitable for stowed engines, limit on expansion ratio is set.	$\epsilon_2 \leq 150$
Summerfield Constraint	This constraint ensures that flow separation is avoided at the nozzle exit [73, 3]	$\frac{P_{e1}}{P_a} \geq 0.4$

Table 4.2: Constraints considered in the Design Module

[1] Also known as package density is the proportion of the surface covered by the circles [23]

No. of Engines	Surface Filling Efficiency
2	0.5
3	0.65
4	0.69
5	0.68
6	0.67
7	0.78
8	0.73
9	0.69

Table 4.3: Engine surface filling Efficiency [22]

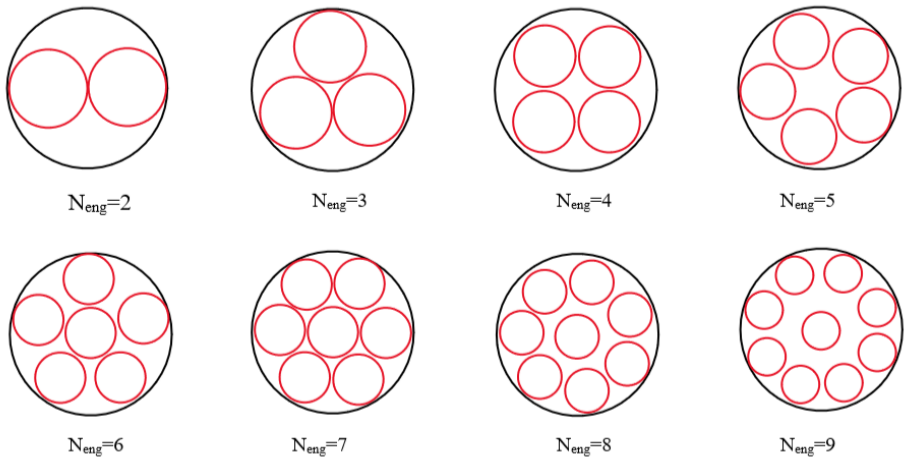

Figure 4.1: Multiple Engine Configuration

4.1.4. Optimization Algorithm

The optimization algorithm considered in this study is a Hybrid algorithm combining both Genetic Algorithm (GA) and Sequential Quadratic Programming (SQP). Most design process, including design process of Contant, consider only Genetic Algorithm. GA is an Evolutionary Optimization algorithm, based on the principles of natural selection and survival of the fittest [72]. The optimization first generates an initial population from the design variables. Different combinations of design variables are evaluated through different generations. The fitness of each individual design variable is determined through the fitness function. The probability that an individual is selected is determined by this fitness function. The fittest individuals from each generation are selected. This process keeps iterating until a generation with the fittest individuals is identified. The main advantage of GA is the ability to find the global optimum.

However, towards the last period of the evolutionary optimization process, the convergence rate of the optimization significantly decreases, which can lead to premature convergence [72]. To avoid this premature convergence, a second optimization is performed to refine the results obtained by GA. The second optimization algorithm implemented is the gradient-based SQP optimization, which guarantees local minima at much lower computation times. The results

obtained by GA are set as an initial point for the optimization by SQP. A fundamental disadvantage of SQP algorithm is the inability to work with integer based design variables (Number of engines in this current study). Unlike SQP, GA optimization can work with integer based design variables. Therefore, the second optimization loop considers a fixed optimum number of engines determined by GA and fine-tunes the remaining design variables.

The optimization process implemented in the study is shown in Figure 4.2. The refined results of this Hybrid optimization for a GTO mission, hydrolox launcher can be seen in Table 4.4. It can be seen that the hybrid optimization algorithm leads to a more optimum launcher design in terms of GLOM, by tuning the optimum design variable values, in this case, the burn time and chamber pressure values.

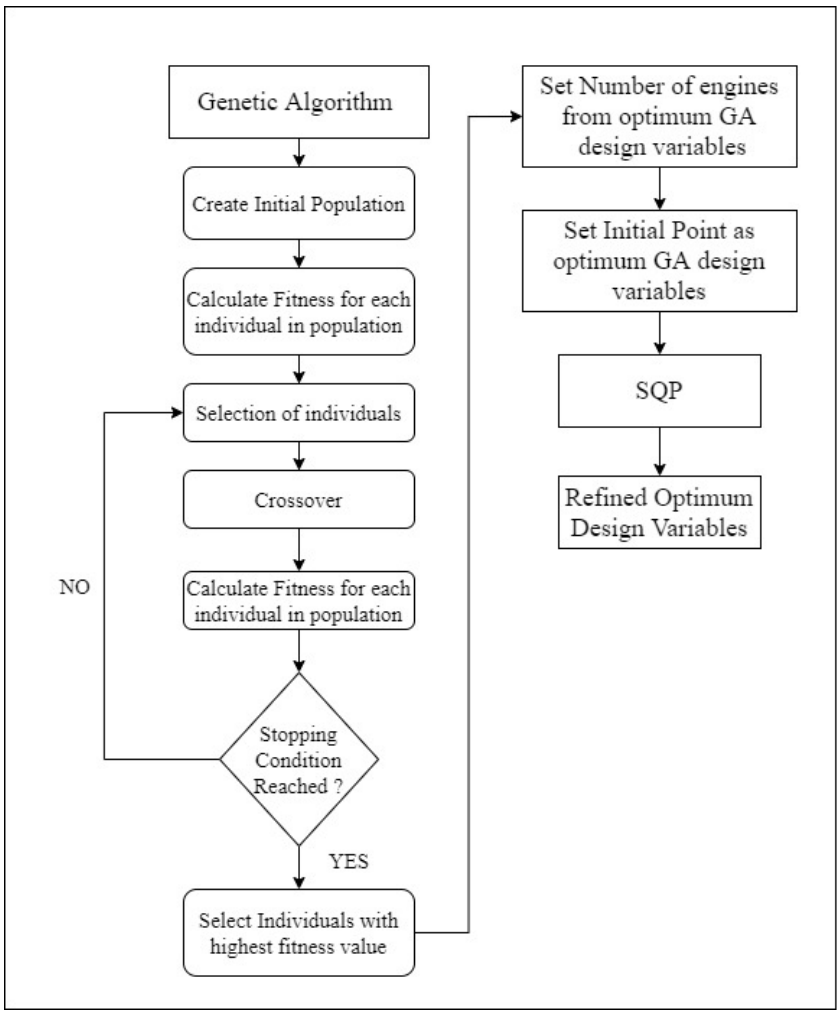

Figure 4.2: Hybrid GA-SQP Optimization Algorithm

Parameter [units]	Genetic Algorithm	Hybrid GA-SQP
GLOM [ton]	215	213
Total Propellant Mass [ton]	186	185
Total Dry Mass [ton]	24	23
Launcher Length [m]	72	70
Stage 1		
Chamber Pressure [bar]	196	200
Mixture Ratio [-]	5	5
Burn time [s]	165	184
Exit Pressure [bar]	0.4	0.4
N_{eng} [-]	5	5
Stage 2		
Chamber Pressure [bar]	151	137
Mixture Ratio [-]	6	6
Burn time [s]	429	422
Exit Pressure [bar]	0.08	0.07
N_{eng} [-]	2	2

Table 4.4: Optimization Algorithm Comparison

This concludes the description of the MDAO design process implemented in the current study with the MDA process models discussed in Chapter 3 and the optimization scheme discussed above. How this design module is linked to the existing FRT tool is described in the next section.

4.2. Overall Tool Architecture

As discussed in Chapter 2, the FRT was designed for resizing and analysing existing launchers for reusability. The tool lacks the capability to design new launchers. For the analysing Methane-based launchers, the existing tool is extended to include a design module. The architecture of the overall tool used in the current study is shown in Figure 4.3.

The new design module now allows a user to design expendable launchers by providing top level user inputs. An overview of the inputs, outputs, and constants considered in the design module is presented in Appendix D. The design module designs an optimum launch vehicle based on the user inputs, as per the objectives and constraint described in Section 4.1. This optimized launcher can then be redesigned to include reusability using the existing FRT tool. It is important to highlight that the new design module does not perform a trajectory optimization. This is to avoid repetition of same launcher trajectory simulation in both the design module and the FRT and to limit the overall simulation time. Rather than repeating the trajectory simulation, the design module considers trajectory requirements as design constraints, described in detail in Section 4.1. Once an optimum launcher design is obtained from the design module, the launcher geometry and mass characteristics can now be used as input for the FRT tool. The FRT tool, before running the optimization loop, checks for the initial ascent of the designed launcher to ensure it reaches orbit. This is performed by ensuring the Thrust-to weight at lift-off is greater than 1 and that the launcher has sufficient Δ V. Both of these parameters are

considered as constraint in the design module. Once the initial ascent check is complete, the optimization begins. For the FRT simulation, the key part is the optimization loop. The loop is run for multiple ascent and descent trajectory, for each the cost per flight is stored. Once, the maximum function evaluations are reached, the cost optimal recovery hardware, recovery hardware mass and cost optimal trajectory are determined. To limit simulation time, re-designed launchers with infeasible ΔV are removed. To minimize the number of ascent trajectories to be optimized, the optimization is done by including a database and an exclusion system. Trajectories with the highest ideal ΔV, that still cannot reach target orbit, are excluded. This is discussed in more detail in the work of Rozemeijer [55]. Once, the FRT simulation is complete a check is performed, to ensure, the assumed design trajectory loss and actual trajectory loss from FRT are similar. This is performed, as the design module does not consider trajectory modelling and designs launcher based on some assumed trajectory loss. To perform this check, a loop is created that compares the actual trajectory losses and design trajectory losses. A disadvantage of this method is the uncertainty in the number of iterations required, to ensure design trajectory loss and actual trajectory loss are similar. Therefore, a limit of 3% difference is set on the two losses to lower the number of potential iterations required. This limit is subject to a sensitivity analysis, discussed in detail in Chapter 6. If the difference between the two losses is less than or equal to 3%, the results are stored, and the simulation is complete. In case, the difference is more than 3%, the design module is run again, now with the updated trajectory loss from FRT and the process is continued.

4.2.1. Simulation Time

The design module simulation time is somewhere between 10 and 15 minutes. The time-consuming part of the design process is the genetic algorithm part. However, this optimization is essential as the second optimization algorithm, SQP, cannot work with integer design variables, number of engines in the current study. The trajectory optimization is the key part of the simulation run. Therefore, the most time-consuming part. During simulations, it was noticed that the run time for medium/heavy lift launchers is between 1 and 2 hours for a single iteration. However, for fairly new launcher design or Small launch vehicles, the run time was quite long - with small launcher configuration simulation taking more than 24 hours for a single iteration. A reason for this is the way the trajectory optimization takes place—via a database. The work by Rozemeijer focused on medium/heavy lift launchers, therefore the FRT already included a database for these launcher trajectories, expediting the simulation process for the current study. The overall simulation, with the design module and FRT for multiple iterations, can take somewhere between 3-6 hours, depending on the number of iterations required to meet the 3% trajectory loss check.

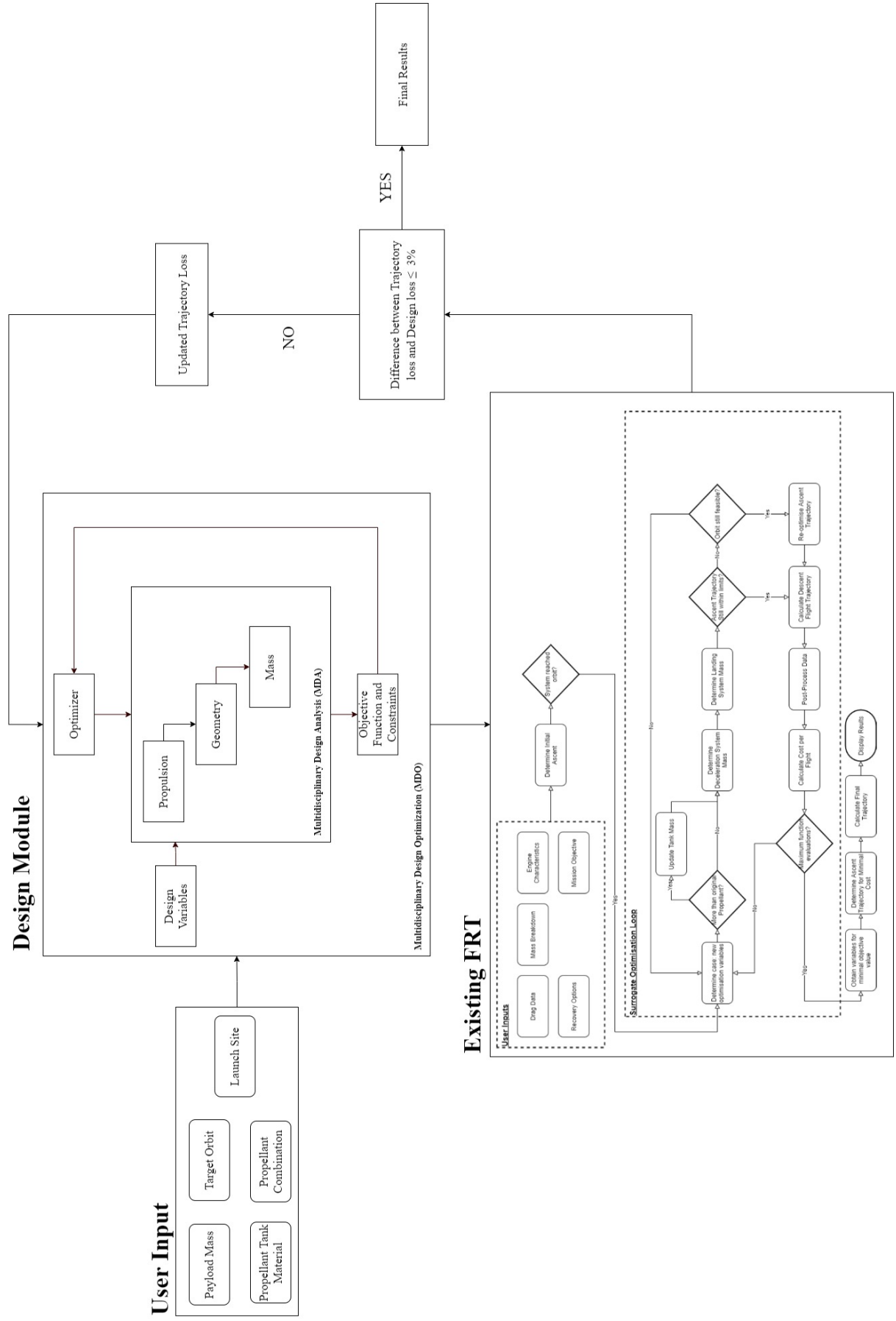

Figure 4.3: Improved First Stage Recovery Tool Architecture

5

Results & Discussion

In earlier chapters, the models implemented, their validity and the implementation of the design module to the existing First Stage Recovery Tool have been described. The validation process performed in Chapter 3 shows the relative error of the propulsion model, geometry and mass model are within 10%. This chapter presents an overview of the simulations performed for the current study. The results for different propellant configurations for different missions are presented. These results are discussed and compared on the basis of both design and cost, for both expendable and reusable configuration and different missions. The results presented in this chapter help answer the main research question—if methalox based launchers can achieve lower cost characteristics compared to hydrolox and kerolox launchers.

The first section details the different simulation cases performed in this study. This is followed by a description of the process of simulation. The remainder of the chapter presents and discusses the results of the simulations performed for different propellant combinations, for both GTO and LEO in expendable and reusable launcher configurations. For ease of the reader and clarity, the results section is presented as a comparison. First, the propellant combinations are compared based on design and cost, for a given mission and configuration, Section 5.3. This section helps determine the influence of propellant choice on design and cost. Next, launcher configurations - ELV and RLV—are compared cost wise for a given mission to determine whether launcher configuration influences propellant comparison Section 5.4. Finally, the missions themselves are compared, to determine the influence of mission type on the propellant comparison, Section 5.5. The results in this chapter are presented rounded to the closest integer, unless the difference is minor or in the case of percentages, the data is presented rounding off to the nearest tenth or hundredth [16].

5.1. Simulation Overview

Two missions are simulated for the current study. These are based on the Starlink Mission—circular Low Earth Orbit (LEO) Mission and the SES-10 mission—highly elliptical Geostationary Transfer Orbit (GTO) Mission. These missions are satellite internet constellation mission and communication satellite mission respectively. Market analysis forecasts growth in these missions in the coming decades [30]. Furthermore, both these missions have different Δ V requirements. For both the missions, the launch site was set to the Kennedy Space Center

(KSC) at longitude -80.61 deg and latitude 28.4 deg. An overview of the mission is presented in Table 5.1. The Δ V values listed in Table 5.1 are approximate values obtained from literature [71] and a more accurate value depends on the launcher design and trajectory flown and is tabulated in the results section.

Parameter	**LEO**	**GTO**
Apogee Altitude [km]	290	32827
Perigee Altitude [km]	290	218
Inclination [deg]	28.4	28.4
Payload Mass [kg]	15600	5000
Δ V [km/s]	10.3	12.7

Table 5.1: Mission overview

Each of these case missions are run for both Expendable and Reusable launcher configuration, for different propellant combinations, to enable propellant comparison. It is important to note the scope of this study is limited to purely liquid two—stage launchers. Liquid propellants are considered for the stages as they are capable of being throttled and restarted. Furthermore, Two stages to Orbit configuration is considered as literature shows that for the current payload range, two stage launchers are more cost optimum compared to three stage launchers [12, 57]. An overview of propellant combinations is shown in Table 5.2. The different propellant cases cover both pure and mixed propellant combinations. The mixed propellant combinations are focused on switching stage 1 propellant from traditional propellants to methalox. Case 4 is studied to compare the costs with Case 1. Case 5 and 6 are studied to confirm literature that suggests performance and design advantages and disadvantages of methalox and kerolox propellants cancel out each other [10, 15] and to determine whether the cost properties remain fairly similar.

Case	**Stage 1 Propellant**	**Stage 2 Propellant**
1	LOX/LH_2	LOX/LH_2
2	LOX/RP1	LOX/RP1
3	LOX/CH_4	LOX/CH_4
4	LOX/CH_4	LOX/LH_2
5	LOX/CH_4	LOX/RP1
6	LOX/RP1	LOX/CH_4

Table 5.2: Propellant Combination overview

For the reusable launcher configuration, there is a further division into the type of wingless (ballistic) recovery method implemented—Non-propulsive recovery and Propulsive Recovery. This division is based on the literature review, that shows winged (powered or glide back) recovery leads to larger dry mass compared to wingless (ballistic) recovery, as recovery hardware such as wing and landing gear for winged recovery is much heavier than parachutes, grid fins or landing gear for wingless recovery [30]. This larger structural mass may lead to higher cost characteristics. The launcher configuration case overview is presented in Table 5.3. The aim of studying different propellant combinations for these different recovery methods is to analyse whether recovery method influences propellant comparison.

Case	Description
1	Expendable Launcher Configuration
2	Reusable Launcher Configuration with Non-propulsive Recovery
3	Reusable Launcher Configuration with Propulsive Recovery

Table 5.3: Launcher Configuration overview

Figure 5.1 shows the different potential combinations that have been analysed in the current study. These different combinations allow the comparison of the different propellants for not only different missions, but also different launcher configurations.

Figure 5.1: Simulation Overview

5.2. Simulation Set-up

A brief description of how the simulation cases are performed is described below.

1. The user selects the mission and propellant combination.

2. An expendable launcher configuration is designed for the selected mission and propellant combination by the design module described in Chapter 4.
3. The First Stage Recovery Tool is implemented to run the trajectory optimization and the cost analysis.
4. As mentioned in Chapter 4, the preliminary design of the expendable launcher is based on assuming trajectory losses from literature [71]. Once a primary FRT run is performed, the trajectory losses are extracted and the expendable launcher is redesigned.
5. The FRT and expendable launcher design iteration is continued till the designed trajectory losses are within 3% of the actual trajectory loss. This trajectory loss parameter is subject to a sensitivity analysis in Chapter 6.
6. For reusable configuration, the type of recovery method is selected—Non-propulsive or Propulsive recovery method.
7. Next, the FRT is implemented to run the trajectory optimization and the cost analysis.
8. Results for optimum recovery method, recovery hardware mass, trajectory, and cost are extracted, for both expendable and reusable launcher configuration, from the FRT.

This methodology is a slight variation of what is found in literature. In literature, the expendable or reusable launchers are designed either based on fixed trajectory losses or performing trajectory optimization in combination with design optimization [57, 15] for a given recovery method. As discussed in Chapter 4, trajectory optimization is the most time-consuming task in the FRT, with typical GTO cases taking up to 2 hours. For this reason, rather than performing this trajectory optimization twice (once in the ELV design and once in FRT), it was decided to consider the trajectory requirements as design constraints and perform an iteration to achieve $\pm$ 3% difference between design trajectory loss and FRT trajectory loss. This factor of $\pm$ 3% is subject to sensitivity analysis in Chapter 6. Furthermore, most literature focuses on a particular recovery method rather than determining the optimum recovery hardware from a range of recovery options. Therefore, combined optimization of launcher design, trajectory optimization and optimum recovery option could lead to increased simulation time.

5.3. Propellant Comparison

This section presents comparison between the design characteristics of expendable launchers with different propellant combinations listed in Table 5.2 for a given mission, followed by the cost comparison. The mission considered is the highly elliptical, 32827 $\times$ 218 km Geostationary Transfer Orbit, with a payload mass of 5000 kg.

5.3.1. Design Comparison

The optimum results for the launcher design are presented in Table 5.4.

Parameter [units]	LOX/LH_2 LOX/LH_2	LOX/RP1 LOX/RP1	LOX/CH_4 LOX/CH_4	LOX/CH_4 LOX/LH_2	LOX/CH_4 LOX/RP1	LOX/RP1 LOX/CH_4
Stage 1						
P_C [bar]	200	200	200	200	200	200
OF [-]	5	3	3.35	1.6	3.35	3
t_b [s]	184	163	169	100	170	155
P_e [bar]	0.41	0.42	0.41	0.49	0.41	0.41
D_e [m]	1.1	1.7	1.5	1.1	1.2	1.7
D_s [m]	4.7	4.2	4.3	4.4	4.3	4.2
N_{eng} [-]	5	4	5	3	8	4
Stage 2						
P_C [bar]	137	90	125	152	85	128
OF [-]	6	3	3.35	6	3	3.35
t_b [s]	422	347	356	500	346	360
P_e [bar]	0.07	0.05	0.07	0.06	0.05	0.07
D_e [m]	1.4	3	1.4	2.3	3	1.4
D_s [m]	3	3	3	3	3	3
N_{eng} [-]	2	1	3	1	1	3

Table 5.4: GTO mission Expendable Launcher Optimum Design Variable

The optimizer drives towards higher chamber pressures for both the first stage and upper stage in all the propellant combinations. The reason for this being that an increased chamber pressure can lead to more efficient engine performance, i.e, higher specific impulse for a given mixture ratio. The thrust efficiency is inversely proportional to the mass of the molecule being expelled [64]. This is why most hydrolox engines are operated at fuel-rich mixture ratios, as hydrogen is much lighter than oxygen. On the contrary, hydrocarbon powered engines are operated at oxygen-rich mixture ratios since hydrocarbons are much heavier than oxygen and to prevent soot formation. This can be seen in the optimum mass mixture ratios in the case of same/similar propellant combinations (purely hydrolox, purely kerolox, purely methalox, methalox-kerolox), Table 5.4. Furthermore, because the mixture ratio range considered is based on optimum mixture ratios of different propellants identified from literature [6]. This is also why the optimum mixture ratios for same/similar propellant combinations is at the bounds. The second stage diameter is driven to the lower bound by the optimizer, as this results in the lower GLOM while not violating the slenderness ratio constraint set.

The number of engines is considered as a design variable in the current study. It can be seen from Table 5.4, that the optimum number of engines differs for different propellant cases. The reason for this is that the optimizer drives towards the number of engines that can results in the lowest overall engine mass, within the constraints. Table 5.5 shows that although for the same thrust conditions, a single engine results in relatively lower total engine mass, engine size can be significantly lowered by employing multiple engines to produce the same thrust. The current study does not consider reliability or cost in the design process, and the optimum number of engines is derived purely based on mass and dimension characteristics.

	Multi-Engine			Single Engine		Multi-Engine	Single Engine	
Propellant	N_{eng}	M_{eng} [ton]	$M_{eng,tot}$ [ton]	$M_{eng,tot}$ [ton]	**% Change**	L_{eng} [m]	L_{eng} [m]	**% Change**
Stage 1								
LOX/LH_2-LOX/LH_2	5	0.9	4.9	6.1	-20	3.3	4.8	-30
LOX/RP1-LOX/RP1	4	1.87	7.5	7.4	1	3.6	4.9	-27
LOX/CH_4-LOX/CH_4	5	1.80	9.0	8.8	2	3.8	5.5	-31
LOX/CH_4-LOX/LH_2	3	1.5	4.5	4.4	2	3.7	4.7	-22
LOX/CH_4-LOX/RP1	8	1.2	9.5	9.3	3	3.5	5.6	-38
LOX/RP1-LOX/CH_4	4	1.8	7.1	7.0	1	3.5	4.8	-27
Stage 2								
LOX/LH_2-LOX/LH_2	2	0.43	0.85	0.80	6.5	2.7	3.2	-14
LOX/CH_4-LOX/CH_4	3	0.37	1.12	1.05	6.8	2.6	3.4	-22
LOX/RP1-LOX/CH_4	3	0.4	1.15	1.08	7	2.7	3.4	-22

Table 5.5: Optimum Number of Engines

Engine Design

The optimum engine characteristics for the different designs are presented in Table 5.6. What is instantly noticeable is that the area ratio for the upper stage engine is at the constraint bounds. The reason for this is that thrust increases with expansion ratio. This, when combined with high specific impulse, results in complying with the required constraints, while ensuring low GLOM. Furthermore, since this constraint is applied to only upper stage rockets (to ensure realistic designs Chapter 4), the optimizer drives towards this allowed high expansion ratio values. Additionally, the engine mass and length estimation relations do not consider pressure and expansion ratio, and depend only on thrust to ensure they can be universally applied [74, 12].

For same/similar propellants—(pure) hydrolox, kerolox, methalox, methalox/kerolox - this expansion ratio constraint results in optimum pressure ratios and acceptable specific impulse values. However, for the case of methalox/hydrolox, this constraint allows for pressure ratios that result in unrealistic specific impulse value for hydrolox, as there is no constraint set on velocity. Since the optimization is performed for the objective of minimizing the GLOM, the main drive of the optimizer is to increase the specific impulse, which results in lower propellant mass and thus storage mass. However, methalox and hydrolox are significantly different propellant—different density and performance levels. Thus, the optimizer drives towards the

higher I_{sp} value, which in this case is hydrolox, and since the expansion ratio is allowed to reach high level, the optimizer compensates for the low specific impulse value of methalox by driving towards higher I_{sp} possibility of hydrolox. This is not the case for other propellant combinations, as the propellants on both stages are either same or have similar properties, and thus I_{sp} range. This unrealistically high I_{sp} of the upper stage in methalox-hydrolox case would result in an unrealistic launcher design and thus invalidate the comparison. To ensure, relatively realistic designs are compared, for methalox-hydrolox case a constraint is placed on the upper stage I_{sp}, limited to 460s.

Parameter [units]	**LOX/LH_2 LOX/LH_2**	**LOX/RP1 LOX/RP1**	**LOX/CH_4 LOX/CH_4**	**LOX/CH_4 LOX/LH_2**	**LOX/CH_4 LOX/RP1**	**LOX/RP1 LOX/CH_4**
Stage 1						
Propellant	LH_2	RP1	CH_4	CH_4	CH_4	RP1
P_{cc} [bar]	200	200	200	200	200	200
OF [-]	5	3	3.35	1.6	3.35	3
$I_{sp,vac}$ [s]	440	330	347.7	264	347.6	330
$F_{T,vac}$ [kN]	638	1670	1226	1017	805	1587
Area Ratio [-]	48	50	52	31	52	52
D_e [m]	1.1	1.7	1.5	1.1	1.2	1.7
L_{eng} [m]	3.3	3.6	3.8	3.7	3.5	3.5
M_{eng} [ton]	0.9	1.8	1.8	1.5	1.2	1.8
Stage 2						
Propellant	LH_2	RP1	CH_4	LH_2	RP1	CH_4
P_{cc} [bar]	137	90	125	152	85	128
OF [-]	6	3	3.35	6	3	3.35
$I_{sp,vac}$ [s]	463	351	367	537	351	367
$F_{T,vac}$ [kN]	260	784	707	368	736	240
Area Ratio[-]	150	150	150	150	150	150
D_e [m]	1.4	3	1.4	2.3	3	1.4
L_{eng} [m]	2.7	3	2.6	3.4	2.9	2.7
M_{eng} [ton]	0.43	0.89	0.37	1.1	0.84	0.38

Table 5.6: Optimum Engine Data for GTO mission Expendable Launcher Configuration

Table 5.7 shows the relatively realistic engine designs. The upper stage hydrolox engine has a realistic I_{sp} and the optimizer, now with restriction in the potential of upper stage, optimizes the lower methalox powered stage to compensate for this loss. This can be seen from the much lower chamber pressure and expansion ratio requirement of upper stage to satisfy the new constraint. It is important to remember that the engine mass and length estimations do not consider the effect of pressure and expansion ratio to ensure applicability across different engine cycles [12, 74], which explains the low chamber pressure and expansion ratio of the upper stage.

Parameter [units]	**LOX/LH_2 LOX/LH_2**	**LOX/RP1 LOX/RP1**	**LOX/CH_4 LOX/CH_4**	**LOX/CH_4 LOX/LH_2**	**LOX/CH_4 LOX/RP1**	**LOX/RP1 LOX/CH_4**
Stage 1						
Propellant	LH_2	RP1	CH_4	CH_4	CH_4	RP1
P_{cc} [bar]	200	200	200	200	200	200
OF [-]	5	3	3.35	3.35	3.35	3
$I_{sp,vac}$ [s]	440	330	347.7	347.7	347.6	330
$F_{T,vac}$ [kN]	638	1670	1226	509	805	1587
Area Ratio [-]	48	50	52	52	52	52
D_e [m]	1.1	1.7	1.5	0.9	1.2	1.7
L_{eng} [m]	3.3	3.6	3.8	3.1	3.5	3.5
M_{eng} [ton]	0.9	1.8	1.8	0.8	1.2	1.8
N_{eng} [-]	5	4	5	8	8	4
Stage 2						
Propellant	LH_2	RP1	CH_4	LH_2	RP1	CH_4
P_{cc} [bar]	137	90	125	40	85	128
OF [-]	6	3	3.35	6	3	3.35
$I_{sp,vac}$ [s]	463	351	367	460	351	367
$F_{T,vac}$ [kN]	260	784	707	242	736	240
Area Ratio [-]	150	150	150	36.5	150	150
D_e [m]	1.4	3	1.4	1.3	3	1.4
L_{eng} [m]	2.7	3	2.6	2.7	2.9	2.7
M_{eng} [ton]	0.43	0.89	0.37	0.4	0.84	0.38
N_{eng} [-]	2	1	3	3	1	3

Table 5.7: Realistic Optimum Engine Data for GTO mission Expendable Launcher Configuration

Stage Design

The optimum stage design for the different propellant combinations is listed in Table 5.8. The influence of propellant density on the inert mass is instantly noticeable. Although the propellant mass of hydrolox launcher is significantly low, 24% less than the second-lowest propellant mass combination (methalox-hydrolox), the inert mass is relatively similar to other propellant combinations.

The optimum propellant choice from the perspective of GLOM and inert mass is kerolox-methalox based launchers. This is attributed to the high density of the kerolox propellant in combination with the high performance of methalox propellant. This leads to a slight decrease in inert mass compared to pure kerolox design. However, the combination of methalox-kerolox shows an increase in inert mass compared to pure kerolox, despite lower propellant mass. This is because of the relatively low density of methalox compared to kerolox, impact of which cannot be balanced by optimum propellant mass parameters. Therefore, it can be seen that the different combinations of kerolox and methalox propellants have properties similar to or somewhere between the pure configurations. The combined propellant combination of methalox-hydrolox shows potential to achieve lower inert mass compared to pure hydrolox based launchers. This is because of the relatively higher density of methalox combined with the relatively higher performance potential of hydrolox. Although, the GLOM is on the slightly higher end compared to hydrolox, given the low performance potential of methalox.

Parameter [units]	LOX/LH_2 LOX/LH_2	LOX/RP1 LOX/RP1	LOX/CH_4 LOX/CH_4	LOX/CH_4 LOX/LH_2	LOX/CH_4 LOX/RP1	LOX/RP1 LOX/CH_4
Stage 1						
D_s [m]	4.7	4.2	4.3	4.0	4.3	4.2
L_{stage} [m]	35	34	36	22	38	31
M_{inert} [ton]	18	17	19	15	20	15
M_{prop} [ton]	136	338	306	172	323	303
ΔV_1 [km/s]	4.4	4.6	4.8	3.5	4.8	4.6
Stage 2						
D_s [m]	3	3	3	3	3	3
L_{stage} [m]	27	18	19	36	17	19
M_{inert} [ton]	5.4	4.5	4.8	6.5	4.3	4.6
M_{prop} [ton]	49	79	70	70.8	74	72
ΔV_2 [km/s]	7.9	7.7	7.6	8.8	7.5	7.7
Overall						
GLOM [ton]	213	444	406	270	426	401
Length [m]	70	61	64	67	64	60
M_{inert} [ton]	23	21	24	21.8	24	20
M_{prop} [ton]	185	418	377	243	397	376

Table 5.8: Optimum Stage Design for GTO mission Expendable Launcher Configuration

The payload fraction remains between 1-2% for the different propellant combinations. The different combinations of methalox and kerolox propellants show slight variations in distribution of structural and propellant mass, attributing to the fairly similar properties of these propellants. Despite having the relatively lower GLOM, hydrolox based systems are much heavier (larger inert mass to propellant percentage) than methalox or kerolox based systems. This explains why most hydrolox launchers currently employ boosters to provide initial thrust and bring down the inert mass and propellant mass ratio and potentially lower costs. However, this is out of scope of this study and is left as a recommendation for future studies.

5.3.2. Cost Comparison

As discussed in Chapter 1, cost is an important parameter, especially for new technology or propellant. The cost model - TRANSCOST model - is based on historical data and implements different cost coefficients for estimation of cost of different components, Appendix C. For this study, the Cost per Flight (CpF) is considered as the cost comparison criteria. The Launches per Annum (LpA) was set to 10 and the Man Year cost was set to €313250 for the financial year of 2021 [35] . Work by Rozemeijer [55] shows that the optimum LpA for reusable launchers is between 8-15 flights, beyond which the refurbishment cost goes up. Furthermore, according to [48], a minimum of 10 LpA must be regarded for reusable launcher design. Table 5.9 shows the cost per flight for different propellant combinations.

Parameter [units]	**LOX/LH_2 LOX/LH_2**	**LOX/RP1 LOX/RP1**	**LOX/CH_4 LOX/CH_4**	**LOX/CH_4 LOX/LH_2**	**LOX/CH_4 LOX/RP1**	**LOX/RP1 LOX/CH_4**
GLOM [ton]	213	444	406	270	426	401
Length [m]	70	61	64	67	64	60
M_{inert} [ton]	23	21	24	21.8	24	20
M_{prop} [ton]	185	418	377	243	397	376
CpF [M€]	59.6	40	43.6	49.9	43.6	39.5

Table 5.9: Cost per Flight for different propellant combinations for GTO mission ELV configuration

Cost analysis shows that low GLOM doesn't necessarily lead to low costs. Despite having the highest overall GLOM, the cost per flight of kerolox launcher is amongst the lowest. This is because most of the cost is related to the hardware, as propellant costs are low. Therefore, dry mass is a much better indicator of costs. This can be attributed to the production costs contributing significantly to cost per flight. The production cost is based on the cost of production of the stage and engine. This explains why the cost per flight of purely kerolox design is marginally higher than kerolox-methalox, due to marginally higher dry mass.

As already established, propellant cost is marginal, the cost of the different launcher combinations would be expected to have a marginal difference given the relatively similar inert mass. However, for the hydrolox propellant combination, it is noticed that the cost characteristic is significantly high despite having an inert mass lower than some methalox propellant combinations. The reason for this is that hydrolox engines are much more complex to build compared to kerolox or methalox engines, given the extreme cryogenic temperatures of hydrolox. This significantly low temperature requires heavier piping systems, advanced metallurgy to prevent embrittlement of engine material etc [9]. This can be seen from Figure 5.2, that shows that for the same engine cycle, Cost per Newton Thrust of hydrolox propellant is higher than that of kerolox. This factor is taken into account by applying a higher cost coefficient for production of hydrolox engines compared to kerolox [36] - Table 5.10 highlights this. Therefore, not just the inert mass, but also the propellant choice has a significant influence on the cost comparison. Methalox engines are considered in this study to have similar cost coefficients as that of kerolox [27]. Therefore, the comparatively lower cost of methalox-hydrolox propellant launcher compared to hydrolox is a result of the propellant choice. The optimum propellant combination from the point of view of costs is kerolox based design - kerolox-methalox. Although this is only marginally better than existing kerolox based launchers. The reason for this being not only the low inert mass, but also the less complex engine, which is accounted for by the lower cost coefficient.

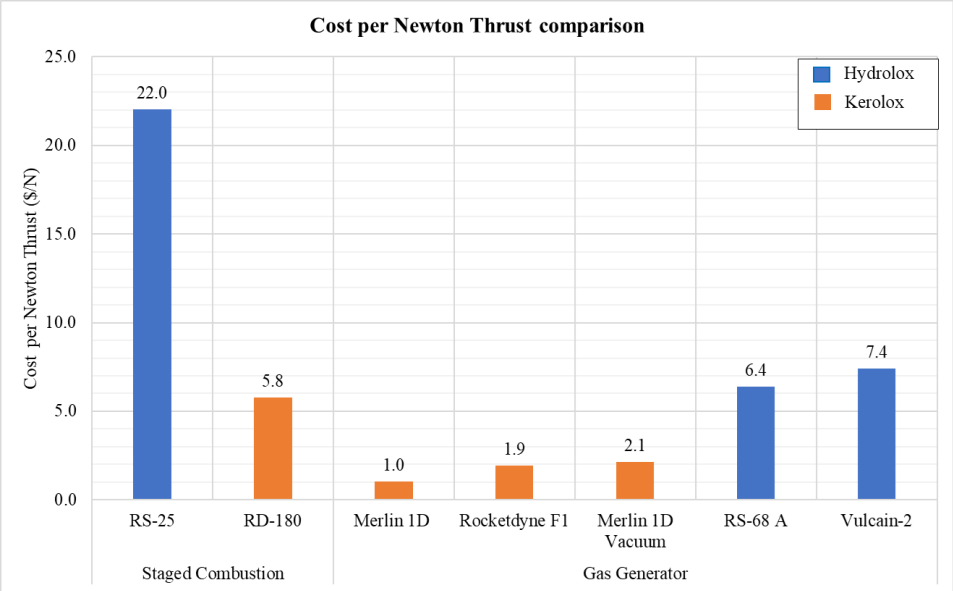

Figure 5.2: Cost per Newton Thrust comparison for different engine cycles [17, 19, 51]

Launcher Component	Propellant	Inert Mass [ton]	Cost [in MY]
Engine	LOX/LH_2	1.1	135
	LOX/RP1	0.9	72

Table 5.10: Cost comparison of upper stages powered by kerolox and hydrolox

5.4. Launcher Configuration Comparison

In this section, the reusable launcher configuration data is presented for the same case as that discussed in Section 5.3 - 5000 kg payload to highly elliptical, 32827 × 218 km Geostationary Transfer Orbit. The reusable launcher configuration is presented and compared for two cases defined in Table 5.3 - Non-propulsive and Propulsive recovery method. This is followed by cost comparison of Reusable and Expendable Launcher cost characteristics.

5.4.1. Non-Propulsive Recovery Reusable Launcher

The expendable launcher is now re-designed for reusability using the First Stage Recovery Tool. Table 5.11 shows the cost optimum recovery method and their masses. The optimum recovery method depends on the launcher design and the trajectory followed. The trajectory data from the FRT is presented in Table 5.12. Recovery of stage 1 involves a system to first decelerate the stage and to land this stage. 'Recovery system 1' represents the systems that provide the initial deceleration, typically at hypersonic or supersonic speeds. 'Recovery system 2' is the system that further slows down the stage within the atmosphere—which can be either parachutes or grid fins. 'Landing systems' is the system that stabilises/ lands the stage. The landing systems depend on the landing location—Mid-Air Retrieval, Landing legs for downrange landing or Airbags for splashdown recovery.

The trend for the launcher GLOM and dry mass characteristics are similar to that of Expendable launcher configuration. The optimum trajectory followed by the different propellants are similar for the kerolox and methalox powered launchers. This is because of the relatively similar launcher design. The low performance capability and low stage 1 Δ V split of methalox - hydrolox launcher can be seen from Table 5.12, with MECO for such a system occurring earlier than other propellant combinations. For the current study, trajectory comparison is not paramount, as the FRT optimizes the trajectory for minimum costs for all the propellant combinations and thus, it is insightful to look at the optimum recovery methods, Table 5.11 and cost characteristics, Table 5.13. The cost optimum recovery method is a combination of HIAD + Subsonic Parachutes + Airbags. This is the case for all the different propellant combinations. The cost optimum deceleration system remains HIAD+Subsonic parachutes, mainly because of HIAD flattens out the deceleration peak across the trajectory, thus making it easier to comply with the acceleration constraint [55]. The optimum deceleration system 2 is subsonic parachutes compared to supersonic. This is attributed to the relatively lower cost of subsonic (Ringsail) parachutes compared to supersonic (Hemisflo) parachute for the same area, [55]. Although, the optimum recovery method is similar for the different propellant designs, the design of these recovery methods is quite different. Therefore, the influence of launcher design on recovery hardware design as in the work of Burkhardt et al. [10] is seen.

Parameter [units]	**LOX/LH_2 LOX/LH_2**	**LOX/RP1 LOX/RP1**	**LOX/CH_4 LOX/CH_4**	**LOX/CH_4 LOX/LH_2**	**LOX/CH_4 LOX/RP1**	**LOX/RP1 LOX/CH_4**
Recovery System 1	HIAD					
Recovery System 2	Subsonic Parachutes					
Landing System	Airbags					
$M_{recovery}$ [ton]	0.7	0.7	1.0	0.5	1.3	1.0
$M_{landing}$ [ton]	1.1	1.5	1.5	2.9	1.2	0.6
GLOM [ton]	215	446	408	273	428	403
M_{inert} [ton]	24.8	23	27	24	27	22

Table 5.11: GTO mission Reusable Launcher Optimum Configuration

Parameter [units]	**LOX/LH_2 LOX/LH_2**	**LOX/RP1 LOX/RP1**	**LOX/CH_4 LOX/CH_4**	**LOX/CH_4 LOX/LH_2**	**LOX/CH_4 LOX/RP1**	**LOX/RP1 LOX/CH_4**
Main Engine Cut Off (MECO)						
Time [s]	171	143	150	115	157	143
Altitude [km]	70	60	55	44	55	74
Orbit Insertion						
Time [s]	767	895	819	955	757	974
Apogee Error [km]	0	0	0	0	0	0
Perigee Error [km]	2.8	0.7	1.7	0.9	1.7	0.9
Re-entry						
Time [s]	300	150	171	218	155	280
Altitude [km]	61	60	56	53	55	60

Table 5.12: GTO mission Reusable Launcher Optimum Trajectory for Non-propulsive Recovery

Parameter [in M€]	LOX/LH_2 LOX/LH_2	LOX/RP1 LOX/RP1	LOX/CH_4 LOX/CH_4	LOX/CH_4 LOX/LH_2	LOX/CH_4 LOX/RP1	LOX/RP1 LOX/CH_4
C_{rec}	0.06	0.06	0.06	0.07	0.12	0.05
C_{ref}	9.8	6.6	7.1	6.4	7.5	6.4
CpF	44.7	30.7	33.3	39.5	32.2	31.2

Table 5.13: GTO mission Reusable Launcher Cost Characteristics

The cost parameters for Reusable launcher configuration are shown in Table 5.13 and are assumed for 10 reuses. C_{rec} represents the Recovery cost, C_{ref} is the retrieval and refurbishment costs and CpF is the cost per flight. From the previous discussion on Expendable launcher vehicle, it has been established that lowest dry mass does not reflect as lower costs. This trend is seen in Reusable launchers as well. In addition to the impact type of propellant has on tank and engine cost, for reusable launchers the cost per flight also includes the cost to rebuild components that are not recovered—upper stage (including fairing) in the current study. Therefore, for reusable launchers, purely kerolox is the cost optimum propellant choice rather than kerolox-methalox combination in the case of expendable launchers Table 5.9. The reason for this is the slightly heavier upper stage in the case of kerolox-methalox launchers. Similarly, purely methalox design is 10% higher than the optimum propellant choice and the reason methalox - kerolox propellant combination performs better cost wise compared to methane alone systems, as the upper stage of these propellant combination is relatively smaller and lighter. The recovery costs depend on the type of recovery hardware and its design, which is influenced by the trajectory. The slightly larger recovery costs for methalox - kerolox are a result of the heavier first stage, which requires a recovery hardware to have larger area and thus higher mass. The retrieval and refurbishment costs are related to the stage 1. The lower retrieval and refurbishment costs of methalox - hydrolox propellant configuration is a result of the relatively much smaller and lighter first stage. It is important to note that for the current study, the refurbishment costs of methalox launchers are considered similar to that of kerolox. However, literature confirms that methalox propellant results in relatively low soot formation and low coking compared to kerolox engine [45, 25] at fuel rich mixture ratios and thus, there exists potential for lower cost per flight for methalox propellant, which can influence the current comparison. Therefore, the refurbishment costs are subject to a sensitivity analysis, described in Chapter 6.

5.4.2. Recovery Method Comparison

GTO mission simulation was performed for both Non-Propulsive and Propulsive Recovery methods, to determine whether type of recovery influences propellant comparison. Table 5.14 shows the cost characteristics of different propellant combinations, which is the cost optimum propellant choice for GTO missions for both Non-propulsive and propulsive recovery. For brevity, only pure propellant combinations are considered, as the combined propellant combination for reusable launcher have cost properties that lie within the range of the pure propellant combinations as seen in Section 5.4.1. 'NP' represents Non-Propulsive recovery, 'Prop' represents Propulsive recovery and 'Diff.' represents the amount of increase or decrease in cost of propulsive recovery compared to non-propulsive recovery. The costs listed in Table 5.14 are in M€. Results indicate, for different propellant combinations, the Non-propulsive Recovery methods have a lower cost per flight. This is because the Propulsive recovery method requires additional propellant for re-entry and landing burns. This additional propellant results

in increased propellant tank mass, which adds to cost. Although, the cost per flight is comparatively higher for propulsive recovery, the cost increase is a few millions, which in terms of the space industry is negligible. This also explains why the interest in propulsive recovery is still widely present in literature and industry. Additionally, this interest is further strengthened given that propulsive recovery is flight proven and has more or less become business as usual for SpaceX's Falcon 9. However, unlike in the comparison between the work of Dresia et al. and that of Burkhardt et al., that showed potential influence of recovery type on propellant comparison, no such variation is found in the current study. This is because the additional mass by incorporating ballistic non-propulsive recovery is a small fraction (under 1% difference in GLOM is noticed between ELV and RLV configurations for all propellant combinations) unlike in the work of Burkhardt et al., that considered winged recovery method. Similarly, for retro-propulsive recovery, the amount of additional propellant and thus increased stage mass is similar across different propellant designs. Therefore, type of recovery methods considered in the current study show no influence on the propellant mass or cost comparison.

	Hydrolox			**Kerolox**			**Methalox**		
Parameter	**NP**	**Prop**	**Diff.**	**NP**	**Prop**	**Diff.**	**NP**	**Prop**	**Diff.**
Stage 1 M_{dry} [ton]	19.7	22.4	2.7	18.9	21.2	2.3	21.7	24.2	2.5
Stage 1 M_{prop} [ton]	136	152	16	338	365	27	306	324	18
Recovery Cost	0.06	0	-0.06	0.06	0	-0.06	0.06	0	-0.06
Retrieval & Refurbishment	9.8	10.8	1.0	6.6	7.6	1	7.1	8.0	0.9
Cost per Flight	44.7	46.2	1.5	30.7	33.3	2.6	33.3	34.1	0.8

Table 5.14: Cost Characteristics Comparison for Non-Propulsive and Propulsive Recovery

5.4.3. Expendable and Reusable launcher Comparison

In this subsection, a cost comparison between expendable and reusable launcher is performed. This is done as it is seen from the previous sections the optimum propellant for Expendable launcher configuration is kerolox-methalox combination, whereas for Reusable configuration it is pure kerolox design, for the same mission and recovery method. The reason for this is explored in this section. For expendable launchers, the cost per flight depends mainly on the production costs of the overall launcher. Whereas, for reusable configuration, the costs are driven typically by the cost of production of components that are not recovered, in addition to refurbishment cost of recovered component. Therefore, a comparison of the inert mass and cost characteristics of the ELV upper stages of the two propellant combinations is performed in Table 5.15. For ELV configuration, the overall launcher cost is important. For the 2 propellant combinations this is fairly similar as seen in Table 5.15, with marginal difference in Cost per flight caused by propellant costs Table 5.9. For reusable configuration, however, the kerolox-methalox propellant has a heavier upper stage, given the relatively lower density of methalox compared to kerolox, which results in higher costs. Therefore, for every new mission, this heavier and expensive upper stage must be built. Although, the stage 1 mass for purely kerolox design is higher, refurbishment costs occupy significantly lower fraction of the cost per flight compared to production costs.

Parameter	Kerolox-Methalox	Pure Kerolox
Stage 1		
Propellant	Kerolox	Kerolox
Tank Mass [ton]	4.9	5.3
Tank Cost [MY]	173	181
Total Engine Mass [ton]	7.1	7.5
Total Engine Cost [MY]	356	367
Stage 2		
Propellant	Methalox	Kerolox
Tank Mass [ton]	1.7	1.5
Tank Cost [MY]	148	138
Total Engine Mass [ton]	1.1	0.9
Total Engine Cost [MY]	81	72
Overall		
Stage 1 Mass [ton]	12	12.8
Stage 1 cost [MY]	529	548
Stage 2 Mass [ton]	2.8	2.4
Stage 2 cost [MY]	229	210
Total cost [MY]	758	758

Table 5.15: Cost comparison of optimum propellants for ELV and RLV configuration

Hence, the type of launcher configuration varies the propellant comparison, however, only a marginal difference in cost is noticed and the variation in propellant comparison is noticed amongst different combinations of kerolox and methalox propellant. This confirms studies in literature that suggest kerolox and methalox propellant launchers could have similar cost characteristics, given the similar properties of these propellants [30]. In a broader sense however, it can be concluded that the cost characteristics of different propellant combinations lie somewhere between the pure propellant configurations and the trend among pure hydrolox, kerolox and methalox design remains same regardless of launcher configuration.

5.5. Mission Comparison

In this section, the launcher cost characteristics for circular 290 × 290 km Low Earth Orbit, with a payload mass of, 15600 kg mission is compared to the GTO mission discussed in the previous sections. This comparison is performed for purely hydrolox, kerolox and methalox propellant combinations, to determine whether the type of mission influences propellant comparison. Table 5.16 shows comparison of launcher overall mass, dry mass and cost characteristics.

The overall launcher mass characteristics for LEO case vary significantly from that of GTO case, particularly for purely hydrolox launcher. The reason for this is the much larger payload mass, leading to a much larger payload adapter (almost 3 times that for GTO payload case). Additionally, the increased payload mass leads to the need for larger thrust capability to satisfy Thrust-to-weight constraints, achieved by increased mass flow rate and thus propellant mass. Given the low density of hydrolox propellant, this leads to a significant increase in tank volume and thus inert mass. Therefore, despite lower Δ V requirement for LEO case, the higher

payload mass has a significant impact on the overall design. This again highlights reason why typical hydrolox launchers use boosters to provide initial thrust and lower overall inert mass to propellant ratio. For purely kerolox and methalox powered launchers, the overall GLOM variation is relatively less compared to GTO case. The reason for this is the much lower Δ V requirements of the LEO case compared to GTO case, which significantly lowers the propellant mass and thus lowers the propellant tank storage mass. The increased payload mass has minimal impact on the launcher mass, as the increased propellant mass comes at minimal increase of dry mass, given the relatively high density of these propellants. The impact of this can also be seen in the cost behaviour of these launchers. Kerolox and methalox propellant combinations are fairly similar to those of GTO case, with cost increase for LEO case under 1.5%. However, for hydrolox propellant combinations, the cost difference is significantly large given the large difference in the inert mass. Therefore, the assumption that lower dry mass leads to lower costs is only valid while comparing launchers with similar propellant combinations.However, the type of mission shows no variation in propellant comparison trend.

	Hydrolox			**Kerolox**			**Methalox**		
Parameter	**GTO**	**LEO**	**Diff.**	**GTO**	**LEO**	**Diff.**	**GTO**	**LEO**	**Diff.**
GLOM [ton]	213	250	+37	444	426	-18	405	397	-8
$M_{dry,tot}$ [ton]	23	27	+4	21	21.4	+0.4	24	25	+1
$M_{prop,tot}$ [ton]	185	206	+21	418	389	-29	377	356	-21
Stage 1 M_{dry} [ton]	17.8	20	+2.2	16.8	16	-0.8	19.3	18.7	-0.6
Stage 1 $M_{prop,tot}$ [ton]	136	132	-4	338	273	-65	306	250	-56
Stage 2 M_{dry} [ton]	5.4	7	+1.6	4.5	5.4	+0.9	4.8	6	+1.2
Stage 2 M_{prop} [ton]	48.6	75	+26.4	79	116	+37	70	106	+36
ΔV_1 [km/s]	4.42	3.26	-26.2	4.65	3.31	-28.8	4.79	3.40	-29
ΔV_2 [km/s]	7.88	6.63	-15.8	7.71	6.44	-16.5	7.57	6.40	-15
Cost per Flight	59.6	66.5	+6.9	40	40.5	+0.5	43.6	44.2	+0.6

Table 5.16: Cost Characteristics Comparison for different Missions (ELV)

5.6. Summary

Results from the different simulations show that kerolox propellant based launchers are the cost wise optimum—either in pure configuration or in combination with methalox. This is because of the relatively large density of kerolox, which compensates for the low performance capability, and therefore the additional propellant required, as a result of low performance, comes at minimal inert mass increase, courtesy the larger density. This low inert mass reflects as lower cost per flight. However, low inert mass does not reflect to lower costs in all cases - hydrolox based engines are much complex to build, and therefore this complexity is accounted for in the cost estimation of these engines. This complexity is not present in the case of methalox or kerolox. Therefore, despite hydrolox having lower inert mass in certain cases, across all simulations hydrolox propellant based launchers have the highest cost characteristics. Methalox based launchers have cost characteristics slightly higher than kerolox based launchers. Comparison between different launcher configurations shows slight variation in propellant comparison. This is attributed to the fact that while expendable configuration cost characteristics depend on the overall launcher, reusable launcher costs are driven by the recurring costs, while is characterised by cost of components that are not recovered—in this study

the upper stage. Thus, for reusable configuration, pure kerolox design showed optimum cost per flight compared to kerolox-methalox combination for expendable configuration. The type of recovery method showed no influence on the propellant comparison. The type of mission has minimal effect on cost parameters of relatively higher density propellant combinations of kerolox and methalox. This is because the impact of larger payload requirement on inert mass is negated by the much lower ΔV requirements. However, this is not the case for hydrolox propellant, as the increased payload requirement results in larger overall mass and increased propellant mass to comply with thrust to weight constraint. Overall, for different missions, the propellant comparison trend remains the same. It is noticed throughout the different simulations that the cost characteristics of combined propellants lie somewhere in between or have marginal difference to their respective pure configuration, especially in the case of kerolox or methalox combinations—this also confirms literature that suggests cost characteristics of kerolox and methalox based designs would be fairly similar, given their similar properties.

6

Sensitivity Analysis

Sensitivity analysis is performed to analyse the robustness of the optimal results to uncertainties in the mathematical models implemented in the tool, described in Chapter 3 and Chapter 4. For the current study, it is important to analyse uncertainty in which parameter is the model output most sensitive to and to determine whether the comparison performed in this study would change as a result of these uncertainties. This is of particular interest for Methane based launchers, since the launcher design is based on assumptions from literature with regard to engine design and propellant tank design.

Sensitivity Analysis is performed using two approaches—One-at-a-time approach (OAT) and Monte-Carlo analysis (MC). These two methods are widely utilised in literature to perform sensitivity study [11, 12, 55, 18]. The first section presents an overview of the OAT analysis performed in this study. This is followed by the Monte Carlo Analysis. The influence of uncertainties on the Cost parameters and Launcher mass characteristics is studied. The influence of uncertainty in cost coefficients and the trajectory parameters are already performed in literature and are not repeated here [12, 55]. Finally, a sensitivity analysis of refurbishment costs is performed by introducing a refurbishment factor, to particularly analyse influence on comparison between kerolox and methalox propellant combinations, as most literature suggests methalox would be a better propellant choice for reusable engines compared to kerolox, given the relatively low soot and coking of methane fuel, confirmed in the works by Hernandez et al. and Nickerson et al. [25, 45].

6.1. One-at-a-time Approach (OAT)

The one-at-a-time approach (OAT) is one of the most widely used sensitivity analysis in literature across different fields [20]. In this approach, only one parameter is changed at a time. This method is helpful in assessing the influence of variation of this particular parameter on the model output. The parameter is varied by a percentage which is equal to plus and minus the absolute mean error (E), calculated in Chapter 3, which represents the worst case scenario [67].

The OAT is performed for the following cases:

1. Modelling Errors identified in validation process performed in Chapter 3 : This is performed to determine uncertainty in which model influences the launcher cost and design

the most and thus must be improved for future studies. Modelling equations for thrust, specific impulse, stage length and stage inert mass is common regardless of the propellant choice and therefore error in these models will influence the launcher designs in the same manner and therefore does not change the propellant comparison. Whereas, the engine length and mass estimation equations are propellant specific and thus error in these models can influence the comparison and hence must be analysed.

2. Assumptions Uncertainties: For the current study, certain assumptions are considered, which remain constant in the design process. For this study, these assumptions are the different correction factors implemented, tank material stress values, trajectory loss assumptions. Uncertainty in trajectory loss is similar across the different propellant launchers and thus does not vary the comparison. Whereas, literature suggests type of propellant has an influence on the propulsion correction factors [73, 33] and thus this difference may influence propellant comparison. Furthermore, for Methane engine in particular, certain correction factors are derived in Chapter 3, to account for propellant switch from kerolox to methalox. Thus, uncertainty in these correction factors will influence the comparison, in particular the comparison between kerolox and methalox engines. Additionally, the storage temperature of these various propellants is different. The tank material stress varies with temperature and thus influences the design of the launcher and therefore the comparison. Therefore, it is important to determine the extent of influence of these uncertainties on the model output and propellant comparison.

The baseline case for common modelling errors and assumptions is the Hydrolox ELV GTO case and that for propellant specific includes Kerolox, Methalox ELV GTO case,Table 6.1. The data are presented rounded to 1 decimal points, as the differences for different errors for some cases were noticed in the tenths place.

Parameter	Hydrolox	Kerolox	Methalox
GLOM [ton]	212.2	444.3	405.8
Dry Mass [ton]	22.2	21.3	24.1
Cpf [M€]	59.6	40	43.6

Table 6.1: Baseline Case for common and propellant specific OAT analysis

6.1.1. Modelling Error Uncertainty

The different modelling errors considered in the current study are listed below:

1. Common modelling errors:

   (a) Uncertainty in Inert Mass Estimation
   (b) Uncertainty in Stage Length Estimation
   (c) Uncertainty in Thrust Estimation
   (d) Uncertainty in Specific Impulse Estimation

   Table 6.2 and Table 6.3 presents the results of the OAT sensitivity analysis for positive and negative variations, respectively. These uncertainties in the different models are implemented to both the stages simultaneously.

Results indicate that the cost parameter is most sensitive to variation in stage length and inert mass calculations. This is because the cost models are based on the dry mass. The stage length variation is considered as propellant tank length variation, and therefore increase in length of these tanks results in increased tank mass. Variation in specific impulse and thrust shows relatively smaller impact on the cost parameters. Increase in specific impulse works in favour of the optimizer and thus results in a lower cost than the nominal case. Whereas, for a decrease in specific impulse, a marginal increase in cost is noticed. Variation in thrust shows negligible influence on cost parameter.

	Variation	**GLOM**		**Dry Mass**		**Cpf**	
	Nominal	212.2 ton		22.2 ton		59.6M€	
Parameter	[%]	[ton]	[%]	[ton]	[%]	[M€]	[%]
Inert Mass	+18.9	228.0	7.4	25.6	15.2	63.5	6.0
Stage Length	+19.2	227.8	7.3	26.3	18.2	63.9	7.2
Vacuum Thrust	+4.3	206.0	-2.9	22.0	-0.9	59.2	-0.7
Specific Impulse	+1.4	195.3	-7.9	21.0	-5.4	57.8	-3.0

Table 6.2: OAT Analysis of Common Modelling Error for positive variations

	Variation	**GLOM**		**Dry Mass**		**Cpf**	
	Nominal	212.2 ton		22.2 ton		59.6 M€	
Parameter	[%]	[ton]	[%]	[ton]	[%]	[M€]	[%]
Inert Mass	-18.9	191.8	-9.6	18.8	-15.3	55.3	-7.2
Stage Length	-19.2	192.6	-9.2	18.4	-17.2	54.9	-7.8
Vacuum Thrust	-4.3	205.8	-3.0	22.0	-0.9	59.3	-0.5
Specific Impulse	-1.4	217.3	2.4	22.7	2.3	60.2	1.0

Table 6.3: OAT Analysis of Common Modelling Error for negative variations

2. Propellant specific modelling errors:

   (a) Uncertainty in Engine Mass Estimation
   (b) Uncertainty in Engine Length Estimation

Table 6.4 shows the model output for different propellants for engine mass and length modelling errors. First, looking solely at the hydrolox case, it can be seen that the cost parameter is the most sensitive to variation in Engine mass estimation. This trend is noticed in other propellant combinations as well. Despite these modelling errors, there is no difference in the propellant comparison, although the gap in cost may vary. Cost parameters show negligible sensitivity to variation in engine length.

	Variation	GLOM			Dry Mass			Cpf		
	Nominal	212.2	444.3	405.8	22.2	21.3	24.1	59.6	40	43.6
Parameter	[%]	**LH2**	**RP1**	**CH4**	**LH2**	**RP1**	**CH4**	**LH2**	**RP1**	**CH4**
Engine Mass	+22.2	218.2	451.7	416.9	24.1	23.5	26.5	62.6	42.7	46.3
	-22.2	200.4	411.5	371.2	20.1	18.2	19.9	55.8	37.8	40.3
Engine Length	+8.6	211.2	434.5	396.5	22.5	21.1	23.3	58.4	40.5	43.8
	-8.6	206.8	427.6	389.6	21.6	20.4	22.6	57.5	40.1	43.1

Table 6.4: OAT Analysis of Propellant Specific Modelling Error

Sensitivity Analysis of the modelling error shows that cost parameter is most sensitive to error in stage geometry and mass models and engine mass models. For future studies, in particular studies focused on comparing new launcher design to existing launchers, it is recommended to refine these models, such as considering expansion ratio and pressures in engine mass estimation [74].

6.1.2. Assumptions Uncertainties

The uncertainty in common and propellant specific assumptions studied are listed below:

1. Uncertainty in common assumptions present in different propellant based launchers

   (a) Uncertainty in Design Trajectory Loss: Varied $\pm 3\%$ from FRT trajectory loss
   (b) Uncertainty in Discharge Coefficient

   Sensitivity of launcher design and cost characteristics to uncertainty in design trajectory loss and discharge coefficient is shown in Table 6.5. Results indicate that variation of 3% in the design and trajectory losses show negligible influence on the cost parameters. Lowering this difference between design and actual trajectory loss to 1% would result in almost no variation in design and cost parameters, but can lead to increased computation time as a result of more iterations required to reach 1%. Ambiguity in discharge coefficient was discussed in Chapter 3. Considering discharge coefficient value similar to that of Contant shows negligible influence on the optimum cost parameter.

	Value	GLOM		Dry Mass		Cpf	
	Nominal	212.2 ton		22.2 ton		59.6 M€	
Parameter		[ton]	[%]	[ton]	[%]	[M€]	[%]
Design Loss (Nominal: 1.2 km/s)	+3%	211.3	-0.4	22.2	0.0	59.6	0.0
	-3%	206.8	-2.6	21.8	-1.8	59.0	-1.0
C_d	1	209.0	-1.5	22.1	-0.7	59.3	-0.5

Table 6.5: Results of OAT analysis of uncertainty in common modelling assumptions

2. Propellant Specific uncertainty in assumptions:

   (a) Uncertainty in discharge coefficient:

   Literature indicates that at Reynolds number below 100000, the effect of boundary

layer on the nozzle throat can no longer be neglected. The increased boundary layer thickness can lead to blockage in the nozzle throat and thus lower mass flow rate than the expected will be achieved [73]. This performance reduction is accounted for by the discharge coefficient. Furthermore, work by Tang et al. have shown that the discharge coefficient can be related to the Reynolds number by Equation 6.1. The relation shows that the discharge coefficient not only depends on the Reynolds number but also on the type of gas, represented by the γ value.

$$C_d = 1 - \left(\frac{\gamma+1}{2}\right)^{\frac{3}{4}} \left\{\frac{-2.128}{\gamma+1} + 3.266\right\} R^{-0.5} + 0.9428\frac{(\gamma-1)(\gamma+2)}{(\gamma+1)^{0.5}} R^{-1} \tag{6.1}$$

To analyse specifically the influence of propellant on C_d, a fixed Reynolds number, 10000, is considered. Table 6.6 shows the optimization results considering Equation 6.1 to derive an appropriate C_d value. Results indicate that the optimum cost parameter is insensitive to variation in C_d. Hence, no variation in propellant comparison is noticed.

Parameter	**Hydrolox**	**Kerolox**	**Methalox**
GLOM [ton]	209.0	429.3	392.7
Dry Mass [ton]	22.0	20.5	23.0
Cpf [M€]	59.3	40.1	43.4
C_d [-]	0.9851	0.9856	0.9856
γ [-]	1.15	1.13	1.13

Table 6.6: Uncertainty in Discharge Coefficient

(b) Uncertainty in Specific Impulse correction factor:

Rocket Propulsion Analysis (RPA) tool considers different specific impulse correction factor for different propellants. Therefore, influence of different specific impulse correction factor on propellant comparison is analysed. The propellant specific correction factors are considered from RPA. Table 6.7 shows that the propellant comparison trend remains same, despite the different correction factors.

Parameter	**Hydrolox**	**Kerolox**	**Methalox**
GLOM [ton]	176.6	369.7	336.5
Dry Mass [ton]	19.4	18.4	20.6
Cpf [M€]	56.2	38.2	41.4
ξ_s [-]	0.9762	0.9672	0.9692

Table 6.7: Uncertainty in Specific impulse correction factor

(c) Uncertainty in Methane Engine Mass and Length Estimation Correction Factor:

In literature, kerolox engine mass and length estimation relations are considered for methalox engines as well [74]. However, comparing results from these relations

with methalox engines present in literature shows that the relations underestimate the engine mass and length Section 3.2. Furthermore, the work by Pempie et al. [47] also shows that for the same chamber pressure, Methalox engines are heavier than kerolox engines. Therefore, certain correction factors are considered to account for this underestimation, in particular for comparison between kerolox and methalox engines.

Assuming engine mass and length estimation same as that of kerolox engines, i.e, Correction factor = 1. Table 6.8 shows that Cost per flight is highly sensitive to uncertainty in engine mass estimation. Cost per flight is less sensitive to engine length variation, as seen in Section 6.1.1, the difference in cost per flight can thus be attributed to variation in engine mass. Results indicate that considering kerolox engine mass and length estimation relations for methalox shows potential to obtain lower cost compared to kerolox. This is an important result, as this invalidates the propellant comparison performed and shows the potential of methalox to be the cost optimum propellant. For reusable launchers, there could be potential to further reduce the costs if lower refurbishment costs for methalox engines compared to kerolox engines, given the low soot formation and coking, is considered.

GLOM		**Dry Mass**		**Cpf**	
[ton]	[%]	[ton]	[%]	[M€]	[%]
363.6	-10.4	19.2	-20.3	39.8	-8.7

Table 6.8: Results of Methalox launcher with engine mass and length estimation relations same as kerolox

(d) Uncertainty in propellant storage temperature and material stress:

Material yield stress is a function of temperature. At lower temperatures, this yield strength is much higher, leading to a potential for lower tank dry mass. The material stress influences the tank mass and thus can impact the cost per flight. Different propellants are stored at different temperatures. Therefore, the uncertainty in cost as a result of propellant storage temperature must be studied. For this sensitivity study, the same material as that in the nominal cases is considered — Al-Li 2195, as stress levels at different temperatures are available [49].

i. Ultimate Yield Strength: 710 MPa
ii. Yield Strength at Room Temperature (25 degree Celsius): 521.6 MPa
iii. Yield Strength at 80K: 589.9 MPa
iv. Yield Strength at 20K: 608.6 MPa

Table 6.9 shows the variation in optimum for different propellants. Liquid Hydrogen is considered stored at 20K, RP1 at Room temperature [64, 73, 17]. Liquid Methane is assumed to be stored at similar temperature as that of LOX mainly because literature indicates the storage temperature proximity of fuel and oxidizer as an advantage for methalox propellant [10], but also because specific strength of Al-Li 2195 at 80K is available in literature [49]. To calculate yield strength of Al-Li 2195 at liquid methane storage temperature (112K [64]), curve fitting is performed. However, the curve fitting is performed with just 3 data points (yield strength at room temperature, 20K and 80K), which is much less than the rule of thumb — 10

points [63, 74]- and therefore, must be looked at in more depth for future studies. Nonetheless, the results indicate negligible variation in the different parameters for the different storage temperatures of methalox. Overall results show that although there exists a maximum variation of 9% in cost per flight (for kerolox case), the overall trend remains the same despite the different storage temperature.

Parameter	**Hydrolox**	**Kerolox**	**Methalox**	**Methalox**
Storage Temperature	20K	25 °C	80K	112K
GLOM [ton]	218.5	458.4	408.2	409.6
Dry Mass [ton]	23.8	23.4	24.7	24.9
Cpf [M€]	61.5	43.7	44.2	44.3

Table 6.9: Propellant Storage temperature Uncertainty Results

Sensitivity Analysis of modelling assumptions shows that, for most assumptions considered, the optimum result is insensitive to variation in these assumptions. However, this is not the case for uncertainty in engine mass and length estimation relations for methalox propellant. Results indicate potential for variation in propellant comparison, and hence derivation of engine mass and length estimation for methalox propellant is recommended.

6.2. Monte Carlo Analysis

The Monte Carlo analysis is different from the OAT approach. Monte Carlo analysis allows all parameters to be varied randomly at the same time. This approach leads to more realistic deviation from the nominal case, as the individual model uncertainties are combined. For the Monte Carlo analysis, the uncertainties considered are those in the modelling errors, as the OAT approach shows that Cost per flight is more sensitive to uncertainty in modelling error than in error in common assumptions. The errors were randomly varied across the absolute error values, for 150 runs. The mean μ, and standard deviation σ of the Monte Carlo runs are listed in Table 6.10.

Parameter	**GLOM [ton]**	**Dry Mass [ton]**	**CpF [M€]**
Nominal	212.2 ton	22.2 ton	59.6 M€
σ	24.0	5.0	5.9
μ	211.9	22.7	59.8
$\mu - \sigma$	187.9	17.7	53.7
$\mu + \sigma$	235.9	27.7	65.9

Table 6.10: Monte Carlo Analysis Results

Table 6.10 shows the average and the standard deviation of the 150 simulation runs for Hydrolox GTO ELV case. Over the 150 simulation runs, combined effect of different modelling errors deviates from the average, as shown below. Compared to the nominal case, the effect of combined errors shows that the average dry mass is overestimated by 2.3% and average cost is overestimated by under 0.4%. The average GLOM remains fairly similar to nominal case, highlighting that most of the deviation in the average dry mass comes from errors in

the launcher stage geometry and mass modelling and engine mass and length modelling. Figure 6.1 confirms that the common modelling errors does not vary the propellant comparison, that the variation is in cost gap not trend.

- GLOM: ± 11.3 %
- Dry Mass: ± 22.0 %
- Cost per Flight: ± 10.3 %

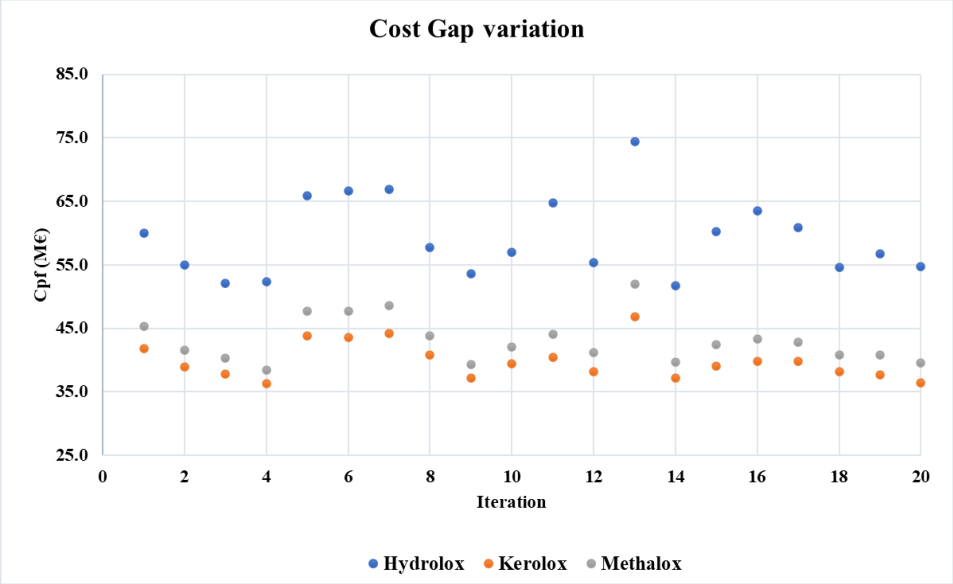

Figure 6.1: Cost per Flight gap variation

It is important to note that the cost variation gap between kerolox and methalox is quite small compared to that between hydrolox. This cost gap can be further reduced if lower refurbishment potential for methalox is considered, which is covered in the next section.

6.3. Refurbishment Cost Uncertainty

As mentioned in Section 5.4.1, the refurbishment costs for reusable launchers is an important parameter, in particular for kerolox and methalox propellant comparison. It was seen that optimum methalox design has only 10% higher cost per flight compared to optimum kerolox —this while not considering the potential of lower refurbishment costs of methalox and taking into account methalox engine correction factors. Assuming methalox engine mass estimation similar to that of kerolox has already showed significant impact in the cost comparison of these two propellant combinations, Section 6.1.2. In this section, the sensitivity of refurbishment factor on refurbishment costs is considered.

Refurbishment costs are calculated using Equation 6.2, where n is the number of reuses and C_{prod} is the production costs. Furthermore, with each reuse, the maintenance requirement increases. This is accounted for by including the parameter 'k' to account for maintenance requirement. Typical value of 'k' is considered between 105-115% [69]. For this study, it is considered as the upper limit of 115%. The production costs are calculated as shown in

Equation 6.3, where 'a' and 'b' represent cost coefficients, M represents the dry mass of the component.

$$C_{ref} = C_{prod} \times \left(0.25.n^{\frac{ln(k)}{ln(2)}}\right) \tag{6.2}$$

$$C_{prod} = a.(M)^b \tag{6.3}$$

To analyse the reusability potential of methalox engine, the refurbishment cost variation is considered with different values of parameter 'k'. The comparison of kerolox and methalox is performed for same thrust level. Equation 6.4 and Equation 6.5 show the refurbishment cost as a percentage of production costs for methalox and kerolox engines. The '1.3' term in Equation 6.4 is from the correction factor derived in Section 3.2. Furthermore, the term 'b' is the same for both kerolox and methalox engines. For kerolox engines, the parameter 'k' is set to 1.15.

$$\left(\frac{C_{ref}}{C_{prod}}\right)_{CH_4} = 1.3^b \times 0.25.n^{\frac{ln(k)}{ln(2)}} \tag{6.4}$$

$$\left(\frac{C_{ref}}{C_{prod}}\right)_{RP1} = 0.25.n^{\frac{ln(1.15)}{ln(2)}} \tag{6.5}$$

The different 'k' factors considered for methalox engines are listed below.

1. Same as Kerolox = 1.15
2. 5% less = 1.1
3. 10% less = 1.05

Figure 6.2 shows the plot of variation of refurbishment cost (as a percentage of production cost) with number of reuses. What can be seen is that for the same 'k' factor as kerolox, methalox engine refurbishment cost, represented by the orange curve—top curve, is higher than that of kerolox and follows a similar trend in increase as that of kerolox, represented by the blue curve—2nd curve. This is because the variation now is driven by the methalox engine mass. Varying the 'k' factor shows interesting results:

- 5% reduction (represented by the yellow curve—3rd curve)—what is noticed is for the first approximately 10 reuses, the influence of 'k' factor is rather small, and the costs are still high for methalox engine given its mass. Beyond 10 reuses, represented by the vertical green line (2nd line), the influence of improved refurbishment is valuable.
- 10% reduction (represented by the purple curve—4th curve)-this significantly lower refurbishment requirement reflects in drastic reduction in refurbishment costs between methalox and kerolox engine after just mere 3 reuses (represented by vertical blue line (1st line)).

Results indicate that just 5% lower refurbishment requirement can drastically change the cost comparisons. Typically, the range of refurbishment costs are between 3-50% [35, 26]. Setting 50% as an indication of major refurbishment (horizontal black line), it can be seen that

methalox engines can be reused more times compared to kerolox engine before major refurbishment. SpaceX's Merlin engines were built with a goal of 10 reuses before major refurbishment [60]. Therefore, for a significant reduction in refurbishment cost compared to current kerolox engines and thus an incentive for switching from kerolox to methalox, the difference between refurbishment requirement reduction for methalox engines must be greater than 5%.

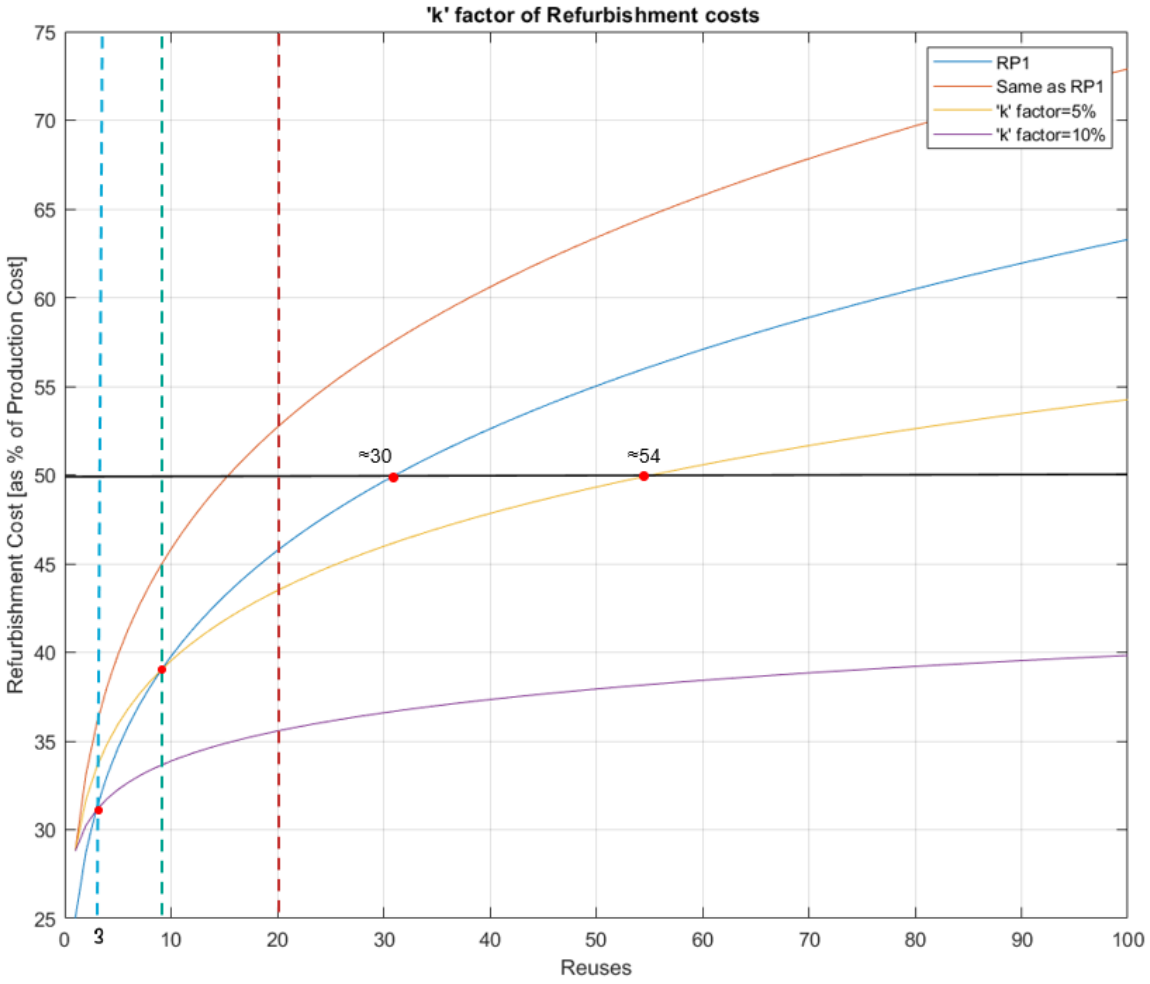

Figure 6.2: Variation in Refurbishment cost for different reusability factor

It is important to note, however, hydrocarbon based engines such as kerolox and methalox are typically run at oxidizer-rich mixture ratio to prevent soot formation. Work by Nickerson et al. [45] shows that the soot formation at fuel rich mixture ratios for kerosene is significant compared to methalox. But at oxidizer rich mixture ratios, there is negligible soot formation by both kerolox and methalox, Figure 2.2. Therefore, the potential of lower refurbishment costs exists only if these engines are run at fuel rich mixture ratios.

7

Conclusion and Recommendations

This chapter presents the conclusions of the research questions laid out for this research and presents recommendations that could improve the current research.

7.1. Conclusion

Research into methalox as a potential propellant to power future launcher missions is extensive in literature [30]. In this study, a cost based comparative study of methalox propellant with existing traditional propellants such as hydrolox and kerolox was performed. To perform this research, two different mission scenarios were considered. In addition to this, different launcher configuration in terms of reusability were considered. Furthermore, to offer a wide range of potential launcher design, different propellant combinations were considered. The main research question for this thesis was:

"Can Liquid Oxygen/Liquid Methane propellant combination achieve lower costs compared to Liquid Oxygen/Liquid Hydrogen and Liquid Oxygen/ Kerosene ?"

From the models developed, and the analysis performed in the current research, it can be concluded that methalox based launchers are cost-effective solution for future missions when compared to hydrolox, regardless of mission type or launcher configuration considered in the current study. Across various simulations considered in this study, pure methalox combination outperformed pure hydrolox propellant designs cost wise. The maximum potential for cost improvement by switching from pure hydrolox to pure methalox was noticed for Low Earth Orbit case, with potential to reduce cost per flight by 33%. Methalox-hydrolox combination also showed potential to reduce cost per flight by 17% compared to pure hydrolox propellant, by merely swapping low density hydrolox first stage for relatively higher density methalox.

Unlike for hydrolox and methalox, where the properties of the two propellants are relatively different and thus a clear influence of these properties on costs is noticed, kerolox and methalox propellant designs showed interesting results. The influence of launcher configuration on propellant comparison was noticeable in the comparison between kerolox and methalox. Across different simulations and propellant combinations, pure methalox designs resulted in higher cost per flight compared to pure kerolox - in the range of 2.5-10%. However, methalox as

upper stage in combination with kerolox as lower stage propellant showed potential for cost reduction compared to kerolox. For the expendable launcher case, the cost optimum propellant was a combination of kerolox-methalox. By switching upper stage to methalox propellant, marginal cost reduction of 1% over pure kerolox can be achieved. On the other hand, for reusable configuration, pure kerolox was the cost optimum propellant combination, just under 2% cost reduction compared to kerolox-methalox combination. Therefore, switching from kerolox upper stage to methalox upper stage shows marginal variation in cost per flight. All other combinations of kerolox and methalox were similar or somewhere in between these two combinations. **Therefore, methalox can achieve lower costs compared to kerolox for expendable launcher configuration with kerolox-methalox design.**

Type of recovery method showed no influence on propellant comparison. The cost optimum recovery method for the different launcher designs was a combination of HIAD, Subsonic Parachutes and Airbags. Furthermore, apart from the case of pure kerolox and kerolox-methalox combination, launcher configuration showed minimal influence on the optimum cost propellant choice. Similarly, the target orbit showed no variation in propellant comparison, however, showed potential of running into increased cost per flight for hydrolox launcher as a consequence of increased payload mass. Across different simulations, the trend of pure hydrolox design having the highest cost per flight, followed by methalox and then kerolox was prevalent. The different propellant combination designs showed potential to either marginally lower costs or have cost per flight within the pure combinations. Sensitivity analysis confirmed that the errors in the models implemented and assumptions considered in the current study do not influence this trend, except in the case of methalox engine mass estimation. Sensitivity analysis of lower refurbishment requirement of methalox compared to kerolox however, shows potential for purely methalox combination to lower the cost gap compared to kerolox, relevant for fuel rich mixture ratios.

The Multidisciplinary Design Analysis and Optimization (MDAO) extension to existing FRT tool meets all the functional requirements set in Chapter 2, with the status of each requirement presented in Table 7.1. The requirements that were not entirely met were the stage inert mass and length predictions.

In conclusion, within the scope of current study, methalox systems to replace hydrolox systems for Earth based missions is justified by the potential to achieve significant cost reductions. However, compared to kerolox, only a marginal cost benefit can be achieved, that too only in the case of expendable configuration and in combination with kerolox. For expendable launcher, the lower refurbishment requirement of methalox over kerolox holds no significant value and therefore replacing kerolox with methalox for marginal cost advantage is questionable. However, for reusable configurations, purely methalox shows potential to achieve costs within 10% of that of kerolox, with potential to further lower this value given the lower refurbishment requirement, if the engines are run at fuel rich mixture ratios.

ID	Requirement	Design Module + FRT
REQ-FUNC-001	The tool shall be able to design launch vehicles.	✓
REQ-FUNC-002	The tool shall be able to incorporate reusability.	✓
REQ-FUNC-003	The tool shall be able to model Methalox launcher system.	✓
REQ-FUNC-004	The tool shall include recovery method models for Propulsive and Non-Propulsive ballistic methods.	✓
REQ-FUNC-005	The tool shall be able to simulate missions to Low Earth Orbit and Geostationary Transfer Orbit.	✓
REQ-FUNC-006	The tool shall include costing models for both expendable and reusable configuration.	✓
REQ-FUNC-007	The tool shall be able to output the Expendable launcher Geometry, mass, and cost parameters for comparative analysis.	✓
REQ-FUNC-008	The tool shall be able to output the Reusable launcher Geometry, mass, and cost parameters for comparative analysis.	✓
REQ-FUNC-009	The tool shall be able to output optimal ascent and descent trajectory parameters.	✓
REQ-PER-001	The design module shall be able to model the liquid stage thrust within 10% accuracy.	✓
REQ-PER-002	The design module shall be able to model the liquid stage Specific Impulse within 10% accuracy.	✓
REQ-PER-003	The design module shall be able to model the Engine Length within 10% accuracy.	✓
REQ-PER-004	The design module shall be able to model the Engine Mass within 10% accuracy.	Partial
REQ-PER-005	The design module shall be able to model the Launch Vehicle Inert Mass within 10% accuracy.	Partial
REQ-PER-006	The design module shall be able to model the Launch Vehicle stage length within 10% accuracy.	Partial
REQ-PER-006	The design module shall be able to model the Launch Vehicle Gross Lift-Off Mass within 10% accuracy.	✓

Table 7.1: Status of requirements set for tool developed for current study

7.2. Recommendations

In this section, recommendations are made regarding potential improvements to the new design model and tool.

- **Methalox system Recommendations**
  - The current study does not consider reliability as a factor. Especially for a new propellant combination such as methalox reliability must be factored into the design and costing process. Estimating the reliability of methane based systems is

especially important to provide a holistic comparison of methane based systems to traditional, flight proven propellants. The work of Soares [58] presents a methodology to incorporate reliability in terms of cost of failure.
  - Sensitivity analysis indicates the potential of methalox to perform better than kerolox cost wise, if refurbishment potential is considered. Although, work by Nickerson et al. shows that soot formation for kerosene is significant compared to methane only at fuel rich mixture ratio [45]. At oxidizer-rich mixture ratio, the soot formation of the two propellants is similar and negligible. Therefore, whether soot formation is a serious issue for kerolox based engines compared to methalox must be analysed.
  - The current methalox models are based on those identified in literature and typically comparable to kerolox systems, with minor factors introduced to account for propellant change. These factors were derived based on Russian kerolox engines that were redesigned for methane. Furthermore, sensitivity analysis shows uncertainty in this parameter affects propellant comparison. Therefore, these models can be refined based on recent literature.

- **Modelling and Tool Recommendations**

  - Sensitivity Analysis shows that the Launcher length and inert mass calculations have large margins of error. Potential improvements in the form of correction factors, refined modelling or detailed launcher geometry and mass modelling must be considered.
  - The current Multidisciplinary Design Analysis and Optimization (MDAO) model can be improved by including the cost analysis in the design loop to obtain truly, cost optimum designs.
  - The trajectory optimization in the FRT tool is based on a database system. The trajectory optimization of the tool, for launchers similar to Falcon 9, can be performed relatively quickly. Any new design, such as a small launcher, takes a longer time. Therefore, the trajectory optimization algorithm can be improved to lower the simulation time.
  - It is assumed, both in the MDAO model and the FRT tool, that the designed launchers can sustain flight loads. This may not always be the case. Therefore, additional mass based on these loads would lead to a comparatively realistic case.
  - In the current MDAO model, the optimum number of engines is obtained from the perspective of mass. However, literature suggests in addition to mass, the optimum number of engines is driven by the cost and reliability levels [37]. To improve the optimum number of engines estimation, these factors must be accounted for, especially given that engines are the most expensive component (higher cost per kg) of the launch vehicle.

- The current study does not factor into the influence of objective function on propellant comparison. This can be an interesting addition to the current findings.
- For hydrolox launcher design, inclusion of boosters is recommended to analyse how the cost comparison would vary, given in reality purely hydrolox launchers make use of boosters for initial thrust.

References

[1] Kevin Spencer G Anglim. *Minimum-fuel optimal trajectory for reusable first-stage rocket landing using Particle Swarm Optimization*. California State University, Long Beach, 2016.

[2] SV Antonenko and SA Belavskiy. "Mid-Air Retrieval technology for returning of reusable launch vehicles' boosters". In: *Progress in Propulsion Physics* 1 (2009), pp. 481–494.

[3] Mathieu Balesdent. "Multidisciplinary design optimization of launch vehicles". PhD thesis. Ecole Centrale de Nantes (ECN), 2011.

[4] Mathieu Balesdent et al. "A survey of multidisciplinary design optimization methods in launch vehicle design". In: *Structural and Multidisciplinary optimization* 45.5 (2012), pp. 619–642.

[5] Douglas J Bayley et al. "Design optimization of a space launch vehicle using a genetic algorithm". In: *Journal of Spacecraft and Rockets* 45.4 (2008), pp. 733–740.

[6] Robert A Braeunig. *Rocket and space technology*. 2005.

[7] Robert D Braun, Arlene A Moore, and Ilan M Kroo. "Collaborative approach to launch vehicle design". In: *Journal of spacecraft and rockets* 34.4 (1997), pp. 478–486.

[8] Gordon P Briggs and John F Milthorpe. "Strategic Propellant Choices for an Australian Medium Launch Vehicle". In: *7th Australian Space Science Conference, Sydney, Australia*. 2007.

[9] Kendall K Brown. *Technology Challenges for Operationally Responsive Spacelift*. Airpower Research Institute, College of Aerospace Doctrine, Research and …, 2004.

[10] Holger Burkhardt et al. "Comparative study of kerosene and methane propellant engines for reusable liquid booster stages". In: *4th international conference on launcher technology" Space Launcher Liquid Propulsion*. 2002, pp. 3–6.

[11] Francesco Castellini. "Multidisciplinary design optimization for expendable launch vehicles". In: (2012).

[12] Stephane Contant. "Design and Optimization of a Small Reusable Launch Vehicle Using Vertical Landing Techniques". In: (2019).

[13] Bret G Drake, Stephen J Hoffman, and David W Beaty. "Human exploration of Mars, design reference architecture 5.0". In: *2010 IEEE Aerospace Conference*. IEEE. 2010, pp. 1–24.

[14] NT Drenthe et al. "Cost estimating of commercial smallsat launch vehicles". In: *Acta Astronautica* 155 (2019), pp. 160–169.

[15] Kai Dresia et al. "Multidisciplinary design optimization of reusable launch vehicles for different propellants and objectives". In: *Journal of Spacecraft and Rockets* 58.4 (2021), pp. 1017–1029.

[16] Andrew SC Ehrenberg. “Rudiments of numeracy”. In: *Journal of the Royal Statistical Society: Series A (General)* 140.3 (1977), pp. 277–297.

[17] *Engine Database*. URL: `http://www.astronautix.com/`.

[18] RRL Ernst. “Liquid Rocket Analysis (LiRA): development of a liquid bi-propellant rocket engine design, analysis and optimization tool”. In: (2014).

[19] *Evolution of SpaceX Merlin Engines*. URL: `http://www.b14643.de/Spacerockets_2/United_States_1/Falcon-9/Merlin/index.htm`.

[20] Federico Ferretti, Andrea Saltelli, and Stefano Tarantola. “Trends in sensitivity analysis practice in the last decade”. In: *Science of the total environment* 568 (2016), pp. 666–670.

[21] Bryan C Fuqua. *ENRE 655 Class Project. Development of the Initial Main Parachute Failure Probability for the Constellation Program (CxP) Orion Crew Exploration Vehicle (CEV) Parachute Assembly System (CPAS)*. Tech. rep. 2010.

[22] Ronald L Graham et al. “Dense packings of congruent circles in a circle”. In: *Discrete Mathematics* 181.1-3 (1998), pp. 139–154.

[23] H Groemer. “Some basic properties of packing and covering constants”. In: *Discrete & Computational Geometry* 1.2 (1986), pp. 183–193.

[24] RJG Hermsen. “Cryogenic propellant tank pressurization”. In: (2017).

[25] Rosemary Hernandez and STEVE MERCER. “Carbon deposition characteristics of LO2/HC propellants”. In: *23rd Joint Propulsion Conference*. 1987, p. 1855.

[26] Todd Herrmann and David Akin. “A critical parameter optimization of launch vehicle costs”. In: *Space 2005*. 2005, p. 6680.

[27] SAKAGUCHI Hiroyuki. “Development of methane engine enabling reusable launch vehicle and long-term in-space operations”. In: *IHI Engineering Review* 51.2 (2018).

[28] Majid Hosseini et al. “Multidisciplinary design optimization of an expendable launch vehicle”. In: *Proceedings of 5th International Conference on Recent Advances in Space Technologies-RAST2011*. IEEE. 2011, pp. 702–707.

[29] Dieter K Huzel. *Modern engineering for design of liquid-propellant rocket engines*. Vol. 147. AiAA, 1992.

[30] Swati Shridhar Iyer. “Literature Study of Liquid Oxygen/Liquid Methane Propellant for Low Cost Reusable Launch Vehicle”. In: *TU Delft* (2021).

[31] Simon Jentzsch. “Optimization of a Reusable Launch Vehicle Using Genetic Algorithms”. PhD thesis. RWTH Aachen, 2020.

[32] Jahangir Jodei, Masoud Ebrahimi, and Jafar Roshanian. “Multidisciplinary design optimization of a small solid propellant launch vehicle using system sensitivity analysis”. In: *Structural and Multidisciplinary Optimization* 38.1 (2009), pp. 93–100.

[33] Aaron N Johnson et al. “Numerical characterization of the discharge coefficient in critical nozzles”. In: *NCSL Conference Proceedings, Albuquerque, NM*. 1998, pp. 407–422.

[34] Harry Jones. “The recent large reduction in space launch cost”. In: 48th International Conference on Environmental Systems. 2018.

[35] Dietrich E Koelle. “Handbook of cost engineering for space transportation systems with transcost 7.0”. In: *TCS—Trans Cost Systems, Ottobrunn* (2000).

[36] Dietrich E Koelle. “The transcost-model for launch vehicle cost estimation and its application to future systems analysis”. In: *Acta Astronautica* 11.12 (1984), pp. 803–817.

[37] Geoffrey A Landis. “How Many Engines Should a Rocket Have?” In: *49th AIAA/ASME/SAE/ASEE Joint PropulsionConference*. 2013, p. 4176.

[38] Wiley J Larson et al. *Applied space systems engineering*. CEI, 2018.

[39] *Launch Vehicle Database*. URL: `https://www.spacelaunchreport.com/`.

[40] Minjiao Li, Xiaoting Rui, and Laith K Abbas. “Elastic dynamic effects on the trajectory of a flexible launch vehicle”. In: *Journal of Spacecraft and Rockets* 52.6 (2015), pp. 1586–1602.

[41] John Livingston. “Comparative Analysis of Rocket and Airbreathing Launch Vehicles”. In: *Space 2004 Conference and Exhibit*. 2004, p. 5948.

[42] Todd Mosher. “Spacecraft design using a genetic algorithm optimization approach”. In: *1998 IEEE Aerospace Conference Proceedings (Cat. No. 98TH8339)*. Vol. 3. IEEE. 1998, pp. 123–134.

[43] Elon Musk. “Making humans a multi-planetary species”. In: *New Space* 5.2 (2017), pp. 46–61.

[44] RV Mykhalchyshyn, MS Brezgin, and DA Lomskoi. “METHANE, KEROSENE, AND HYDROGEN COMPARISON AS A ROCKET FUEL FOR LAUNCH VEHICLE PHSS DEVELOPMENT”. In: *Космічні енергетика і двигуни* (2018), p. 12.

[45] G Nickerson and C Johnson. “A soot prediction model for the TDK computer program”. In: *28th Joint Propulsion Conference and Exhibit*. 1992, p. 3391.

[46] *Optimum Expansion Ratio*. URL: `http://www.braeunig.us/space/`.

[47] Pascal Pempie, Thomas Froehlich, and Hilda Vernin. “LOX/methane and LOX/kerosene high thrust engine trade-off”. In: *37th Joint Propulsion Conference and Exhibit*. 2001, p. 3542.

[48] Pascal Pempie and Hilda Vernin. “Reusable expendable launcher cost analysis”. In: *36th AIAA/ASME/SAE/ASEE Joint Propulsion Conference and Exhibit*. 2000, p. 3738.

[49] Steven S Pietrobon. “Analysis of propellant tank masses”. In: *Submitted to Review of US Human Space Flight Plans Committee* 6 (2009).

[50] D Preclik et al. “Reusability aspects for space transportation rocket engines: programmatic status and outlook”. In: *CEAS Space Journal* 1.1 (2011), pp. 71–82.

[51] *Price (or cost) of rocket engines*. URL: `https://forum.nasaspaceflight.com/index.php?topic=43053.0`.

[52] Amer Farhan Rafique et al. “Multidisciplinary design of air launched satellite launch vehicle: Performance comparison of heuristic optimization methods”. In: *Acta Astronautica* 67.7-8 (2010), pp. 826–844.

[53] Mohamed Ragab and F McNeil Cheatwood. “Launch vehicle recovery and reuse”. In: *AIAA Space 2015 Conference and Exposition*. 2015, p. 4490.

[54] Daniel Rasky, R Bruce Pittman, and Mark Newfield. “The reusable launch vehicle challenge”. In: *Space 2006*. 2006, p. 7208.

[55] Mark Rozemeijer. “Launch Vehicle First Stage Reusability: a study to compare different recovery options for a reusable launch vehicle”. In: (2020).

[56] *Russian space-rocket and missile liquid-propellant engines*. URL: http://www.b14643.de/Spacerockets/Specials/Russian_Rocket_engines/engines.htm.

[57] Martin Sippel et al. “High-Performance, Partially Reusable Launchers for Europe”. In: *Proceedings of the International Astronautical Congress, IAC*. 2020.

[58] Gonçalo Soares dos Santos Vera-Cruz Pinto. “Reliability and Cost Modeling of Reusable Launch Vehicles: Predicting, Preventing and Mitigating the Cost of Failure”. In: (2022).

[59] *SpaceX Grid fins*. URL: https://space.stackexchange.com/questions/22096/how-are-the-spacex-falcon-9-mod-3-and-mod-4-grid-fins-different.

[60] *SpaceX Rocket Flies 10 Times as Reusability Gets Surprisingly Routine*. URL: https://singularityhub.com/2021/05/17/spacex-milestone-signals-reusable-rockets-are-becoming-mainstream/.

[61] *SpaceX Starship SN9 Simulation*. URL: https://spaceexplored.com/2020/12/09/spacex-starship-sn8-aced-launch-and-bellyflop-maneuver-landing-explosive-data-collected/.

[62] *SpaceX’s upgraded Crew Dragon parachutes breeze through 13 drop tests*. URL: https://newatlas.com/space/spacexs-upgraded-crew-dragon-parachutes-13-drop-tests/.

[63] Jill C Stoltzfus. “Logistic regression: a brief primer”. In: *Academic Emergency Medicine* 18.10 (2011), pp. 1099–1104.

[64] George P Sutton and Oscar Biblarz. *Rocket propulsion elements*. John Wiley & Sons, 2016.

[65] Paul V Tartabini et al. *Payload Performance Analysis for a Reusable Two-Stage-to-Orbit Vehicle*. Tech. rep. 2015.

[66] Dominique Valentian et al. “Green propellants options for launchers, manned capsules and interplanetary missions”. In: *ESA Special Publication*. Vol. 557. 2004.

[67] MW Van Kesteren. “Air launch versus ground launch: a multidisciplinary design optimization study of expendable launch vehicles on cost and performance”. In: (2013).

[68] JMV Vandamme. “Assisted-launch performance analysis: Using trajectory and vehicle optimization”. In: (2012).

[69] James R Wertz. “Economic model of reusable vs. expendable launch vehicles”. In: *IAF, International Astronautical Congress, 51 st, Rio de Janeiro, Brazil*. 2000.

[70] *Will LandSpace be China’s SpaceX?* URL: https://www.thespacereview.com/article/3787/1.

[71] David Michael Woodward et al. “Space Launch Vehicle Design: Conceptual Design of Rocket Powered, Vertical Takeoff, Fully Expendable and First Stage Boostback Space Launch Vehicles”. PhD thesis. 2018.

[72] Firas Yengui et al. “A hybrid GA-SQP algorithm for analog circuits sizing”. In: (2012).

[73] Barry Zandbergen. “Thermal rocket propulsion”. In: *Delft University of Technology* 2 (2003).

[74] BTC Zandbergen. “Simple mass and size estimation relationships of pump fed rocket engines for launch vehicle conceptual design”. In: *6th European Conference for Aeronautics and Space Sciences (EUCASS)*. 2015.

[75] T Zedníček. “Commercial versus cots+ versus qualified passive components in space applications”. In: *SA/ESTEC, Noordwijk, The Netherlands* (2016).

A

Engine Database

Table A.1 shows the Engine database used for the verification and validation in Chapter 3.

Engine	**Propellant**	**P_c [bar]**	**OF [-]**	**ϵ [-]**	**$\dot{m}$ [kg/s]**	**t_b [s]**	**D_e [m]**	**L_{engine} [m]**	**$F_{T,vac}$ [kN]**	**I_{sp} [s]**	**M_{engine} [kg]**
RS-68 A	LOX/LH_2	102.6	5.97	21.5	-	245	2.43	5.2	3137	411	6685
Merlin 1A	LOX/RP1	53.92	2.2	14.5	130.5	169	1.68	2.89	378	300	760
Merlin 1C	LOX/RP1	67.7	2.2	14.5	161.5	169	1.43	2.86	614	304	630
Rocketdyne H-1	LOX/RP1	40	2.23	8	244	150	0.82	2.13	947	289	635
RD-171	LOX/RP1	245.2	2.63	36.87	2392.5	150	3.78	4.02	7900	337	9500
RD-180	LOX/RP1	256.6	2.72	36.4	1250	270	3.15	3.56	4150	339	5480
Merlin 1D	LOX/RP1	97	2.34	16	236.6	180	0.92	2.18	981	311	470
RD-108	LOX/RP1	51	2.39	18.86	76.16	340	0.67	2.86	941	315	1250
Rocketdyne F1	LOX/RP1	70	2.27	16	2578	161	3.7	5.6	7770	304	8400
Vulcain-2	LOX/LH_2	116	6.7	61.5	326.6	540	2.09	3.44	1350	434	811
NK-33	LOX/RP1	145.7	2.8	27	517.9	600	1.5	3.71	1638	331	1222
RS-27	LOX/RP1	49	2.25	8	361	274	1.07	3.63	1023	295	1027
Vulcain 1	LOX/LH_2	100	5.3	45	235.9	605	1.76	3.05	1140	431	1300
Rocketdyne J-2	LOX/LH_2	52.61	5.5	27.5	240.72	500	2.1	3.4	1033	421	1788.1
RD-120	LOX/RP1	162.8	2.6	106.7	242.9	315	1.95	3.87	834	350	1125
RD-8	LOX/RP1	76.5	2.4	-	-	1100	4	1.67	78.45	342	380
RL10A-4-2	LOX/LH_2	39	5.5	84	16	740	1.2	2.29	99	451	167
Merlin 1DV	LOX/RP1	97.2	2.36	164	236.56	375	2.89	3.3	934	347	490
RD-0109	LOX/RP1	50	2.14	79.4	17.1	430	0.73	1.56	54.5	323.5	121
HM7B	LOX/LH_2	37	5	83.1	14.8	945	0.99	2.01	64.8	444.6	165
RL-10B-2	LOX/LH_2	44.12	5.88	250	24.1	700	2.15	4.15	110	462	310.2
RD-160	LOX/CH_4	118	3.69	352	-	900	0.76	1.7	1.9	381	129

Table A.1: Engine Database consolidated from Literature [4, 5, 17, 9, 3]

B

Discharge Coefficient Comparison

B.1. Correction Factor Comparison

Figure B.1a and Figure B.1b shows a comparison of vacuum specific impulse and vacuum thrust estimated by the work of Contant [3], the current study and the value found in literature. The vacuum specific impulse prediction is fairly similar to that of Contant. It is evident that the current study, compared to that of Contant, underestimates the vacuum thrust. The reason for this is the mass flow rate correction performed in the current study, work by Contant only corrects for specific impulse. Although, the current correction factors underestimate thrust, the accuracy achieved is still within the 10% limit as seen in Section 3.4. Furthermore, Chapter 6, shows that for minimal impact on costs as a result of thrust modelling error. The current thrust model estimates thrust with 2.35% accuracy.

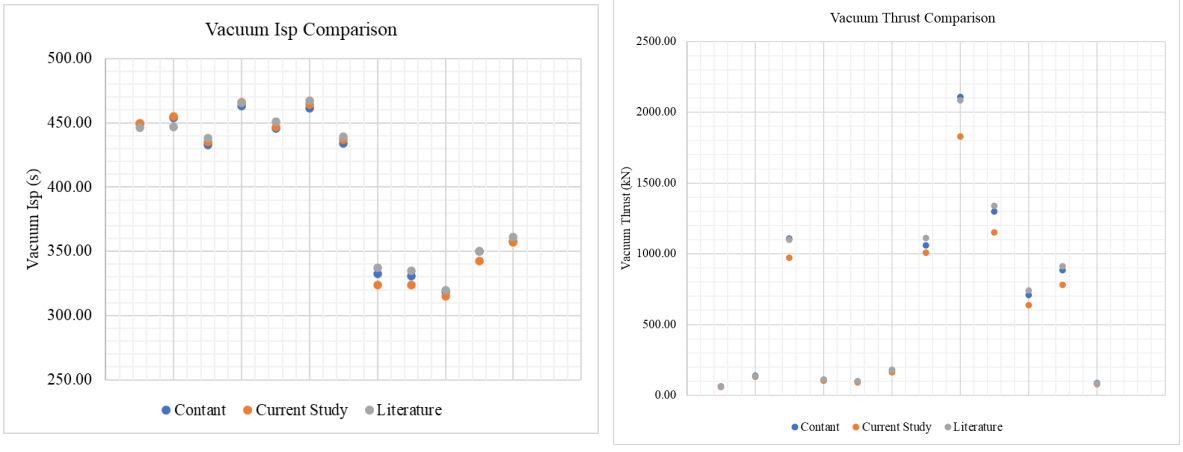

(a) Specific Impulse Comparison

(b) Vacuum Thrust Comparison

Figure B.1: Correction Factor Comparison

For future studies, it is recommended to derive mass flow rate correction factor from the thrust and specific impulse, Equation B.1. The reason for this being, the thrust data for engines is much easily available, unlike the mass flow rate. Furthermore, there remains ambiguity around the engine conditions for the mass flow rate values from literature. Another alternative is to consider the IRT value of mass flow rate. Figure B.2 shows slight overestimation of thrust

with the improved mass flow rate correction factor.

$$C_d = \frac{F_{real} \times I_{sp,ideal}}{F_{ideal} \times I_{sp,real}} \tag{B.1}$$

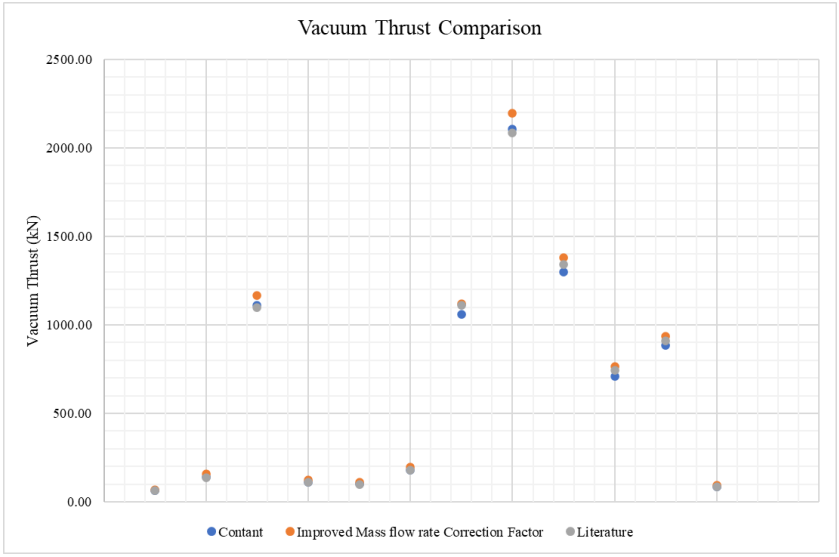

Figure B.2: Improved Vacuum Thrust Comparison

C

Aerodynamics, Trajectory and Cost Models

In this section, a brief discussion of the aerodynamics, trajectory, and cost model implemented in existing FRT is presented. These models have been validated in the work of Rozemeijer [16].

C.1. Aerodynamics Model

The general drag model is based on the standard equation presented in Equation C.1, where C_D is the drag coefficient, q is the dynamic pressure and S represents the wetted area. For reusable launchers, recovery methods such as—landing legs, grid fins—are stowed during ascent and does not change the overall launcher area and no additional impact of recovery hardware on the general drag model is needed [16, 3]. However, during recovery using parachutes, the deployed parachutes have a significant impact on the drag forces. The FRT therefore considers two drag models, one for the general case and an additional parachute inflation model. A more detailed description of this model can be found in the work of Rozemeijer [16].

$$F_D = C_D.q.S \tag{C.1}$$

For the general drag model, the entire launcher is treated as a lumped mass and since for most recovery hardware the overall area of the launcher remains constant, the C_D varies only with the Mach Number. In the FRT, this C_D-Mach relation is considered as an input. This relation is calculated using existing open source RASAero II. The RASAero II is a well known open source tool that can calculate the drag coefficient between Mach 0 and Mach 25 for a given launcher configuration. The RASAero II assumes that the angle of attack of the vehicle remains zero during the flight. A similar assumption is considered by ParSim, which is a tool developed by Delft Aerospace Rocket Engineering (DARE) to calculate the force generated from parachute deployment in mid-air. The tool has been used in precious research and is validated [11, 12]. The ParSim tool considers a similar zero Angle of Attack assumption and results in trajectory error within 5%. The RASAero II is widely used in literature and compares well with the Wind tunnel model as shown in Figure C.1. A comparison of the Altitude prediction of RASAero II, showed an average error of 3.38%, Figure C.2 and 78% of the simulation cases have all parameters within 10% of the flight data. Other widely used drag prediction model is the Missile DATCOM. However, this model is not open source and furthermore, the existing open source tool is sufficiently accurate for conceptual design phase.

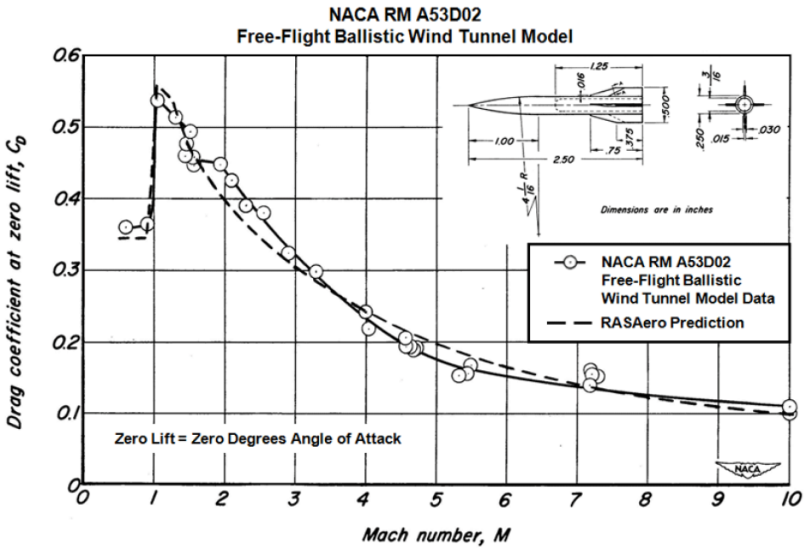

Figure C.1: RASAero II comparison with Wind Tunnel results [15]

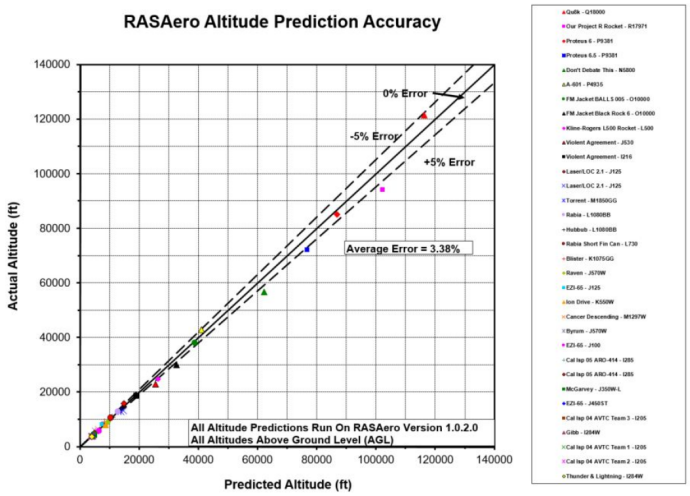

Figure C.2: RASAero II Altitude Prediction Accuracy [15]

Figure C.3 shows the typical drag variation with Mach number for launcher with different propellants. The drag variation with Mach for kerolox and methalox is similar, given the fairly similar launcher design. Hydrolox based launchers are slightly longer, given the lower density of hydrolox and the slenderness ratio constraint in the MDO process. This results in a slightly larger drag compared to kerolox and methalox.

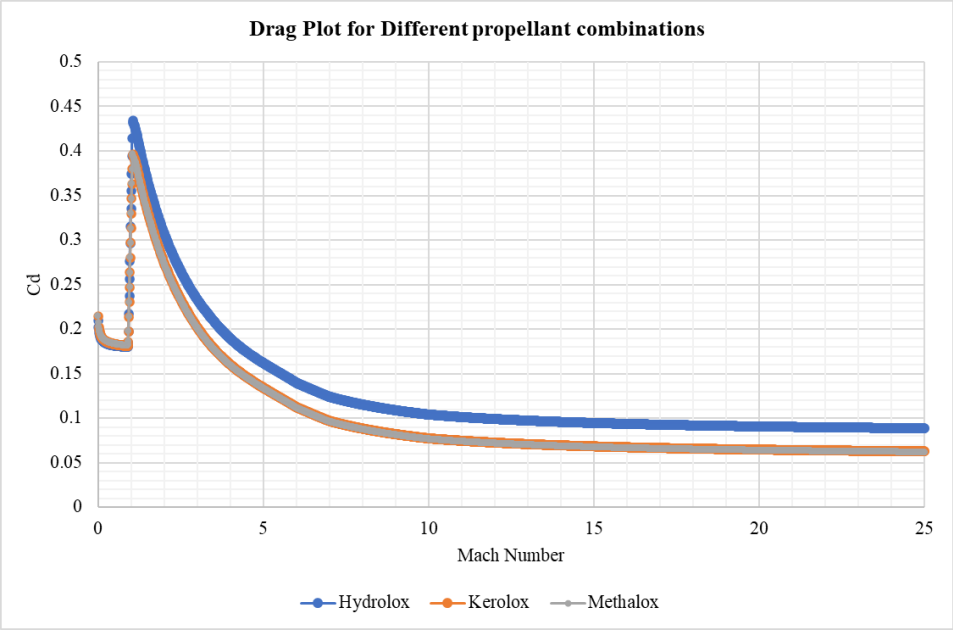

Figure C.3: Drag variation with Mach number for different propellant designs

C.2. Trajectory Model

The general trajectory equations of motion are implemented from the validated ParSim tool [12]. The axis-system considered for the trajectory model is seen in Figure C.4a. Since the current study is focused on Earth mission orbits, the perturbations from remaining planets and moons are ignored in the trajectory modelling. The typical equations of motion of the launcher in a rotational geocentric Reference frame or Earth-centered, Earth fixed reference frame (Figure C.4b) in spherical coordinates are presented through Equation C.2 and Equation C.7. For the current study, zero-lift launchers are considered and therefore, the lift terms in the below equations are zero i.e, L= 0. These models have been validated in [11, 12] and show under 2% error in calculating the altitude, velocity, and time of flight.

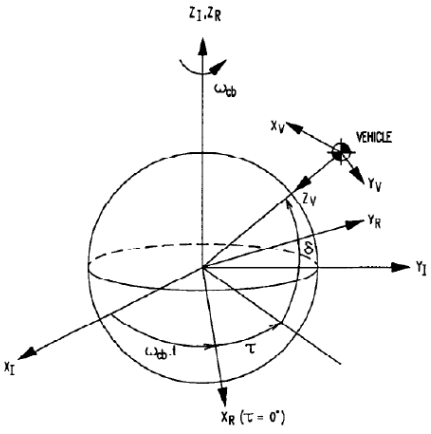

(a) Inertial and Local Horizon Frame [19]

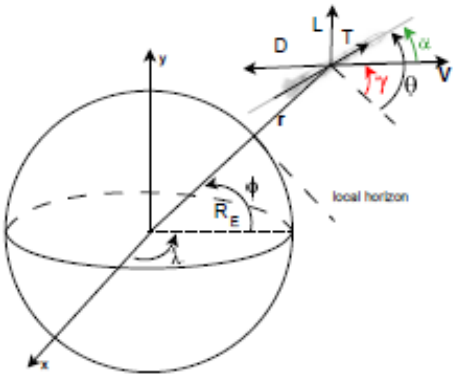

(b) Earth-centered, Earth fixed Reference frame [2]

Figure C.4: Trajectory Reference Frame

$$\dot{r} = Vsin(\gamma) \tag{C.2}$$

$$\dot{V} = \frac{Tcos(\theta-\gamma) - D}{m} - gsin(\gamma) + \omega_E.rcos(\delta)(sin(\gamma)cos(\delta) - sin(\delta)cos(\gamma)cos(\chi)) \tag{C.3}$$

$$\begin{aligned}\dot{\gamma} = \frac{[L + Tsin(\theta-\gamma)]cos(\mu)}{mV} + (\frac{V}{r} - \frac{g}{V})cos(\gamma) + 2\omega_E.sin(\chi)cos(\delta) \\ + \frac{\omega_E^2.rcos(\delta)(cos(\gamma)cos(\delta) + sin(\gamma)sin(\delta)cos(\chi))}{V}\end{aligned} \tag{C.4}$$

$$\dot{\tau} = \frac{Vcos(\gamma)sin(\chi)}{rcos(\delta)} \tag{C.5}$$

$$\dot{\delta} = \frac{Vcos(\gamma)cos(\chi)}{r} \tag{C.6}$$

$$\begin{aligned}\dot{\chi} = \frac{[L + Tsin(\theta-\gamma)]sin(\mu)}{mVcos(\gamma)} + \frac{Vcos(\gamma)sin(\chi)tan(\delta)}{r} \\ + 2\omega_E(sin(\delta) - cos(\chi)cos(\delta)tan(\gamma)) + \frac{\omega_E^2.rsin(\delta)cos(\delta)sin(\chi)}{Vcos(\gamma)}\end{aligned} \tag{C.7}$$

The gravity model implemented in the FRT is the central gravity field, which only depends on the distance from Earth's centre. The tool does provide the option to use spherical harmonics Gravity model, however for the current study the central gravity model is used as it is less complex, computationally less time-consuming and the work of Vandamme [20] shows that the effect of J_2 and J_3 harmonics is under 5%. The atmosphere model implemented is the 1976 COESA (Committee on Extension to the Standard Atmosphere). This atmosphere model is widely used in trajectory modelling and optimization in literature and has a range between 0 and, 84852 m [2, 19]. Beyond this altitude, the temperature, and pressure are extrapolated, linear for temperature and logarithmically for pressure [10].

The ascent trajectory is divided into different phases, shown in Figure C.5. The first stage burn is performed as a continuous burn, with capability of throttling until 15 km.Above 15 km the launcher returns to 100% thrust until MECO. Stage separation follows MECO. Stage 2 ignition, is performed to raise the apogee of current orbit to perigee to target orbit. After this, the first SECO is performed. This is followed by a coasting phase until upper stage reaches point of re-ignition to reach the final orbit. The descent is split according to recovery method—propulsive or non-propulsive. This is because of the need for a landing burn in the case of propulsive recovery. The FRT tool only considers Down range landing, as literature shows potential of payload loss of 40% when Return to launch site is considered for medium to heavy lift launchers [18].

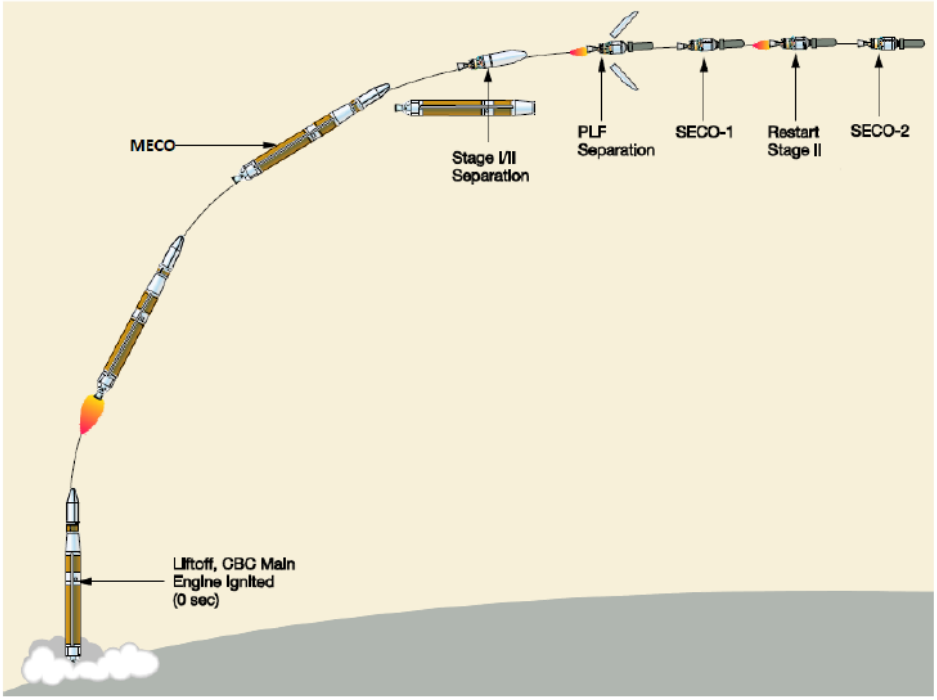

Figure C.5: Different phases in the ascent trajectory [16]

C.3. Cost Modelling

The TRANSCOST Model is a cost estimation model developed by Koelle [8]. The model was developed to provide cost estimation during the conceptual design phase. The model is organized in three major parts which are coupled, Figure C.6.

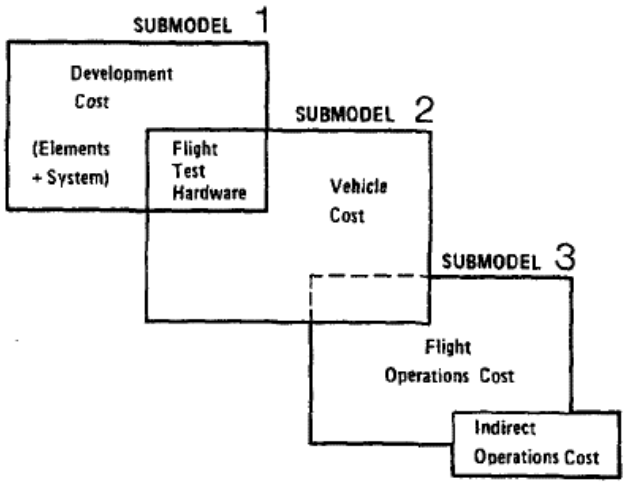

Fig. 1. Organization of the TRANSCOST-Model in three major submodels.

Figure C.6: TRANSCOST Model Organization [8]

The cost data considered in the estimation are the development cost, Vehicle cost, Operations cost. Each of the development and vehicle submodel include different technical groups including different propellant systems-Liquid Propellant Rocket engines, Solid Propellant Rocket

Motors, Pressure fed engines etc—type of launch vehicle – expendable, winged, crewed capsules. The cost estimation of all these models is based on the inert mass (M) and is calculated in terms of Man Years (MY), Equation C.8 – where 'a' is the system specific constant value and 'b'is the system specific cost to mass sensitivity factor, which have been derived based on historical data and vary for different propellants, Figure C.7. A more detailed derivation of the different submodels can be found in [7]. For methane based launchers, coefficients similar to that for kerolox is considered [6].

$$C = aM^b \tag{C.8}$$

Model	a	b	M
Development Cost			
pump fed liquid engine	277	0.48	Engine mass
solid engine	16.8	0.54	Engine Mass
stage development	98.5	0.555	stage empty mass
solid engine stage	22.4	0.54	stage empty mass
First Unit Production Cost			
RP1/LOX Engine Production	1.9	0.535	Engine Mass
LH2/LOX Engine Production	3.15	0.535	Engine Mass
RP1/LOX Tank Mass	1.84	0.59	Tank Mass
LH2/LOX Tank Mass	1.265	0.59	Tank Mass
Solid Engine & Stage	2.75	0.412	Stage Mass

Figure C.7: TRANSCOST Model Coefficients [16, 7]

The TRANSCOST model does not consider reusability and therefore lacks Reusability Cost models. Basic reusability cost model in literature considers recovery hardware cost models, retrieval costs and refurbishment costs [16, 13]. Recovery hardware costs are typically made up of the material cost and the production cost. Retrieval costs depend on the workforce required in terms of personnel and the cost of either the ship (for DRL) or the aeroplane/helicopter (for MAR). Refurbishment costs encompass all the costs involved from the point the stage is retrieved to the launcher ready at the launch pad, excluding the operations cost. The validation data of these equations is summarized in Appendix E.

D

Overview of Inputs, Outputs, and Constants

This section presents the inputs required to run the new design module. The typical output that can be saved from the module is presented. Finally, the constants considered in this design module are listed.

D.1. Inputs

The top level inputs required to run the design module are:

- Payload Mass [kg]
- Apogee Altitude [km]
- Perigee Altitude [km]
- Launch site Longitude [deg]
- Launch site Latitude [deg]
- Propellant Choice: The propellant choice is entered as an array, for e.g, [1 2] implies LOX/LH_2 propellant for stage 1 and LOX/RP1 for stage 2. To select a particular propellant, just enter the designated propellant number:
  - 1 : LOX/LH_2
  - 2: LOX/RP1
  - 3: LOX/CH_4
- Material Choice: the user can select the propellant tank material, by entering the designated material number:
  - 1: Al 7075-T6
  - 2: Al-Li 2195
  - 3: Al 2014-T6
  - 4: 4340 Steel
  - 5: Ti 6Al-4V
  - 6: CFRP
- Objective Function: The objective function can be selected by entering the designated objective function number:

- 1: Minimize GLOM
- 2: Minimize Dry Mass

D.2. Output

The typical outputs from the design module are listed below. These outputs are saved as .mat and .dat files. The outputs are listed for both stage 1 and stage 2.

Optimum Design Variables
- Chamber Pressure
- Mixture Ratio
- Burn Time
- Exit Pressure
- Engine Exit Diameter
- Stage Diameter
-Number of Engines

Propulsion Characteristics
- Vacuum Thrust
- Specific Impulse
- ΔV split
- Expansion Ratio

Geometry Characteristics
- Engine Length
- Tank Length
- Interstage Length
- Fairing Length

Mass Characteristics
- Propellant Mass
- Total Engine Mass
- Tank Mass
- Interstage Mass
- Avionics Mass
- EPS Mass - Payload Adapter Mass
- Fairing Mass
- Launch Pad interface mass
- Stage Dry Mass

Vehicle Overview
- Gross Lift-off Weight
- Total Propellant Mass
- Total Dry Mass
- Launch Vehicle Length

D.3. Constants

Table D.1 presents the parameters that remain constant in the current study. These parameters can be altered, in the "constants" Matlab file, as per the user preference.

Parameter [units]	Symbol	Value	Source
Mass Flow Rate Correction Factor [-]	C_d	0.95	Chapter 3
Vacuum I_{sp} Correction Factor [-]	ξ_s	0.93	Chapter 3
Residual Propellant factor [-]	k_{unused}	0.32%	[3, 16]
Safety Factor [-]	SF	1.4	[3, 16]
Methane Engine Mass Correction Factor [-]	ξ_{mass}	1.3	Chapter 3
Methane Engine Length Correction Factor [-]	ξ_{len}	1.2	Chapter 3
Tank Pressure [bar]	P_{tank}	4	[3, 21]

Table D.1: Values that remain constant in Modelling

D.4. Material Choices

The new design module allows the user to select the propellant storage tank material. In the current study, it is assumed that the propellant tanks form part of the primary launcher core structure. The material choices and structural parameters are listed in Table D.2. Material selection is typically based on 'specific strength' i.e, ratio of the strength to density. A higher specific strength indicates a stronger or lighter structure. For the current study, "Al-Li 2195" material is selected. The material is Aluminium Lithium alloy including Copper [1]. This material choice has a high specific strength and relatively low density, which results in lower inert mass Figure D.1. On average, reduction of 26% can be achieved by switching from Al 2219 material to Al-Li 2195 [14].

Material	Allowable Stress (MPa)	Density [kg/m^3]
Al 7075-T6	570	2810
Al-Li 2195	710	2600
Al 2014-T6	483	2700
4340 Steel	1793	7833
Ti 6Al-4V	1030	4420
CFRP	810	1600

Table D.2: Material Choices

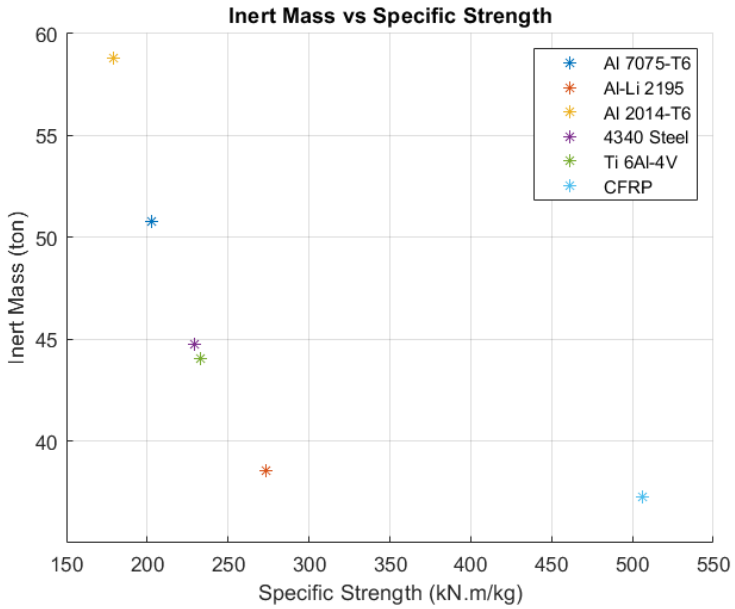

Figure D.1: Inert Mass vs Specific Strength for different materials

E

Model Error Overview

Table E.1 summarizes the error in the different models that make up the MDA and the overall tool implemented in the current study.

Model	Equation	Error [%]	Source	Remark
Specific Impulse	Equation 3.11	± 0.9	Table 3.19	Within performance requirements
Thrust	Equation 3.12	± 2.4	Table 3.19	Within performance requirements
Engine Mass	Equation 3.22	± 22.2	Table 3.21	Error can be reduced using equations listed in [22]. However, engine cycle type differentiation is not considered in the current study
Engine Length	Equation 3.17	± 9.0	Table 3.21	Within performance requirements
Stage Inert mass	Equation 3.15	± 18.9	Table 3.23	Error due to ambiguity in launcher data from literature
Stage length	Equation 3.14	± 19.1	Table 3.23	Error due to ambiguity in launcher data from literature
Extra Tank mass		± 6.1	[16]	-
Landing legs mass		± 10	[16]	-
Airbag mass		± 43.8	[16]	Accepted as sensitivity analysis performed in [16] show minimal impact of this error on cost estimation
Grid fin mass		± 24.4	[16]	Accepted as sensitivity analysis performed in [16] show minimal impact of this error on cost estimation
Hemisflo Mass		± 20	[16]	Accepted as sensitivity analysis performed in [16] show minimal impact of this error on cost estimation
Ringsail Mass		± 14	[16]	Accepted as sensitivity analysis performed in [16] show minimal impact of this error on cost estimation
HIAD Mass		± 4	[16]	-
RASAero II Drag	Equation C.1	± 10	Appendix C	Accepted as sensitivity analysis performed in [16] show minimal impact of this error on cost estimation
Parachute Inflation model		± 5	[16]	-
TRANSCOST model		± 20	[7]	-
Recovery hardware Cost model		± 50	[16]	Accepted as sensitivity analysis performed in [16] show minimal impact of this error on cost estimation

Table E.1: Model Accuracy

Appendix References

[1] *"NASA Facts: Super Lightweight External Tank" (PDF) (Press release). Huntsville, Alabama*. URL: https://www.nasa.gov/centers/marshall/pdf/113020main_shuttle_lightweight.pdf.

[2] Mathieu Balesdent. "Multidisciplinary design optimization of launch vehicles". PhD thesis. Ecole Centrale de Nantes (ECN), 2011.

[3] Stephane Contant. "Design and Optimization of a Small Reusable Launch Vehicle Using Vertical Landing Techniques". In: (2019).

[4] *Engine Database*. URL: http://www.astronautix.com/.

[5] *Evolution of SpaceX Merlin Engines*. URL: http://www.b14643.de/Spacerockets_2/United_States_1/Falcon-9/Merlin/index.htm.

[6] SAKAGUCHI Hiroyuki. "Development of methane engine enabling reusable launch vehicle and long-term in-space operations". In: *IHI Engineering Review* 51.2 (2018).

[7] Dietrich E Koelle. "Handbook of cost engineering for space transportation systems with transcost 7.0". In: *TCS—Trans Cost Systems, Ottobrunn* (2000).

[8] Dietrich E Koelle. "The transcost-model for launch vehicle cost estimation and its application to future systems analysis". In: *Acta Astronautica* 11.12 (1984), pp. 803–817.

[9] *Launch Vehicle Database*. URL: https://www.spacelaunchreport.com/.

[10] United States. National Oceanic, Atmospheric Administration, and United States. Air Force. *US Standard Atmosphere, 1976*. Vol. 76. 1562. National Oceanic and Atmospheric Administration, 1976.

[11] L Pepermans et al. "Flight Simulations of the Stratos III Parachute Recovery System". In: *IAC, Bremen, Germany* (2018).

[12] L Pepermans et al. "Trajectory simulations and sensitivity for the SPEAR parachute test vehicle". In: *IAC, Washington, USA* (2019).

[13] Lars Pepermans. "Reusable Rocket Upper Stage: Development of a Multidisciplinary Design Optimisation Tool to Determine the Feasibility of Upper Stage Reusability". In: (2019).

[14] Steven S Pietrobon. "Analysis of propellant tank masses". In: *Submitted to Review of US Human Space Flight Plans Committee* 6 (2009).

[15] *RASAero II User Manual*. URL: http://www.rasaero.com/.

[16] Mark Rozemeijer. "Launch Vehicle First Stage Reusability: a study to compare different recovery options for a reusable launch vehicle". In: (2020).

[17] *Russian space-rocket and missile liquid-propellant engines*. URL: http://www.b14643.de/Spacerockets/Specials/Russian_Rocket_engines/engines.htm.

[18] Paul V Tartabini et al. *Payload Performance Analysis for a Reusable Two-Stage-to-Orbit Vehicle*. Tech. rep. 2015.

[19] MW Van Kesteren. “Air launch versus ground launch: a multidisciplinary design optimization study of expendable launch vehicles on cost and performance”. In: (2013).

[20] JMV Vandamme. “Assisted-launch performance analysis: Using trajectory and vehicle optimization”. In: (2012).

[21] Barry Zandbergen. “Thermal rocket propulsion”. In: *Delft University of Technology* 2 (2003).

[22] BTC Zandbergen. “Simple mass and size estimation relationships of pump fed rocket engines for launch vehicle conceptual design”. In: *6th European Conference for Aeronautics and Space Sciences (EUCASS)*. 2015.